

**Universität  
Basel**

Fakultät für  
Psychologie



# **Vor dem Vergessen: Verbesserung der Früherkennung der Alzheimer-Krankheit durch innovative kognitive und strukturelle Marker**

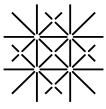
**Inauguraldissertation** zur Erlangung der Würde eines Doktors der Philosophie vorgelegt der  
Fakultät für Psychologie der Universität Basel von

**Nicolas Alexander Henzen**

aus Ferden, VS

Basel, 2024

Originaldokument gespeichert auf dem Dokumentenserver der Universität Basel [edoc.unibas.ch](https://edoc.unibas.ch)



Universität  
Basel

Fakultät für  
Psychologie



Genehmigt von der Fakultät für Psychologie auf Antrag von

PD Dr. phil. Sabine Krumm

Prof. Dr. phil. Klaus Opwis

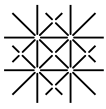
Prof. em. Dr. phil. Andreas U. Monsch

Datum des Doktoratsexamen: 16.07.2024

---

Prof. Dr. phil. Rainer Greifeneder

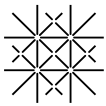
Dekan der Fakultät für Psychologie



## Erklärung zur wissenschaftlichen Lauterkeit

Ich erkläre hiermit, dass ich die vorliegende Arbeit ohne die Hilfe Dritter und ohne Benutzung anderer als der angegebenen Hilfsmittel selbstständig verfasst habe. Zu Hilfe genommene Quellen sind als solche gekennzeichnet. Die veröffentlichten oder zur Veröffentlichung in Zeitschriften eingereichten Manuskripte wurden in Zusammenarbeit mit den Koautoren erstellt und von keinem der Beteiligten an anderer Stelle publiziert, zur Publikation eingereicht, oder einer anderen Prüfungsbehörde als Qualifikationsarbeit vorgelegt. Es handelt sich dabei um folgende Manuskripte:

- I. Frei, M., Berres, M., Kivisaari, S. L., **Henzen, N. A.**, Monsch, A. U., Reinhardt, J., Blatow, M., Kressig, R. W., & Krumm, S. (2023). Can you find it? Novel oddity detection task for the early detection of Alzheimer's disease. *Neuropsychology*, 37(7), 717–740. doi:10.1037/neu0000859.
- II. **Henzen, N. A.**, Reinhardt, J., Blatow, M., Kressig, R. W., & Krumm, S. (2023). Excellent Interrater Reliability for Manual Segmentation of the Medial Perirhinal Cortex. *Brain Sciences*, 13(6), Article 6. doi:10.3390/brainsci13060850.
- III. **Henzen, N. A.**, Abdulkadir A., Reinhardt, J., Blatow, M., Kressig, R. W., & Krumm, S. Automated segmentation for cortical thickness of the medial perirhinal cortex. **Eingereicht.**



## Spezifizierung des eigenen Forschungsbeitrags zu den Manuskripten:

### I. Eigener Beitrag nach [CRediT](#)<sup>1</sup>:

- |  |  |   |
|--|--|---|
| <input type="checkbox"/> Conceptualization                     | <input type="checkbox"/> Data curation | <input type="checkbox"/> Formal Analysis          |
| <input type="checkbox"/> Funding acquisition                   | <input type="checkbox"/> Investigation | <input checked="" type="checkbox"/> Methodology   |
| <input type="checkbox"/> Project administration                | <input type="checkbox"/> Resources     | <input type="checkbox"/> Software                 |
| <input type="checkbox"/> Supervision                           | <input type="checkbox"/> Validation    | <input checked="" type="checkbox"/> Visualization |
| <input checked="" type="checkbox"/> Writing – original draft   |  |   |
| <input checked="" type="checkbox"/> Writing – review & editing |  |   |

Das Manuskript wurde bisher für keine anderen Qualifikationsarbeiten eingereicht.

### II. Eigener Beitrag nach [CRediT](#)<sup>1</sup>:

- |  |  |   |
|--|--|---|
| <input checked="" type="checkbox"/> Conceptualization          | <input type="checkbox"/> Data curation | <input checked="" type="checkbox"/> Formal Analysis |
| <input type="checkbox"/> Funding acquisition                   | <input type="checkbox"/> Investigation | <input checked="" type="checkbox"/> Methodology     |
| <input type="checkbox"/> Project administration                | <input type="checkbox"/> Resources     | <input type="checkbox"/> Software                   |
| <input type="checkbox"/> Supervision                           | <input type="checkbox"/> Validation    | <input checked="" type="checkbox"/> Visualization   |
| <input checked="" type="checkbox"/> Writing – original draft   |  |   |
| <input checked="" type="checkbox"/> Writing – review & editing |  |   |

Das Manuskript wurde bisher für keine anderen Qualifikationsarbeiten eingereicht.

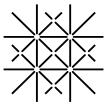
### III. Eigener Beitrag nach [CRediT](#)<sup>1</sup>:

- |  |  |   |
|--|--|---|
| <input checked="" type="checkbox"/> Conceptualization        | <input type="checkbox"/> Data curation | <input checked="" type="checkbox"/> Formal Analysis |
| <input type="checkbox"/> Funding acquisition                 | <input type="checkbox"/> Investigation | <input checked="" type="checkbox"/> Methodology     |
| <input type="checkbox"/> Project administration              | <input type="checkbox"/> Resources     | <input type="checkbox"/> Software                   |
| <input type="checkbox"/> Supervision                         | <input type="checkbox"/> Validation    | <input checked="" type="checkbox"/> Visualization   |
| <input checked="" type="checkbox"/> Writing – original draft |  |   |
| <input type="checkbox"/> Writing – review & editing          |  |   |

Das Manuskript wurde bisher für keine anderen Qualifikationsarbeiten eingereicht.

---

<sup>1</sup> <https://casrai.org/credit/>



### Open-Science Aspekte der Manuskripte:

- I. Preregistration:  ja  nein  
Open-Access-Publikation:  ja  nein  
Open-Access-Data/Analyse:  ja  nein  
Ort/URL der Daten und Analysen: N/A

- II. Preregistration:  ja  nein  
Open-Access-Publikation:  ja  nein  
Open-Access-Data/Analyse:  ja  nein  
Ort/URL der Daten und Analysen: N/A

- III. Preregistration:  ja  nein  
Open-Access-Publikation:  ja  nein  
Open-Access-Data/Analyse:  ja  nein  
Ort/URL der Daten und Analysen: N/A

Ort, Datum

Basel, den 29. April 2024

Signatur

  
.....

Vorname Nachname

Nicolas Alexander Henzen

## **DANKSAGUNG**

An dieser Stelle möchte ich die Gelegenheit nutzen, um all jenen zu danken, deren Unterstützung die Realisierung dieser Dissertation erst möglich gemacht haben:

Von ganzem Herzen möchte ich meiner Doktormutter, Frau PD Dr. phil. Sabine Krumm, für ihre unschätzbare Unterstützung danken. Ihr tiefgreifendes Wissen und die Leidenschaft, mit der sie Forschung betreibt, sind nicht nur beeindruckend, sondern waren auch eine stetige Inspirationsquelle für mich. Ich hätte mir keine bessere Doktormutter und Mentorin vorstellen können.

Mein besonderer Dank gilt Herrn Prof. em. Dr. phil. Andreas U. Monsch für seine hochgeschätzte Grosszügigkeit, die es mir ermöglichte, meine Dissertation an der Memory Clinic Basel zu verfassen sowie begleitend die Weiterbildung zum Fachtitel Neuropsychologie zu verfolgen. Herrn Prof. Dr. phil. Klaus Opwis möchte ich für die begleitende Betreuungsrolle meiner Dissertation danken.

Weiter möchte ich Herrn Dr.-Ing. Ahmed Abdulkadir danken, welcher mit seinem umfassenden Know-how und seinem unermüdlichen Einsatz die Realisierung unserer computergestützten Methodik erst ermöglichte. Zudem möchte ich auch Marlen Frei meinen Dank aussprechen für die spannende und engagierte Zusammenarbeit bei unserer gemeinsamen Publikation.

Bei dieser Gelegenheit möchte ich auch dem Team der Memory Clinic Basel meinen Dank aussprechen. Ihre Bereitschaft zu Diskussionen und die wertvollen Inputs waren von grosser Hilfe. Ein besonderer Dank geht an Frau Dr. phil. Alexandra Wüest und Herrn Dr. phil. Stefan Bläsi, deren geschätzte Rückmeldungen während der Finalisierung meiner Dissertation besonders zielführend waren.

Herzlich danken möchte ich auch meiner wunderbaren Frau für ihre stetige Unterstützung und Geduld, die massgeblich zu meinem Durchhaltevermögen beigetragen haben. Ich bin unglaublich dankbar, dich an meiner Seite zu haben. Nicht zu vergessen ist unser treuer Begleiter Grey, der mit regelmässigen Spaziergängen an der frischen Luft geholfen hat, meinen Geist zu klären und Denkblockaden zu lösen.

## **INHALTSVERZEICHNIS**

ZUSAMMENFASSUNG	2
ABKÜRZUNGEN	3
1. HINTERGRUND UND EINFÜHRUNG	4
1.1. Vorteile und Herausforderungen einer frühen Alzheimer-Diagnose	5
1.2. Neuropathologie der Alzheimer-Krankheit	7
1.3. Klinische Manifestation der Alzheimer-Krankheit	9
1.4. Verbesserung der Alzheimer-Frühdagnostik	12
1.4.1. Die Funktion des perirhinalen Kortex – ein kognitiver Marker	13
1.4.2. Der mediale perirhinale Kortex – ein struktureller Marker	15
1.5. Hauptziele der vorgestellten Studien	19
2. LISTE DER WISSENSCHAFTLICHEN ORIGINALPUBLIKATIONEN	20
2.1. Studie I: Can you find it? Novel oddity detection task for the early detection of Alzheimer's disease	21
2.2. Studie II: Excellent Interrater Reliability for Manual Segmentation of the Medial Perirhinal Cortex	46
2.3. Studie III: Automated segmentation for cortical thickness of the medial perirhinal cortex	60
3. GENERELLE DISKUSSION	80
3.1. Der Odd-One-Out für die Früherkennung der Alzheimer-Krankheit	80
3.2. Manuelle und automatisierte Segmentierung des medialen perirhinalen Kortex	85
3.3. Der PRC/mPRC vor dem Hintergrund der Früherkennung der Alzheimer-Krankheit	88
4. AUSBLICK	92
5. REFERENZLISTE	95
CURRICULUM VITAE	105

## ZUSAMMENFASSUNG

Die Demenz und insbesondere die Alzheimer-Krankheit (AK) als ihre Hauptursache stellen eine der grössten gesundheitlichen Herausforderungen des 21. Jahrhunderts dar. Die frühzeitige Identifikation der kognitiven und strukturellen Veränderungen, die mit der AK einhergehen, ist daher von ausserordentlichem Interesse. Charakteristisch für die AK ist das fortschreitende Verteilungsmuster neurofibrilläres Bündel (NFT), beginnend im medialen perirhinalen Kortex (mPRC), sich ausbreitend über den entorhinalen Kortex (ERC) mit späterer Beteiligung des lateralen perirhinalen Kortex (IPRC), Hippocampus und Rest des Gehirns. Angesichts des engen Zusammenhangs zwischen der Ansammlung von NFT und Nervenzellverlust in betroffenen Regionen, erweist sich der mPRC bzw. der perirhinale Kortex (PRC) als vielversprechender struktureller und kognitiver Marker für die Frühdiagnostik der AK.

Studie I präsentierte eine neue visuelle Diskriminationsaufgabe zur Bewertung der PRC-Funktion. In einer Pilotstudie wurden optimale Testitems für die Differenzierung zwischen einer frühen Alzheimer-Gruppe (N=50) und gesunden Kontrollen (N=50) identifiziert. Eine nachfolgende Validierungsstudie setzte den adaptierten Test an einer Stichprobe mit einer frühen Alzheimer-Gruppe (N=27), gesunden Kontrollen (N=25) und einer Depressionsgruppe (N=26) ein. Die Ergebnisse zeigten, dass die Testleistung erfolgreich zwischen der Alzheimer-Gruppe und gesunden Kontrollen unterscheiden konnte. Die Analyse der ergänzende MRT-Bildgebung wies signifikante Unterschiede in der kortikalen Dicke des mPRC und ERC in der Alzheimer-Gruppe im Vergleich zu den anderen zwei Gruppen auf. Zusätzlich konnte die Testleistung mittels voxel-basierter Morphometrie mit parahippocampalen Regionen, inkl. PRC und ERC, in Verbindung gebracht werden.

Studie II untersuchte die Übereinstimmung zwischen zwei Ratern bei der manuellen Segmentierung parahippocampaler Regionen (mPRC, IPRC und ERC) in strukturellen MRT-Bildern (N=44). Das verwendete manuelle Segmentierungsprotokoll ermöglichte es den Ratern, bemerkenswert ähnliche Werte für die kortikale Dicke zu erzielen. Angesichts des hohen Zeitaufwands für die manuelle Segmentierung in Studie II, wurde in Studie III ein automatisiertes Segmentierungstool für die Berechnung der kortikale Dicke parahippocampaler Regionen (z.B. mPRC und ERC) erstellt. Das Modell wurde auf einem Trainingsdatensatz (N=126) mit manuell segmentierten Labels trainiert und wurde anschliessend auf einen unabhängigen Testdatensatz angewendet (N=103; Stichprobe aus der Studie von Krümm et al., 2016). Wir fanden eine hohe Übereinstimmung zwischen den manuell und automatisiert generierten Werten für die kortikale Dicke. Analog zu den Befunden von Krümm et al. (2016) zeigte sich eine signifikante Atrophie in der Alzheimer-Gruppe im Vergleich zu gesunden Kontrollen im mPRC, ERC und IPRC. Beim Vergleich einer amnestischen mild cognitive impairment Gruppe mit den gesunden Kontrollen fand sich ein signifikanter Unterschied im ERC, jedoch nicht, wie bei Krümm et al. (2016), auch im mPRC.

Die Ergebnisse präsentieren den neu entwickelten spezifischen PRC-Funktionstest sowie das automatisierte Segmentierungstool zur Beurteilung der kortikalen Dicke des mPRC, als wertvolle Instrumente, um die Alzheimer-Forschung voranzutreiben. Der künftige Einsatz in Langzeitstudien, um dadurch entscheidend zur Verbesserung der Früherkennung und Diagnostik der AK beizutragen wird reflektiert und diskutiert.



## ABKÜRZUNGEN

<b>A<math>\beta</math></b>	Amyloid- $\beta$
<b>AK</b>	Alzheimer-Krankheit
<b>aMCI</b>	Amnesic Mild Cognitive Impairment
<b>DSM-5</b>	Diagnostic and Statistical Manual of Mental Disorders 5
<b>ERC</b>	Entorhinaler Kortex
<b>fMRT</b>	Funktionelle Magnetresonanztomographie
<b>HC</b>	Hippocampus
<b>IPRC</b>	Lateraler perirhinaler Kortex
<b>MCI</b>	Mild Cognitive Impairment
<b>mPRC</b>	Medialer perirhinaler Kortex
<b>MRT</b>	Magnetresonanztomographie
<b>MTA</b>	Mediale Temporallappen Atrophie
<b>MTL</b>	Medialer Temporallappen
<b>NFT</b>	Neurofibrilläre Bündel («neurofibrillary tangles»)
<b>PHC</b>	Parahippocampaler Kortex
<b>PRC</b>	Perirhinaler Kortex
<b>ROI</b>	Regions of Interest
<b>VBM</b>	Voxel-basierte Morphometrie

## 1. HINTERGRUND UND EINFÜHRUNG

„Ich habe mich sozusagen verloren.“ - Auguste D.

Zu Beginn des 20. Jahrhunderts stand der deutsche Arzt Alois Alzheimer vor einem medizinischen Rätsel. Fasziniert von seiner Patientin Auguste D. beobachtete er unerklärliche Symptome eines fortschreitenden Gedächtnis- und Sprachverlusts, begleitet von Desorientierung und Halluzinationen. Die post-mortem Untersuchung ihres Gehirns enthüllte Ansammlungen von extra- und intrazellulären Proteinablagerungen sowie ein gleichmässig atrophes Gehirn. Alois Alzheimer zog daraus den Schluss, dass diese neuropathologischen Veränderungen, die beobachteten klinischen Symptome verursachten. Damit setzte er den Grundstein für die Erforschung der später nach ihm benannten Alzheimer-Krankheit (AK; Alzheimer, 1907; Goedert & Ghetti, 2007).

Die AK ist eine langsam fortschreitende, neurodegenerative Erkrankung und betrifft insbesondere Menschen jenseits des 65. Lebensjahres (Kumar et al., 2023). Klinisch zeigt sich die AK typischerweise durch progrediente Gedächtnis- und Lernschwierigkeiten, gefolgt von Störungen der Exekutivfunktionen, der Sprache und der Aufmerksamkeit. Im fortgeschrittenen Verlauf, dem Demenz-Stadium, führt sie zu nicht mehr kompensierbaren Beeinträchtigungen in Aktivitäten des täglichen Lebens und beraubt die Betroffenen ihrer Selbstständigkeit (Jack et al., 2011; McKhann et al., 2011). In der Schweiz leben rund 150'000 Menschen mit einer Demenz (Alzheimer Schweiz, 2023), wobei die AK die häufigste Ursache darstellt. Laut Prognosen der Weltgesundheitsorganisation (WHO) wird der Anteil der weltweit über 60-Jährigen von 12% im Jahr 2015 auf 22% im Jahr 2050 ansteigen (WHO, 2023). Da das Alter der grösste Risikofaktor für die Entwicklung einer Demenz darstellt, ist entsprechend mit einer Verdopplung der Demenzfälle bis zum Jahr 2050 zu rechnen. Eine Veränderung, welche enorme sozioökonomischen Kosten mit sich bringt. Bereits heute belaufen sich die Demenz-Kosten in der Schweiz auf geschätzte 11.8 Milliarden Franken jährlich, wovon etwa die Hälfte durch die unbezahlte Betreuungs- und Pflegeleistungen von Angehörigen getragen wird (Alzheimer Schweiz, 2023; Monsch et al., 2012). Weiter werden die Aussichten dadurch getrübt, dass trotz intensiver Forschung zum jetzigen Zeitpunkt noch keine Therapie existiert, welche den Krankheitsverlauf der AK stoppen, geschweige denn heilen kann. Ein

Konsensus besteht darüber, dass eine frühzeitige Diagnose und Intervention die beste Grundlage bieten, den verheerenden Verlauf dieser Krankheit zu ändern. Es ist jedoch nicht nur von Bedeutung, die Relevanz einer frühen Diagnose zu erkennen, sondern auch ihre Vorteile und Herausforderungen zu verstehen.

Im Rahmen dieser Dissertation bezieht sich der Begriff "Alzheimer-Krankheit" auf die sporadische Form, die etwa 95% aller Fälle repräsentiert und üblicherweise bei Personen jenseits des 65. Lebensjahres auftritt. Die verbleibenden Fälle beziehen sich auf die familiäre Form, die bereits im Alter zwischen 30 und 65 Jahren beginnen kann (Piaceri et al., 2013). Weiter verwendet die vorliegende Arbeit den Begriff «Früherkennung der Alzheimer-Krankheit» im Kontext erster klinisch objektivierbarer kognitiver Veränderungen und nicht im Sinne eines präklinischen Nachweises der neuropathologischen Hauptcharakteristika Amyloid- $\beta$  (A $\beta$ ) und Tau.

### 1.1. Vorteile und Herausforderungen einer frühen Alzheimer-Diagnose

Frühe Anzeichen der AK, insbesondere leichte Veränderungen in der Gedächtnisleistung, werden meist früh im Verlauf von Betroffenen und ihren Angehörigen bemerkt. Obgleich neuropsychologische Tests, wie semantische und episodische Gedächtnisaufgaben, diese subtilen Veränderungen erfassen könnten, erfolgt in vielen Fällen eine klinische Untersuchung und Diagnosestellung erst in einem Stadium, in dem schon erhebliche kognitive Defizite und signifikante Hirnschädigungen vorhanden sind (Monsch et al., 2012). Eine frühe Diagnose hat für Betroffene, ihre Angehörige und die Gesellschaft hohe Relevanz (Dubois et al., 2016). Sie liefert eine Erklärung für beobachtete Symptome und erleichtert eine entsprechende zukünftige Planung (Rasmussen & Langerman, 2019). Darüber hinaus öffnet sie nicht nur den Zugang zu etablierten medikamentösen (z.B. Acetylcholinesterase-Hemmern) und nicht-medikamentösen (z.B. eine aktive Alltagsgestaltung) Behandlungsmöglichkeiten, sondern ebnet auch den Weg für den Einsatz von neuen (z.B. Lecanemab; van Dyck et al., 2023) und zukünftigen krankheitsmodifizierenden Therapieansätzen. Die aktuellen symptomatischen Behandlungen zielen darauf ab, die Lebensqualität der Betroffenen zu verbessern und den Zeitpunkt einer Institutionalisierung

hinauszuzögern (Littlewood et al., 2010; Lopez et al., 2009). Insbesondere die längere Selbstständigkeit sowie der frühzeitige Zugang zu professioneller Hilfe führt bei Angehörigen zu einer psychosozialen und physischen Entlastung (Monsch et al., 2012). Eine frühestmögliche Diagnose ist also entscheidend für die Nutzung aktueller Behandlungsmöglichkeiten. Sie ist aber genauso bedeutend im Rahmen der Alzheimer-Forschung, um den Krankheitsverlauf besser zu verstehen und die Entwicklung krankheitsmodifizierender Medikamente zu unterstützen (Dubois et al., 2016; Rasmussen & Langerman, 2019). Ein wesentlicher Punkt, der die Wichtigkeit einer frühen Diagnose weiter unterstreicht, liegt in der Annahme, dass das Scheitern vieler bisheriger Therapieansätze möglicherweise darauf zurückzuführen ist, dass sie zu einem Zeitpunkt angewendet wurden, an dem die Krankheit bereits zu weit fortgeschritten war (Aisen et al., 2011).

Trotz der entscheidenden Bedeutung einer frühen Alzheimer-Diagnose stehen wir auch vor Herausforderungen und Risiken. Eine frühzeitige Diagnose kann zu Stigmatisierung führen und kritische Fragen hinsichtlich der Kompetenzen und der Entscheidungsfähigkeit der Betroffenen aufwerfen (Gauthier et al., 2013; Mattsson et al., 2010). Darüber hinaus besteht das Risiko einer Fehldiagnose, die entweder zu unnötigen Behandlungen führt oder aber einer angemessenen Therapie für eine möglicherweise behandelbare Ursache im Wege steht (Gaugler et al., 2013). Diese Überlegungen verdeutlichen die Notwendigkeit sensitiver, aber auch reliabler kognitiver Marker für die Früherkennung der AK. Ein fundamentaler Ansatz ist hierbei ein theoriegeleitetes Vorgehen, das die Beziehung zwischen der topografischen Verteilung der Alzheimer-typischen Neuropathologie und kognitiven Theorien über die Funktion der betroffenen Gehirnregionen nutzt. Dies eröffnet die Möglichkeit, kognitive Veränderungen, als Folge der Neuropathologie der AK zu einem frühestmöglichen Zeitpunkt zu untersuchen (Bastin & Delhaye, 2023). Auf dieser Grundlage konzentriert sich der folgende Abschnitt auf die wesentlichen Aspekte der zeitlichen und topografischen Charakteristika der Alzheimer-Pathologie.

## 1.2. Neuropathologie der Alzheimer-Krankheit

Die AK ist eine doppelte Proteinopathie, charakterisiert durch die extrazelluläre Ablagerung von A $\beta$  in Plaques und die intrazelluläre Aggregation von Tau zu neurofibrillären Bündeln (NFT; «neurifibrillary tangles»; Braak & Braak, 1991a; DeTure & Dickson, 2019). Amyloid-Plaques setzen sich vorwiegend aus A $\beta$ -Peptiden zusammen, welche durch die Spaltung des Amyloid-Precursor-Proteins entstehen. Anstatt effektiv abgebaut zu werden, aggregieren gewisse Peptidfragmente und formen Plaques (Chen et al., 2017). NFT bestehen aus intrazellulären Ansammlungen von hyperphosphorylierten, mikrotubuli-assoziierten Tau-Proteinen. Im gesunden Hirn spielen diese Tau-Proteine eine wichtige Rolle bei der Stabilisierung der Mikrotubuli und dem axonalen Transport innerhalb der Nervenzellen. Bei der AK führt eine Hyperphosphorylierung der Tau-Proteine dazu, dass sie sich von den Mikrotubuli loslösen. Diese Tau-Proteine aggregieren dann zu unlöslichen spiralförmigen Filamenten, welche letztendlich NFT bilden. Dieser Prozess führt zum Funktionsverlust und Absterben der betroffenen Nervenzellen (Ballatore et al., 2007; Spillantini & Goedert, 2013). Heutige technologische Fortschritte ermöglichen es, A $\beta$  und Tau in vivo zu messen, beispielsweise mittels Liquor-Analyse oder molekularer Bildgebung (Rullmann et al., 2022; Scheltens et al., 2021). Solche Untersuchungen haben aufgezeigt, dass diese neuropathologischen Veränderungen der AK bereits Jahrzehnte vor den ersten klinischen Symptomen beginnen (Dubois et al., 2016; Jack Jr. et al., 2018; Price & Morris, 1999). Angesichts dessen reflektiert die AK ein Kontinuum, dargestellt in Abbildung 1, das sich von einer langen präklinischen Phase, über ein Stadium leichter kognitiver Beeinträchtigungen (MCI; «mild cognitive impairment») bis hin zur ausgeprägten Alzheimer-Demenz spannt (Sperling et al., 2011).

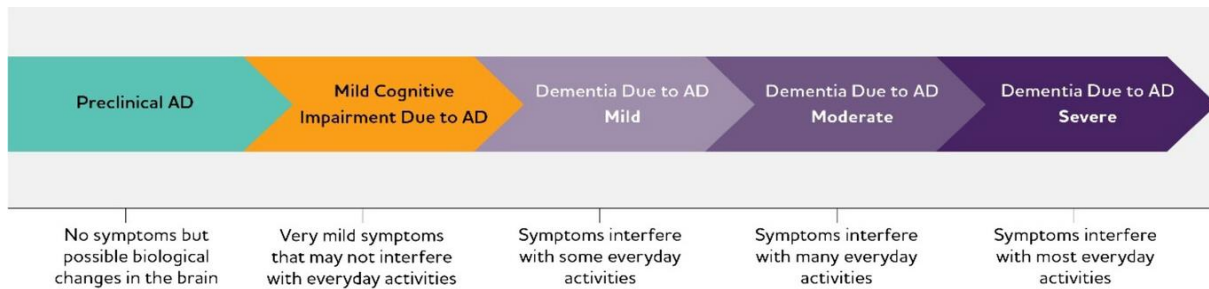


Abbildung 1. Kontinuum der Alzheimer Krankheit (Alzheimer's disease facts and figures, Alzheimers dement. 2023).

Beide Proteinopathien zeichnen sich durch ein unterschiedliches topografisches Muster aus. Gemäss Thal-Phasen manifestiert sich A $\beta$  zuerst im Neokortex, insbesondere in frontalen Bereichen, bevor im Verlauf Ansammlungen im Hippocampus (HC) und dem entorhinalen Kortex (ERC) auftreten (Thal et al., 2002). Bei der neurofibrillären Taupathologie ist laut Braak-Stadien der mediale perirhinale Kortex (mPRC; auch als transentorhinaler Kortex bekannt) als erste kortikale Region von NFT betroffen. Im Verlauf der Krankheit breiten sich die NFT zunächst auf den benachbarten ERC aus, bevor der HC, der laterale perirhinale Kortex (IPRC) und im späteren Verlauf der Krankheit der Rest des Gehirns betroffen ist (Braak et al., 2006; Braak & Braak, 1991b; Rullmann et al., 2022; Taylor & Probst, 2008). In den wissenschaftlichen Diskussionen wird bei der AK oftmals das Augenmerk auf A $\beta$  gelegt. In Bezug auf die Auswirkungen der AK spielt die neurofibrilläre Taupathologie jedoch eine weitaus präzisere und relevantere Rolle. Im Vergleich zu A $\beta$  steht die neurofibrilläre Taupathologie in einem wesentlich engeren Zusammenhang mit Art und Ausprägung der kognitiven Defizite (Giannakopoulos et al., 2003, 2009). Weiter ist die Akkumulation von NFT eng mit dem Verlust von Nervenzellen in den betroffenen Gehirnregionen verbunden (Bobinski et al., 1997; Braak & Braak, 1991a) und steht in kausalem Zusammenhang mit zerebraler Atrophie (Gómez-Isla et al., 1997). Diese direkte Manifestation der schädigenden Auswirkungen der AK auf das Gehirn ist somit ein entscheidender Faktor bei der Entwicklung kognitiver Beeinträchtigungen. In Anbetracht dessen nimmt die neurofibrilläre Taupathologie nicht nur für das Verständnis der Mechanismen der AK eine Schlüsselrolle ein, sondern ist auch essenziell für die diagnostische Früherkennung mittels kognitiver und biologischer Marker sowie die

Erforschung therapeutischer Ansätze. Vor diesem Hintergrund legt die vorliegende Promotionsarbeit den Schwerpunkt auf die neurofibrilläre Taupathologie der AK, insbesondere in ihrer initialen Manifestation im mPRC.

### 1.3. Klinische Manifestation der Alzheimer-Krankheit

Obwohl es bedeutende Fortschritte in der präklinischen Bestimmung von Alzheimer-typischen neuropathologischen Veränderungen gibt, können die Biomarker A $\beta$  und Tau nicht zuverlässig die Entwicklung kognitiver Defizite vorhersagen. Eine systematische post-mortem Studie zeigte, dass etwa zwei Drittel der über 70-Jährigen eine Alzheimer-typische Neuropathologie aufwiesen, unabhängig von ihrem klinischen Zustand (Braak et al., 2011). Ähnlich fanden in vivo Untersuchungen mittels molekularer Bildgebung vergleichbare Mengen an A $\beta$  und Tau sowohl bei gesunden als auch bei kognitiv beeinträchtigten Individuen (Maass et al., 2017; Timmers et al., 2019). Der genaue Zusammenhang zwischen dem Vorhandensein der zwei neuropathologischen Hauptcharakteristika der AK und der Entstehung von kognitivem Abbau und Neurodegeneration auf individueller Ebene ist weiterhin unklar. Es werden zwei mögliche Modelle diskutiert: eines, in dem A $\beta$  und Tau einen langen und asymptomatischen Verlauf repräsentieren sowie eines, in welchem A $\beta$  und Tau mit einem höheren Risiko einhergehen, den klinischen Phänotyp der AK zu entwickeln (Dubois et al., 2021). Protektive Faktoren, wie beispielsweise eine über die Lebenszeit aufgebaute kognitive Reserve, werden als mögliche Gründe diskutiert, wieso ein Teil der Betroffenen zu Lebzeiten nie klinische Symptome entwickeln (Brookmeyer & Abdalla, 2018; Stern, 2012). Umso wichtiger ist es, die ersten subtilen kognitiven Veränderungen zu erfassen, da sie ein Hinweis für den Beginn eines symptomatischen Alzheimer-Stadiums sein könnten.

Vor diesem Hintergrund spielt die umfassende neuropsychologische Untersuchung eine entscheidende Rolle. Einleitend mit einem Anamnesegespräch wird die Sichtweise der Patientinnen und Patienten sowie die Perspektive ihrer Angehörigen erhoben. In diesem Gespräch ist es besonders wichtig, wahrgenommene Veränderungen in Bereichen der Hirnleistungen (z.B. dem Gedächtnis), der

Alltagsfunktionalität (z.B. bei administrativen Aufgaben), der Psychopathologie (z.B. die Stimmungslage) sowie dem Verhalten zu identifizieren. Im Anschluss folgt eine dezidierte testpsychologische Abklärung, um das Ausmass der kognitiven Defizite zu objektivieren. In der klinischen Praxis kommen dafür domänenspezifische neuropsychologische Testinstrumente zum Einsatz, was beispielsweise die Beurteilung der Aufmerksamkeit, des Lernens und des Gedächtnisses, der Sprache oder der exekutiven Funktionen erlaubt. Klinisch liegt der Schwerpunkt in der Alzheimer-Diagnostik auf neuropsychologischen Tests, die primär die Funktion des ERC und HC evaluieren, etwa durch Erfassen der episodischen Gedächtnisleistung (Hirni et al., 2013; Lipton & Eichenbaum, 2008). Ein zusätzlich eingesetzter Test, der die semantische Gedächtnisleistung misst (semantische Flüssigkeitsaufgabe) korreliert zwar mit der Integrität des perirhinalen Kortex (PRC), gleichzeitig aber auch mit dem ERC und dem HC (Hirni et al., 2013). Obwohl der mPRC initial in der Alzheimer-Pathologie betroffen ist, kommt aktuell kein spezifischer PRC-Funktionstest routinemässig in der klinischen Diagnostik zum Einsatz.

Nachdem durch die Neuropsychologie in einem ersten Schritt die kognitiven Beeinträchtigungen betreffend Art und Ausmass objektiviert wurden, geht es im nächsten Schritt darum, deren Ursache herauszufinden. Am Beispiel der Memory Clinic in Basel findet im Anschluss im Sinne einer fundierten Differenzialdiagnostik eine geriatrisch-neurologische Abklärung statt, die Aussagen zum Somato- und Neurostatus liefert. Darüber hinaus wird standardmässig eine strukturelle Bildgebung durchgeführt (z.B. mittels Magnetresonanz-Tomographie [MRT]). Während die Bildgebung ursprünglich zur Ausschlussdiagnostik von sekundären Ursachen, wie Tumoren oder einem Hydrozephalus diente (Wu et al., 2003), bietet sie heutzutage in Verbindung mit der Neuropsychologie einen zusätzlichen diagnostischen Mehrwert (Klöppel et al., 2015). Im Fokus der ergänzenden MRT-Bildgebung steht die visuelle Beurteilung von Atrophie, beispielsweise der ERC Atrophie Score (ERICA; Enkirch et al., 2018) oder der mediale Temporallappen Atrophie (MTA) Score. Beim MTA-Score steht der HC im Fokus und er wird in Bezug auf eine Volumenabnahme sowie im Vergleich zu umliegenden Bereichen, wie der Fissura choroidea und den Seitenventrikel bewertet. Der MTA-Score kann Werte von 0 keiner Atrophie bis 4 eine schwere Atrophie angeben (Scheltens & Pol, 2012). Ergänzend führen radiologische Zentren zunehmend



automatisierte volumetrische MRT-Analysen durch, die es ermöglichen, Volumina von ganzen Hirnlappen (z.B. dem Temporallappen) oder einzelnen Strukturen (wie dem ERC und HC) zu berechnen. Obwohl der mPRC initial in der Alzheimer-Pathologie betroffen ist, wird er in der strukturellen klinischen Diagnostik häufig vernachlässigt. Wenn er berücksichtigt wird, geschieht dies meist nur im Rahmen des gesamten PRC.

Ergänzend zu den bisher erwähnten Untersuchungen und in erster Linie bei unzureichender Diagnosesicherheit, können weitere Biomarker erhoben werden (z.B. Liquor-Analyse oder molekulare Bildgebungsverfahren). Dieses interdisziplinäre differentialdiagnostische Vorgehen ist von grosser Bedeutung, da kognitive Probleme unterschiedliche Ursachen haben können, welche teilweise reversibel sind (z.B. Depression oder Schlafprobleme). Die Neuropsychologie nimmt eine zentrale Rolle ein, denn sie erlaubt es eine Hirnleistungsstörung zu objektivieren, damit weiterführend nach einer Ursache gesucht werden kann. Auch bei der Differentialdiagnose liefert die Neuropsychologie wichtige Hinweise, da unterschiedliche neuropsychologische Testprofile auf unterschiedliche Ätiologien hinweisen können. Dies unterstreicht erneut die Wichtigkeit von Testinstrumenten, welche die ersten subtilen kognitiven Veränderungen im Rahmen der AK erfassen können.

Bei der AK stützt sich die aktuelle klinische Diagnostik massgeblich auf die diagnostischen Leitlinien des National Institute on Aging und der Alzheimer's Association (NIA-AA) aus dem Jahre 2011 (Albert et al., 2011; Jack et al., 2011; McKhann et al., 2011; Sperling et al., 2011). In den symptomatischen Alzheimer-Stadien, also dem MCI und der Demenz, stehen die klinischen Kriterien im Vordergrund, während Biomarker (z.B. bildgebende Verfahren oder Liquor-Analysen) eine unterstützende Funktion einnehmen. Dies ermöglicht die Anwendung der diagnostischen Hauptkriterien auch dort, wo keine Biomarker zur Verfügung stehen. Das MCI (im Diagnostic and Statistical Manual of Mental Disorders 5 [DSM-5] als «leichte neurokognitive Störung» bezeichnet) wird oft als Vorstufe einer Demenz betrachtet und repräsentiert den frühestmöglichen Zeitpunkt, um eine klinische Alzheimer-Diagnose zu stellen. Das MCI-Stadium ist charakterisiert durch eine leichte Beeinträchtigung der kognitiven Fähigkeiten, welche im Vergleich zu einem vorherigen Leistungsniveau neu aufgetreten oder zugenommen hat, die betroffene

Person jedoch nicht in ihrer Alltagsfunktionalität einschränkt (Albert et al., 2011). Einer Alzheimer-Demenz geht häufig ein sogenanntes amnestisches MCI mit initial Gedächtnisproblemen voraus (Albert et al., 2011; Winblad et al., 2004). Im Gegensatz dazu führen die kognitiven Defizite im Demenz-Stadium (im DSM-5 als «majore neurokognitive Störung» bezeichnet) zu einer Beeinträchtigung der Selbstständigkeit im Alltag. Die Bedeutung von Biomarkern wird besonders deutlich angesichts atypischer nicht-amnestischer Präsentationen der AK (Murray et al., 2011; Polsinelli & Apostolova, 2022). Darunter fallen die posteriore kortikale Atrophie (PCA; Crutch et al., 2017), mit überwiegend visuell-räumlichen Defiziten, die logopenische Variante der primär progressiven Aphasie (lvPPA; Gorno-Tempini et al., 2011), mit im Vordergrund stehenden Sprachschwierigkeiten, die verhaltensbezogene/dysexekutive Variante (bvAD; Ossenkoppele et al., 2015 / dAD; Townley et al., 2020), charakterisiert durch Verhaltensauffälligkeiten und Defizite in exekutiven Funktionen sowie das corticobasale Syndrom (CBS; Armstrong et al., 2013), gekennzeichnet durch motorische Störungen. Vor dem Hintergrund der aktuellen klinischen Alzheimer-Diagnostik wird der PRC bzw. der mPRC im Folgenden als vielversprechender kognitiver und struktureller Marker näher thematisiert.

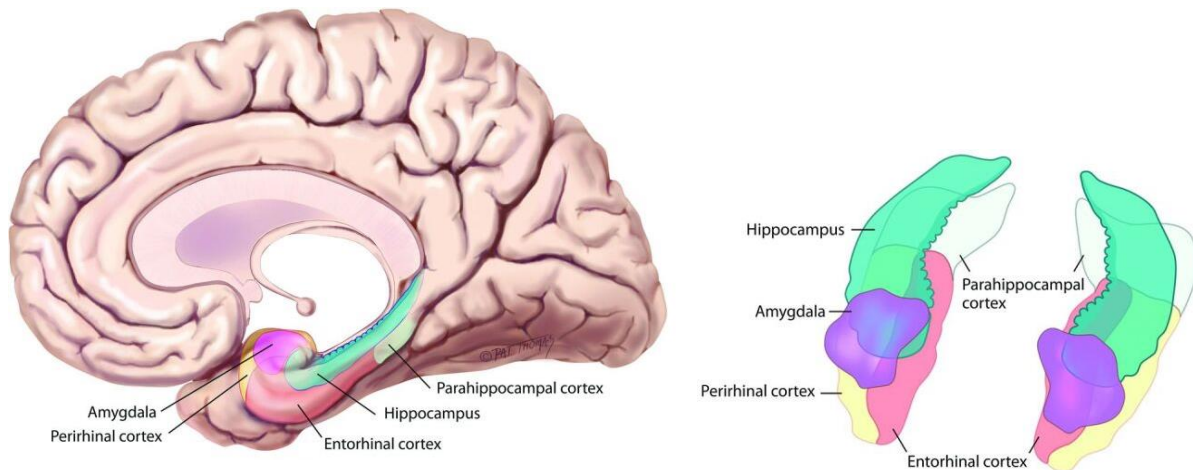
#### 1.4. Verbesserung der Alzheimer-Frühdagnostik

Eine präzise Frühdagnostik der AK ist weiterhin eine der grössten Herausforderungen und zugleich Chancen im Bereich der Gesundheitswissenschaften. Die aktuellen Forschungskriterien für ein MCI im Kontext der AK (Albert et al., 2011) und die Definition des präklinischen Stadiums anhand Biomarker (Sperling et al., 2011) empfehlen die kombinierte Nutzung neuropsychologischer Marker und Biomarker (z.B. MRT). Wenn die neurofibrilläre Taupathologie im Frühstadium der AK auf den mPRC beschränkt ist, können bereits subtile kognitive Veränderungen vorhanden sein. Diese sind im Alltag oft nicht wahrnehmbar und können mit herkömmlichen Diagnosewerkzeugen noch nicht erfasst werden. Der mPRC, initial in der Pathogenese der AK betroffen, bietet sich daher als Schlüsselregion für die Entwicklung neuer diagnostischer Marker an. Deutliche Gedächtnisstörungen manifestieren sich typischerweise, wenn die Pathologie den HC involviert. Der mPRC, obgleich früher von der neurofibrillären Taupathologie

betroffen, wird wie bereits erwähnt in der aktuellen Diagnostik mehrheitlich vernachlässigt. Ein Atrophie-Score, der die Integrität des mPRC - beispielsweise anhand der kortikalen Dicke - misst, zusammen mit kognitiven Tests, welche spezifisch die PRC-Funktion erfassen, könnten die Frühdiagnose der AK massgeblich verbessern. Da MRT-Biomarker auch zukünftig eine zentrale Rolle in der Alzheimer-Diagnostik spielen werden, ist es entscheidend, diese Instrumente weiter zu verfeinern. Die MRT-Bildgebung besticht durch ihre weite Verfügbarkeit, Kosteneffizienz sowie ihre nicht-invasive und strahlungsfreie Anwendung und stellt daher ein besonders überzeugendes Werkzeug in der Auswahl möglicher Alzheimer-Biomarker dar (Villa et al., 2020).

#### 1.4.1. Die Funktion des perirhinalen Kortex – ein kognitiver Marker

Der mediale Temporallappen (MTL; siehe Abbildung 2) spielt eine zentrale Rolle für das deklarative Gedächtnis, das sich aus dem episodischen (z.B. die Erinnerung an den letzten Urlaub) und dem semantischen Gedächtnis (z.B. Welt- und Faktenwissen) zusammensetzt. Historisch betrachtet wurden der HC und andere Strukturen des MTL oft als eine einheitliche Funktionseinheit angesehen, die hauptsächlich für Gedächtnisprozesse verantwortlich ist (Corkin, 1984; Squire et al., 2004; Tulving, 1972). Aktuellere neurowissenschaftliche Studien legen nahe, dass den verschiedenen Subregionen des MTL, wie beispielsweise dem PRC und dem ERC, unterschiedliche funktionelle Aufgaben zukommen (siehe z.B. Davachi, 2006). Die lange vorherrschende Auffassung eines gesamtheitlichen Modells hat das Verständnis für die spezialisierten Funktionen einzelner MTL-Strukturen behindert. Dies ist vermutlich einer der Hauptgründe dafür, dass im klinischen Bereich aktuell keine spezifischen PRC-Funktionstests routinemässig zum Einsatz kommen. Das Wissen um diese funktionelle Spezialisierung der MTL-Subregionen ist von herausragender Bedeutung, da es zur detaillierten Erforschung der jeweiligen Strukturen motiviert.



*Abbildung 2.* Links: Sagittalschnitt des Gehirns mit farblich hervorgehobenen Strukturen des rechten medialen Temporallappens. Rechts: Detaillierte, isolierte Ansicht dieser Strukturen für beide Hemisphären in entsprechender Farbcodierung (adaptiert aus Raslau et al., 2015).

Ein Grossteil unseres heutigen Wissens über den PRC stammt aus Tierstudien. Diese zeigen, dass der PRC am Ende des ventralen visuellen Stroms lokalisiert ist und eine Schlüsselrolle bei der visuellen Objektverarbeitung innehat (Murray et al., 2007; Murray & Richmond, 2001). Ausgehend vom primären visuellen Kortex im Okzipitallappen nimmt die Komplexität der repräsentierten Eigenschaften entlang des ventralen visuellen Stroms zu, an dessen Spitze der PRC die komplexesten visuellen Analysen übernimmt. Solche Analysen ermöglichen es beispielsweise, Objekte mit ähnlichen Merkmalen voneinander zu differenzieren (z.B. ein Löwe von einem Tiger) oder zuvor betrachtete von neuen Objekten zu unterscheiden (Brown & Aggleton, 2001; Bussey et al., 2005). Dieses Modell wird sowohl durch Läsionsstudien als auch durch zahlreiche funktionelle MRT-Ergebnisse im menschlichen visuellen Verarbeitungssystem bestätigt (z.B. Lerner et al., 2001; Moss et al., 2005; Tyler et al., 2004). Vor diesem Hintergrund untersuchte Studie I mit einer neu entwickelten visuellen Diskriminationsaufgabe die Fähigkeit von Alzheimer-Patienten, aus einzelnen visuellen Merkmalen eine integrierte Wahrnehmungsrepräsentation zu erstellen (siehe Abbildung 3 für eine Beispielaufgabe). Die visuellen Reize wurden gemäss Gestalttheorie entwickelt, die Kriterien wie Nähe, Verbundenheit und ein klares Objekt-Hintergrund-Verhältnis berücksichtigen (Cate & Köhler, 2006; O'Neil et al., 2009; Palmer & Rock, 1994). Damit sollte sichergestellt werden, dass jede der sechs visuellen Reize als individuelles Objekt

wahrgenommen wird oder zumindest einer visuellen Repräsentation entspricht, für welche die Beteiligung des PRC benötigt wird. Entsprechend wird erwartet, dass Alzheimer-Patienten aufgrund reduzierter PRC-Integrität eine schlechtere Testleistung erzielen als Personen mit intaktem PRC. Ein solcher Test hat das Potential, noch früher als bisherige Instrumente, die ersten kognitiven Veränderungen der AK zu erfassen, ohne dass in diesem frühen Stadium andere Hirnareale die Defizite des PRC kompensieren können. Zudem erlaubt der Test eine kostengünstige sowie breit anwendbare und von soziokulturellen Faktoren (z.B. Sprache) unabhängige Anwendung.

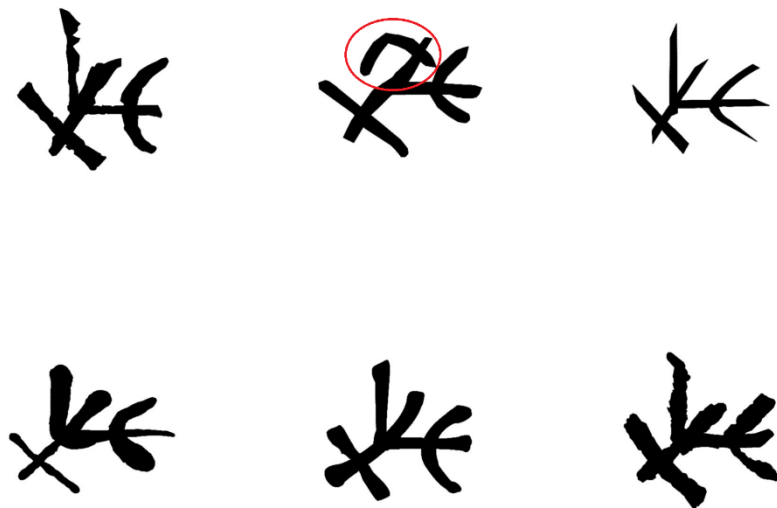


Abbildung 3. Beispielaufgabe der visuellen Diskriminationsaufgabe aus Studie I.

#### 1.4.2. Der mediale perirhinale Kortex – ein struktureller Marker

Wie eingehend erwähnt, wird der PRC bzw. der mPRC trotz früher Beteiligung in der Alzheimer-Pathologie sowohl in der Forschung als auch der Klinik mehrheitlich vernachlässigt. Ein Grund hierfür mag die anhaltende Debatte über die exakte anatomische Lokalisation des menschlichen PRC sein (Suzuki & Amaral, 2003). Braak und Braak (1985) führten erstmals die Bezeichnung "transentorhinale Region" für einen Übergangsbereich zwischen dem ERC und dem Neokortex ein. Ein Bereich, der laut Taylor und Probst (2008) dem mPRC entspricht. Charakteristisch für diese Region ist eine besondere Schicht schräg

verlaufender Pyramidenzellen, welche besonders empfindlich gegenüber neurofibrillären Veränderungen sind und der erste kortikale Entstehungsort von NFT in der typischen AK repräsentieren (Braak & Braak, 1985, 1991b). Kivisaari et al. (2013) beschrieben, basierend auf der zytoarchitektonischen Studie von Insausti et al. (1998), Orientierungspunkte für die Segmentierung von MTL-Subregionen (inklusive mPRC und IPRC) auf MRT-Schnittbildern. Ein solches Protokoll erlaubt eine getrennte Untersuchung von mPRC und IPRC, was entscheidend ist, da wie bereits erwähnt, der mPRC bei der AK früher von NFT betroffen ist als der IPRC. Dennoch haben nur sehr wenig Forschungsarbeiten, trotz verfügbarer manueller Segmentierungsprotokolle, eine solche Unterteilung vorgenommen (Kivisaari et al., 2013; Krumm et al., 2016). Ein bedeutendes Hindernis bei der Segmentierung dieser beiden Regionen ist die hohe inter- und intraindividuelle anatomische Variabilität des angrenzenden Sulcus collateralis. Das bedeutet, dass dieser Sulcus nicht nur zwischen verschiedenen Individuen stark variieren kann, sondern auch innerhalb derselben Person, sogar innerhalb einer einzelnen Hirnhemisphäre. Abbildung 4 zeigt, wie beispielsweise abhängig der Länge des Sulcus collateralis die anatomischen Grenzen des mPRC und IPRC variieren (Insausti et al., 1998; Taylor & Probst, 2008). Es ist wichtig zu betonen, dass die neurofibrilläre Taupathologie keinen Einfluss auf die zytoarchitektonischen Grenzen hat und auch nicht zu einer Verflachung von Sulci führt (z.B. Änderung der Länge). Stattdessen bewirkt sie eine Erweiterung der Sulci infolge der reduzierten kortikalen Dicke. Daher gelten die beschriebenen anatomischen Grenzen unabhängig von neurodegenerativen Prozessen und sind somit sowohl für Alzheimer-Patienten als auch für gesunde Personen oder im Kontext anderer Krankheitsprozesse anwendbar (Kivisaari et al., 2013; Taylor & Probst, 2008).

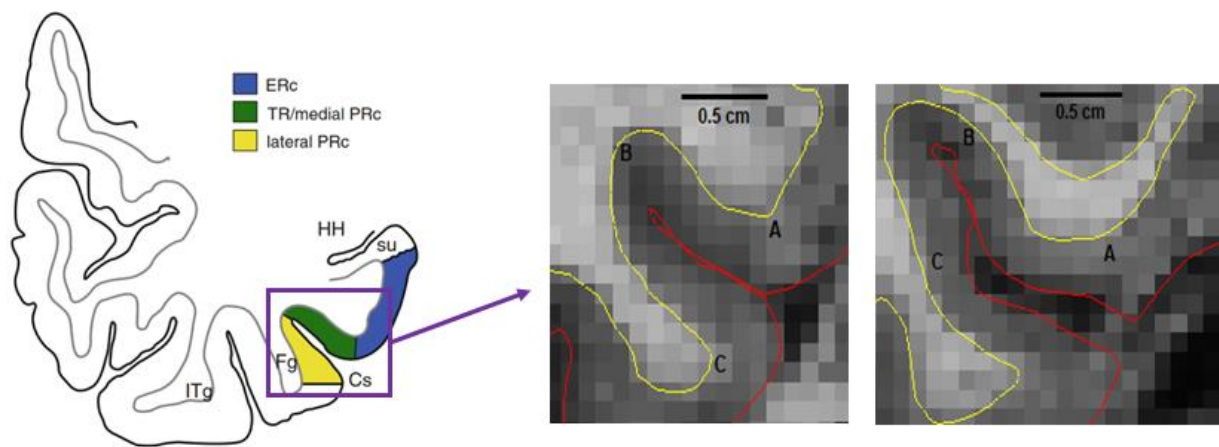


Abbildung 4. Links: Koronale Ansicht des rechten medialen Temporallappens (modifiziert von Kivisaari et al., 2013). Rechts: Zwei vergrösserte Ausschnitte des Sulcus collateralis (links: Länge < 1.5cm; rechts: Länge > 1.5cm) und deren Auswirkungen auf die Grenzen des mPRC und IPRC. (modifiziert von Studie II). Anmerkung. A. mediale Grenze des mPRC, B. laterale Grenze des mPRC/mediale Grenze des IPRC, C. laterale Grenze des IPRC. Für mehr Informationen siehe Studie II.

In der Arbeit von Krumm et al. (2016) wird das oben erwähnte manuelle Segmentierungsprotokoll, welches die Variabilität des Sulcus collateralis berücksichtigt, zusammengefasst. Es ist ausserdem eine der wenigen Publikationen, die den mPRC und IPRC im Kontext der AK getrennt untersucht haben. Sie wiesen nach, dass der mPRC und der ERC bei Patienten mit amnestischen MCI im Vergleich zu gesunden Kontrollen signifikant atrophiert waren. Der IPRC hingegen zeigte erst im Stadium der Alzheimer-Demenz signifikante Unterschiede (Krumm et al., 2016). Dieser Befund entspricht der oben beschriebenen hierarchischen Ordnung der NFT-Ausbreitung und unterstreicht erneut die Relevanz einer getrennten Bewertung von mPRC und IPRC im frühen Alzheimer-Stadium. Eine Beurteilung des gesamten PRC, wie es in den meisten Forschungsarbeiten der Fall ist, unterschätzt möglicherweise den Krankheitszustand (Braak & Braak, 1991b; Krumm et al., 2016). Eine Studie von Sone et al. (2017) ergab, dass Personen, die später ein MCI entwickelten, bereits viele Jahre zuvor eine signifikant verringerte kortikale Dicke des mPRC aufwiesen. Dies zeigt, wie wichtig eine präzise Segmentierung und Analyse der mPRC-Integrität (z.B. der kortikalen Dicke) für das Verständnis und die Früherkennung der AK ist.

Ein manuelles Segmentierungsprotokoll beschreibt anatomische Orientierungspunkte, welche einer Person erlauben, mithilfe spezialisierter Software (z.B. FreeSurfer; Reuter et al., 2012) auf MRT-Schnittbildern bestimmte Strukturen oder Bereiche zu identifizieren und abzugrenzen. Ein solches Protokoll sollte in Hinblick auf Standardisierung und Reliabilität überprüft werden, eine Aufgabe, welcher sich Studie II der vorliegenden Promotionsarbeit widmete. Das Ziel war die Beurteilung der Inter-Rater Reliabilität der manuellen Segmentierung von parahippocampalen Regionen (mPRC, IPRC und ERC) zwischen zwei Ratern. Dies ist eine wichtige Voraussetzung für solide wissenschaftliche Erkenntnisse und den Vergleich zwischen verschiedenen Studien. Die Zuverlässigkeit eines solchen manuellen Segmentierungsprotokolls ist zudem essentiell für die Entwicklung und Validierung automatisierter Segmentierungsmethoden (Wisse et al., 2021), eine Herausforderung, der sich Studie III annahm. Ein wichtiger Schritt, da die manuelle Segmentierung sehr zeitintensiv ist und für umfangreiche Datensätze oder den klinischen Einsatz schlichtweg nicht effizient genug ist. Fortschritte in Algorithmen und Rechenkapazitäten haben die Entwicklung verschiedener automatisierter Segmentierungstechniken für die MRT-Bildgebung vorangetrieben, darunter beispielsweise FreeSurfer (Reuter et al., 2012) oder Statistical Parametric Mapping (SPM; Ashburner & Friston, 2005). Darüber hinaus gewinnen Ansätze des maschinellen Lernens, die auf sogenannten künstlichen neuronalen Netzwerken («Convolutional Neural Networks») basieren, an Beliebtheit (Alzubaidi et al., 2021). Vor diesem Hintergrund befasste sich Studie III mit der Entwicklung eines automatisierten Segmentierungstools, basierend auf U-Net, einem Deep-Learning-basierten Softwarepaket, welches ursprünglich für die Segmentierung von Zellen in biomedizinischen Bildern entwickelt wurde (Ronneberger et al., 2015). Es bietet den Vorteil, dass es anhand einer «Ground Truth» (in diesem Fall die manuell segmentierten Label der parahippocampalen Regionen) trainiert und auf neue Daten angewendet werden kann. Zudem ist es konfigurierbar, was eine Adaption an spezifische Fragestellungen und Herausforderungen ermöglicht (Çiçek et al., 2016; Ronneberger et al., 2015). Um die Genauigkeit und einen möglichen klinischen Nutzen zu beurteilen, wurde das automatisierte Segmentierungsprotokoll genutzt, um die Ergebnisse der Studie von Krumm et al. (2016) mit derselben Stichprobe zu replizieren.



## 1.5. Hauptziele der vorgestellten Studien

Die vorliegende Dissertation zielte darauf ab, die Früherkennung der AK zu verbessern, indem sie neue Instrumente zur Bewertung der PRC-Funktion und der mPRC-Atrophie untersuchte. Im Zuge dessen wurden in den Studien I-III die folgenden spezifischen Forschungsfragen überprüft:

1. Ist ein neu entwickelter, spezifischer PRC-Funktionstest in der Lage, Patienten mit einer AK von gesunden Kontrollpersonen und Patienten mit einer Depression zu differenzieren? Welche Gehirnregionen korrelieren mit der Testleistung?
2. Erzielen zwei unabhängige Rater mithilfe eines manuellen Segmentierungsprotokolls für parahippocampale Regionen (mPRC, IPRC und ERC) konsistente Messergebnisse, beispielsweise in Bezug auf die kortikale Dicke?
3. Ist ein neu entwickeltes automatisiertes Segmentierungstool in der Lage, Messwerte für die kortikale Dicke parahippocampaler Regionen (z.B. mPRC und ERC) zu erzielen, die mit denen der manuellen Segmentierung vergleichbar sind, und ermöglicht es die Replikation der Ergebnisse der Studie von Krumm et al. (2016) mit derselben Stichprobe?

## 2. LISTE DER WISSENSCHAFTLICHEN ORIGINALPUBLIKATIONEN

Die vorliegende Promotionsschrift basiert auf den folgenden drei wissenschaftlichen Originalpublikationen:

- I. Frei, M., Berres, M., Kivisaari, S. L., **Henzen, N. A.**, Monsch, A. U., Reinhardt, J., Blatow, M., Kressig, R. W., & Krumm, S. (2023). Can you find it? Novel oddity detection task for the early detection of Alzheimer's disease. *Neuropsychology*, *37*(7), 717–740. doi:10.1037/neu0000859.
  
- II. **Henzen, N. A.**, Reinhardt, J., Blatow, M., Kressig, R. W., & Krumm, S. (2023). Excellent Interrater Reliability for Manual Segmentation of the Medial Perirhinal Cortex. *Brain Sciences*, *13*(6), Article 6. doi:10.3390/brainsci13060850.
  
- III. **Henzen, N. A.\***, Abdulkadir A.\*, Reinhardt, J., Blatow, M., Kressig, R. W., & Krumm, S. Automated segmentation for cortical thickness of the medial perirhinal cortex. *Eingereicht*.

\* Henzen N. A. and Abdulkadir A. contributed equally to this study and share first authorship.

## 2.1. Studie I

Can you find it? Novel oddity detection task for the early detection of Alzheimer's disease

# Can You Find It? Novel Oddity Detection Task for the Early Detection of Alzheimer's Disease

Marlen Frei<sup>1</sup>, Manfred Berres<sup>2</sup>, Sasa L. Kivisaari<sup>3</sup>, Nicolas A. Henzen<sup>1, 4</sup>, Andreas U. Monsch<sup>1, 4, 5</sup>, Julia Reinhardt<sup>6, 7, 8</sup>, Maria Blatow<sup>9</sup>, Reto W. Kressig<sup>1, 5</sup>, and Sabine Krumm<sup>1, 5</sup>

<sup>1</sup> University Department of Geriatric Medicine FELIX PLATTER, Basel, Switzerland

<sup>2</sup> Department of Mathematics and Technology, University of Applied Sciences Koblenz

<sup>3</sup> Department of Neuroscience and Biomedical Engineering, Aalto University School of Science

<sup>4</sup> Faculty of Psychology, University of Basel

<sup>5</sup> Faculty of Medicine, University of Basel

<sup>6</sup> Division of Diagnostic and Interventional Neuroradiology, Department of Radiology, University Hospital Basel, University of Basel

<sup>7</sup> Department of Cardiology and Cardiovascular Research Institute Basel, University Hospital Basel, University of Basel

<sup>8</sup> Department of Orthopedic Surgery and Traumatology, University Hospital of Basel, University of Basel

<sup>9</sup> Section of Neuroradiology, Department of Radiology and Nuclear Medicine, Neurocenter, Cantonal Hospital Lucerne, University of Lucerne

**Objective:** We aimed to develop a measure to specifically assess the functioning of the perirhinal cortex (PRC), a brain structure affected very early in Alzheimer's disease (AD) pathology. In this novel task, participants were shown arrays of six complex figures and had to identify the "odd-one." **Method:** The pilot study included 50 normal controls (NCs) and 50 patients in very early stages of AD. Participants completed the task and received MRI scanning. Best differentiating items were determined and applied in a validation study including 25 NCs, 27 early-stage AD patients, and 26 patients with major depression. Logistic regression models investigated if task performance predicted group membership. Task performance was then related to whole-brain gray matter integrity. As proof of concept, cortical thickness values of four regions of interest (ROIs; e.g., medial PRC and entorhinal cortex [ERC]) were compared between the groups. The associations of task performance and cortical thickness of the ROIs were investigated using linear models. **Results:** Task performance showed good discriminative ability between early-stage AD patients and NCs. Whole-brain analyses revealed four significant clusters ( $p < .001$ ) with peak voxels in parahippocampal regions including PRC and ERC. ROI analyses showed distinctly reduced cortical thickness in the AD group compared to both other groups in the medial PRC and ERC ( $p \leq .001$ ). Task performance modeled by ROI cortical thickness did not achieve significant results. **Conclusion:** Although further validation is needed, especially with age-matched participant groups, these findings indicate that the task detects early cognitive impairment related to AD.

Marlen Frei  <https://orcid.org/0000-0002-6218-391X>

Sabine Krumm  <https://orcid.org/0000-0001-6362-699X>

This study was supported by a Grant from the Alfred and Anneliese Sutter-Stöttner Foundation (Andreas U. Monsch and Sabine Krumm). The pilot study was supported by a Grant from the Swiss National Science Foundation (Ambizione fellowship PZ00P1\126493) awarded to Kirsten I. Taylor. The authors have no conflicts of interest to disclose and confirm that the work is original and has not been published elsewhere, nor is it currently under consideration for publication elsewhere. This study's design and its analysis were not preregistered. All analysis code and research materials as well as metadata and/or full data are available upon request. The authors thank Kirsten I. Taylor, who is the principal investigator of the pilot study, developed the novel oddity detection task together with Sasa L. Kivisaari, and who let us use the pilot data set for our analyses.

Marlen Frei played lead role in writing of original draft, supporting role in conceptualization, data curation, formal analysis and investigation and equal role in methodology, visualization and writing of review and editing. Manfred Berres played lead role in formal analysis and supporting role in methodology, visualization, writing of original draft and writing of review

and editing. Sasa L. Kivisaari played supporting role in writing of review and editing and equal role in conceptualization, project administration and software. Nicolas A. Henzen played lead role in writing of review and editing, supporting role in writing of original draft and equal role in methodology and visualization. Andreas U. Monsch played supporting role in writing of review and editing and equal role in funding acquisition, resources and supervision. Julia Reinhardt played supporting role in writing of review and editing and equal role in conceptualization, investigation, methodology and software. Maria Blatow played supporting role in conceptualization and writing of review and editing and equal role in methodology and resources. Reto W. Kressig played supporting role in supervision and writing of review and editing and equal role in resources. Sabine Krumm played lead role in data curation, supporting role in resources, visualization and writing of original draft and equal role in conceptualization, formal analysis, funding acquisition, investigation, methodology, project administration, software, supervision and writing of review and editing.

Correspondence concerning this article should be addressed to Sabine Krumm, University Department of Geriatric Medicine FELIX PLATTER, Burgfelderstrasse 101, Basel CH-4055, Switzerland. Email: [sabine.krumm@felixplatter.ch](mailto:sabine.krumm@felixplatter.ch)

**Key Points**

**Question:** This study examines whether a novel neuropsychological task, developed to specifically assess the functioning of the brain structures affected very early in Alzheimer's disease (AD), can discriminate patients in early stages of AD from healthy adults. **Findings:** AD patients showed distinct lower performance in the discrimination task compared to healthy adults and task performance was associated with gray matter integrity in areas including the perirhinal and entorhinal cortex. **Importance:** It supports the use of functional and structural measures of the perirhinal and entorhinal cortex for the early detection of AD and its differentiation from other etiologies of cognitive impairment. **Next Steps:** Further validation of this task, especially with age-matched participant groups, could contribute to refining the detection of early-stage AD and expand opportunities for targeted therapeutic intervention.

**Keywords:** Alzheimer's disease, perirhinal cortex, early diagnosis, visual discrimination, neuroimaging

The detection of cognitive impairment in very early stages of Alzheimer's disease (AD) is still a challenge in clinical practice since first signs of impending AD can be very subtle. One major neuropathological characteristic of AD is intracellular neurofibrillary tangles, which typically start in the medial part of the perirhinal cortex (PRC) within the parahippocampal gyrus of the medial temporal lobe (MTL). The progressive deposition of neurofibrillary tangles is associated with cortical thinning in these regions (Braak & Braak, 1991; Sone et al., 2017; Taylor & Probst, 2008). Thus, we developed a task based on models of PRC functioning to detect the earliest stage of AD (i.e., when tau pathology has not yet disrupted brain functions in a way that causes impairment of everyday functionality).

The parahippocampal gyrus can be subdivided into the PRC (Brodmann areas 35/36), entorhinal cortex (ERC; Brodmann areas 28/34), and parahippocampal cortex (PHC; Brodmann area 36) based on their cytoarchitectural features (Insausti et al., 1998; Van Hoesen, 1995). The progression of neurofibrillary tau pathology in AD typically begins in the medial perirhinal cortex (mPRC), also referred to by Braak and Braak (1991) as the transentorhinal cortex (Taylor & Probst, 2008). It then progresses on to Layers II and IV of the ERC, hippocampus (limbic stages), and temporal neocortex (Braak & Braak, 1991, 1995; Braak et al., 2006). Regional neurofibrillary deposition in early-stage AD has indeed been associated with cortical thinning in the PRC and ERC, but not in hippocampal subfields (Sone et al., 2017). Still, past efforts to identify early functional-neuroanatomic markers of AD have mostly focused on episodic memory impairment, which is associated with atrophy in hippocampal regions (Naylor et al., 2012; Perri et al., 2007; Sarazin et al., 2007). Episodic memory impairment is, however, a shared symptom between AD and major depression (MD). In clinical practice, such overlapping cognitive symptoms between MD and AD (i.e., episodic memory impairment, executive functions, attention) hamper the distinction between cognitive impairment related to MD from those associated with early stages of AD and may lead to misdiagnosis (Christensen et al., 1997; Rotomskis et al., 2015). Yet, for MD there is little evidence of PRC neurodegeneration (Bocchia et al., 2015; Tsopelas et al., 2011). Therefore, testing the functions of the first areas affected by neurofibrillary pathology (i.e., PRC and ERC) might allow differentiation between the two pathologies in very early stages of AD (Buerger et al., 2003).

The PRC is involved, among others, in visual discrimination of complex objects that are ambiguous, meaning that their low-level

features have a high degree of perceptual overlap (Barens et al., 2012). The representational-hierarchical account posits that the PRC constitutes the apex of the ventral visual stream processing pathway, coding for the most highly integrated complex representations of objects (Cowell et al., 2010). As a result, the PRC provides a representation of complex feature conjunctions (Murray et al., 2007), or of object characteristics in line with Gestalt principles (Cate & Köhler, 2006; O'Neil et al., 2009). Such representations that are more integrated than representations by the posterior ventral visual stream, take a central role when individual features or simple conjunctions of features are not sufficient for object discrimination (O'Neil et al., 2013).

In support of this notion, a multivoxel pattern analysis by Erez et al. (2016) indicated that the PRC codes information regarding an object's feature conjunctions over and above the simple sum of its individual features. Therefore, when PRC integrity is reduced, object discrimination relies on more posterior ventral stream regions coding for simple features shared by many objects (Bussey et al., 2002; Bussey & Saksida, 2002, 2007). Evidence supporting this account has mostly been provided by animal studies that associated PRC abnormalities with impaired ability to discriminate and recognize complex objects while leaving lower level visual processes relatively intact (Bartko et al., 2007; Bussey et al., 2002; McTighe et al., 2010).

Visual object discrimination tasks with minimal or no demand on memory have been applied in humans with brain lesions extending into the PRC (Barens et al., 2005, 2007; Lee & Rudebeck, 2010). Tasks mostly included visual matching paradigms, where the participant has to decide whether trial-unique objects are same or different (Barens et al., 2005), or oddity detection tasks, where the figure that is different from the others has to be detected (Barens et al., 2007). Results revealed that damage to the PRC is indeed associated with difficulties in object discrimination and, most notably, in disambiguating complex objects that are perceptually similar by sharing many features. Importantly, converging evidence from functional MRI (fMRI) studies found the PRC to be active during these paradigms of object matching (Barens et al., 2012; Ryan et al., 2012) and oddity detection (Barens et al., 2011; Lawrence et al., 2020). In the same vein, nonmnemonic object discrimination tasks have been administered to participant groups in various stages of AD-related disease progression. Subjects at risk for AD as well as patients with mild cognitive impairment (MCI), and patients with Alzheimer's dementia were found to have reduced discrimination ability, particularly when the presented objects had

highly overlapping features (Gaynor et al., 2019; Mason et al., 2017). Moreover, a study by Newsome et al. (2012) presented MCI patients with objects that had similar features, leading to high interference of low-level representations. MCI patients were impaired at discriminating ambiguous objects, but their performance improved when the degree of interference between objects was reduced. These findings are in line with the representational-hierarchical account, suggesting, that to resolve the interference of irrelevant, low-level features (e.g., features that are shared between many objects), the ability to maintain an integrated object representation is required. Thus, testing the capacity to form an integrated perceptual representation from similar low-level visual features in a complex object discrimination task may indeed be an early neurocognitive marker for AD.

Nonetheless, there are limitations to the studies outlined above. There are only few studies with AD patients that have directly linked performance on nonmnemonic tasks to brain integrity through neuroimaging (i.e., Delhaye et al., 2019), and most importantly, none has specifically investigated the earliest neurofibrillary pathology site, the mPRC. Previous studies have manipulated ambiguity either by comparing different kinds of stimuli thought to be more or less ambiguous (i.e., faces vs. greebles in Mason et al., 2017), or mental rotation between the stimuli (i.e., Gaynor et al., 2019), or by changing the number of distinctive features that visually differed in their appearance (Newsome et al., 2012). Other developments have, however, proposed that areas corresponding to the mPRC are involved in *spatial arrangement* processing within objects (Knierim et al., 2014). A study by Yeung et al. (2017) evaluated intra-item configural processing in a group of older adults at the earliest stages of cognitive decline. Results indicated that attention to the spatial arrangement and properties of an object's features was predicted by anterolateral ERC volume. Importantly, this region overlaps significantly with the regions described as the mPRC by Kivisaari & Taylor (2012). Thus, the extent to which the anterolateral ERC overlapped with regions of the mPRC might explain its role in configural processing. Taken together, it seems highly promising to apply spatial manipulation within nonmnemonic object discrimination paradigms to detect earliest changes in cognitive processing that are mediated by the mPRC, known to exhibit early neurofibrillary pathology in AD.

Although the role of the PRC in discriminating spatial arrangement *between* objects has been investigated in healthy adults (Lawrence et al., 2020), to our knowledge, the present study is the first to manipulate the spatial arrangement *within* objects to assess PRC functioning as an early neurocognitive marker of AD. We developed a novel oddity detection task that tested participants' ability to choose the "odd-one", the figure that differed most from the other five highly complex figures. Thereby, two concurrent factors that are necessary for PRC recruitment were considered in the development of the visual discrimination task: First, stimuli require common features that are shared between them in a way that they are processed at the level of feature conjunctions or even more highly integrated object representations. Second, a visual discrimination task must be created such that it requires the usage of these complex representations for successful distinction and not just simple features supported by the ventral visual stream (Cowell et al., 2010). Against this theoretical background, figures in our discrimination task were not only created from the same features that were arranged in different ways but also comprised of a high number

of features leading to a high degree of feature ambiguity. Thus, it is necessary to extract an integrated figure representation to solve the task (Newsome et al., 2012). Moreover, the visual stimuli used in the present study were created in line with important classical principles of Gestalt theory, including proximity, connectedness (Palmer & Rock, 1994), and a distinct object-to-ground relationship. This ensures that each of the six visual stimuli is perceived as an individual object or at least complies with the level of conjunctions needed for PRC involvement (Cowell et al., 2010; Wagemans et al., 2012). Last, we intended to develop a cognitive measure for AD, that is affordable and broadly applicable as well as independent of sociocultural factors (e.g., nonverbal; Parra, 2022).

The main objective of this study was to develop and validate a novel neuropsychological instrument for early diagnosis of AD that additionally may support differential diagnosis with other etiologies, such as MD. Based on models of PRC functioning, a novel oddity detection task was designed to assess the capacity to form an integrated and complex perceptual representation from separate visual features. Neuropsychological testing and MRI were applied in samples of older adults. In a pilot study, we investigated which stimuli components differentiated best between healthy older adults and patients in very early stages of AD. Furthermore, test performance was related to whole-brain gray matter integrity to inform neuroanatomical hypotheses for the validation study. After test adaptation based on the pilot study, the validation study assessed whether this novel task could individually predict group membership of patients with early AD relative to cognitively healthy normal controls (NCs) and relative to MD patients. Further, task performance was related to whole-brain gray matter integrity and to assess whether results of the pilot study could be replicated after improvement of the discrimination task. As proof of concept that cortical thinning of neuroanatomical regions of interest (ROIs) within the MTL, including the mPRC, lateral PRC (IPRC), ERC, and PHC, is specific to the AD group, cortical thickness values were compared between participant groups. Further, task performance was related to whole-brain gray matter integrity to assess whether results of the pilot study could be replicated after improvement of the discrimination task. Last, the neuroanatomical hypotheses based on results of the pilot study were tested by relating task performance to cortical thickness of the four ROIs to disentangle their individual contributions.

## The Pilot Study

### Method of the Pilot Study

#### Participants

Data sets of 100 native Swiss-German or German-speaking adults were evaluated. Written informed consent was obtained from all individuals prior to participation and the study was approved by the local ethics committee (Ethikkommission Nordwest- und Zentralschweiz [EKNZ]). The sample consisted of 50 individuals with very early AD, namely 25 patients with amnesic mild cognitive impairment (aMCI), presumed to be in the prodromal phases of AD (Petersen et al., 2006) as well as 25 mildly affected AD patients. Diagnosis of aMCI was made according to the *Diagnostic and Statistical Manual of Mental Disorders, Fourth Edition (DSM-IV;* American Psychiatric Association, 1994) and Winblad et al. (2004) criteria. Alzheimer's dementia was diagnosed according to National Institute of Neurological and Communicative Diseases and

Stroke/Alzheimer's Disease and Related Disorders Association (NINCDS-ADRDA; McKhann et al., 2011) and *DSM-IV* criteria (American Psychiatric Association, 1994). During the diagnostic process, patients received a comprehensive neuropsychological assessment, medical examination, gait analysis, structural MRI, and evaluation of informant questionnaires. Some patients had additional positron emission tomography scans and/or investigation of cerebrospinal fluid measures. All patients were diagnosed in an interdisciplinary consensus conference at the Memory Clinic of the University Department for Geriatric Medicine FELIX PLATTER, Basel, Switzerland. Additionally, 50 NCs were recruited from the Memory Clinic's "Registry of Healthy Individuals Interested to Participate in Research" and matched to the AD group regarding age and education. They had filled out a comprehensive medical questionnaire and undergone extensive neuropsychological testing to ensure that they were cognitively healthy (i.e., neurologically and psychiatrically). Specifically, they had all received normal scores on the Mini-Mental State Examination (MMSE; Folstein et al., 1975), Clock Drawing Test (Thalman et al., 2002), 15-item version of the Boston Naming Test (Kaplan et al., 1978), and the Basel Verbal Learning Test (BVL), and the German equivalent to the California Verbal Learning Test (Delis et al., 1987). All tests were administered in German. Sample characteristics are depicted in Table 1.

### Stimuli Creation and Procedure

Six analogous sets of 17 features using existing letter fonts from an online database (Urban Fonts; <http://www.urbanfonts.com>) were created. Features corresponded to brush strokes manually extracted from letters and symbols and included short and long lines, hooks, and points. Six different fonts were used so that the corresponding individual features (e.g., hook) were perceptually different yet similar in form. Between two and seven of these individual features were combined (number of features [NOF]) to form 74 different Kanji-like figures that contained no apparent meaning. One figure per trial was presented in six different fonts in a  $3 \times 2$  grid. Within each trial, one or two features, referred to as distinctive features (i.e., number of distinctive features [NODF]), were altered in one figure to create the target stimulus, the "odd-one."

Participants completed a practice session (20 trials) for which they received accuracy feedback, before the evaluated task with no more accuracy feedback began (54 trials). Stimuli were shown on a touch screen device using the E-prime 2.0 software. Each trial

started with 1,000 ms silence. Afterward, the participants' task was to tap the target stimulus that was the most different out of the six figures (i.e., the "odd-one") as fast as possible (max. 20,000 ms). In the evaluated task ( $n = 54$  stimuli), the distinctive feature of the target stimulus was manipulated to be different in (a) location only (18 items), (b) type of feature (18 items), or (c) location and type of the distinctive feature (18 items). See Figure 1 for example trials. We assumed that items with high NOF would be more difficult than items with low NOF while items with low NODF would be more difficult than items with high NODF. For items with 2, 3, or 4 NOF we showed six items each with NODF = 1. For items with 5, 6, or 7 NOF we presented six items each with NODF = 1 and six items each with NODF = 2. Font and place of the target figure were approximately counterbalanced across trials. All participants received the same sequence of trials. Responses and reaction times were recorded by the software.

### MRI Measures

**Acquisition and Preprocessing.** The average time interval between diagnostic neuropsychological testing and MRI was 31 days ( $SD$  26). One aMCI participant did not get an MRI scan. All other participants received MRI scanning on the same 3-Tesla scanner (MAGNETOM Verio, Siemens) at the University Hospital in Basel (12 channel headcoil; T1-weighted 3D magnetization-prepared rapid gradient echo imaging [MPRAGE]; inversion time = 1,000 ms; repetition time = 2000 ms; echo time = 3.37 ms; flip angle =  $8^\circ$ ; field of view =  $256 \times 256$ ; acquisition matrix =  $256 \times 256$  mm, voxel size = 1 mm isotropic). Total intracranial volumes (TIV; i.e., the sum of gray matter, white matter, and CSF volumes) were obtained using SPM8 (Wellcome Institute of Cognitive Neurology, [www.fil.ion.ucl.ac.uk](http://www.fil.ion.ucl.ac.uk)) implemented in MATLAB R2010b (Mathworks Inc., Sherborn, Massachusetts, USA).

**Whole-Brain Voxel-Based Morphometry.** T1 MPRAGE images were preprocessed using the DARTEL method (Ashburner, 2007) using SPM8 (Wellcome Institute of Cognitive Neurology, [www.fil.ion.ucl.ac.uk](http://www.fil.ion.ucl.ac.uk)) implemented in MATLAB 2010 (Mathworks Inc., Sherborn, Massachusetts, USA). The anterior commissure was manually set at the origin of the three-dimensional Montreal Neurological Institute (MNI) coordinate system. Images were then automatically segmented into gray matter, white matter, and cerebrospinal fluid volumes, coregistered to the DARTEL template and normalized to MNI space, modulated, and smoothed with an 8 mm full-width at half-maximum Gaussian kernel. Manual correction of gray/white matter voxel misclassifications was skipped, based on the results of Hartmann et al. (2021).

### Analyses

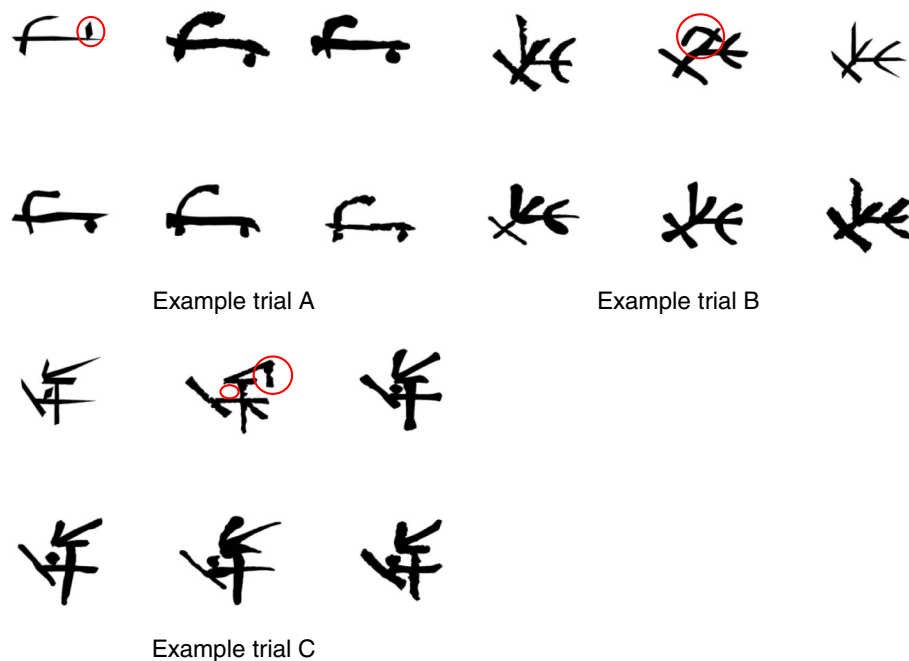
To find the variables that best discriminate between diagnostic groups, we performed mixed-effects logistic regressions of all individual responses. Response was either correct (right answer), commission (wrong answer), or omission (no answer). Predictors are diagnosis, one experimental condition (i.e., font, location, distinctive feature type, NOF, NODF, and a combination of NOF and NODF [NOF.NODF; e.g., 5 NOF with 1 NODF, 6 NOF with 2 NODF]), and the two-way interaction. Based on the behavioral results, voxel-based regression analyses were conducted to relate behavioral measures (i.e., %correct = [number of correct answers]/

**Table 1**  
*Sample Characteristics of the Pilot Study*

Variable	NCs ( $N = 50$ )		aMCI ( $N = 25$ )		Alzheimer's dementia ( $N = 25$ )	
	29/21		12/13		10/15	
Gender (m/f)	<i>M</i>	<i>SD</i>	<i>M</i>	<i>SD</i>	<i>M</i>	<i>SD</i>
Age (years)	75.0	5.71	74.6	8.20	77.3	4.98
Education (years)	12.6	2.77	13.6	3.34	12.4	2.77
MMSE score	29.3	0.76	28.7	1.10	26.2	1.73

*Note.* NCs = normal controls, aMCI = amnesic mild cognitive impairment; m = male; f = female; MMSE = Mini-Mental State Examination.



**Figure 1***Example Trials From the Pilot Study*

*Note.* Three example trials from the pilot study with the different features circled. Figures in example Trial A are comprised of three features with the target figure showing one distinctive feature located in a different space within the figure (spatial type). Figures in example Trial B are comprised of five features with the target figure showing one distinctive feature with a different shape (feature type). Figures in example Trial C are comprised of seven features with the target figure showing two distinctive features, namely one spatial and one feature type. See the online article for the color version of this figure.

100 and %commissions = [number of wrong answers]/100 for distinctive feature type and NOF) to whole gray matter integrity (covariate: TIV) using a general linear model approach in SPM8 (Wellcome Institute of Cognitive Neurology, www.fil.ion.ucl.ac.uk). No masking was applied, and groups were examined in the same model. One aMCI subject did not have an MRI scan and was, thus, not analyzed in the Whole-Brain Voxel-Based Morphometry (VBM) approach. All mappings were thresholded at  $p < .001$  or  $p < .01$  uncorrected at the voxel level and clusters surviving a random-field corrected  $p < .05$  are reported in MNI space. %omissions showed great inconsistencies and a floor effect was apparent as some participants responded to every trial and therefore had no omissions. Due to the rare occurrence of omissions, %commissions was almost complementary to %correct (%commissions  $\approx 100 - \%correct$ ) and was not further analyzed in the validation study. Additionally, %omissions did not appear like a reliable measure and were excluded from all subsequent analyses in the pilot study and the validation study.

### Transparency and Openness

Data were analyzed using R, Version 4.0.0 (R Core Team, 2020) and the package lme4, Version 1.1-23. This study's design and its analyses were not preregistered. All analyses code and research materials as well as metadata and/or full data are available upon request.

## Results of the Pilot Study

### Results of Behavioral Analyses

Analyses of performance in the oddity detection task did not reveal a need for test amendment regarding font, location, or NODF level of the odd item (see Appendix Tables A1–A3 and Figures A1–A3). For items with NOF levels 2, 3, and 4, patients diagnosed with aMCI and Alzheimer's dementia performed relatively similarly, indicating that items with NOF levels 5, 6, and 7 might differentiate better between groups (see Appendix Table A4 and Figure A4). Analyses of the combination of NOF and NODF (NOF.NODF) suggested that items with 5 or 6 NOF and 1 NODF as well as items with 7 NOF and either 1 or 2 NODF are especially promising to differentiate between diagnostic groups (see Appendix Table A5 and Figure A5). Further, variation of a single feature type (i.e., spatial or feature) seemed to be significantly more difficult (i.e., participants had lower %correct scores) than if both types were combined (spatial only compared to both combined types:  $\beta = -0.4240$ ,  $z = -3.65$ ,  $p = .00026$ ; feature only compared to both combined types:  $\beta = -0.7454$ ,  $z = -6.55$ ,  $p = 5.8e^{-11}$ ).

### VBM

Based on the results of behavioral analyses of the pilot study, we only investigated NOF and feature type variation using VBM. We did not examine NOF.NODF, because based on the behavioral



**Table 2**

*Significant Results of Brain–Behavioral Analyses for Distinctive Feature Type Variation and %Correct at Threshold  $p < .001$  in the Pilot Study*

Anatomical region	Side	MNI coordinates Peak voxel			Cluster size (kE)	$p$ (FWE-corr)
		$x$	$y$	$z$		
Feature variation						
Precuneus	Right	14	-47	57	6,006	.001
Insula	Right	31	-15	21	3,160	.040
Spatial variation						
Medial temporal lobe	Left	-45	6	-31	4,007	.014
Frontal medial orbital region	Left	-11	60	0	5,320	.003
Insula	Right	34	7	10	3,854	.017

*Note.* MNI = Montreal Neurological Institute and Hospital; FWE-corr = family-wise-error corrected.

results of the pilot study we assumed that NOF has a substantially bigger impact on NOF.NODF than NODF. For distinctive feature type, we found significant clusters at  $p < .001$  threshold for % correct in the right precuneus and the right insula when the feature type was varied and in the left MTL, left frontal medial orbital region, and right insula when the spatial location of the distinctive feature was varied (see Table 2). Notably, the cluster in the left MTL comprised the parahippocampal gyrus including medial and

lateral perirhinal cortex. No significant brain–behavioral correlations at threshold  $p < .001$  or  $p < .01$  were found when both types (i.e., spatial and feature) were combined and there were no significant clusters for %commissions for any feature type variation at threshold  $p < .001$  or  $p < .01$ .

For %correct and NOF2, we found a significant cluster at threshold  $p < .001$  in the right cerebellum crus 1. At threshold  $p < .01$  we found six significant clusters comprising bilateral parahippocampal gyrus. Peak voxels of the clusters were near the right middle frontal gyrus, in the left and right cerebellum, right cerebellum crus 1, and left and right superior frontal regions. For NOF3 and NOF4 we did not find any significant clusters at threshold  $p < .001$  or threshold  $p < .01$ . Analyses for %correct and NOF5 revealed three significant clusters with peak voxels in the left medial superior frontal lobe, right supraorbital frontal gyrus, and the right insula at threshold  $p < .001$ . Further, at threshold  $p < .01$  we found seven significant clusters with peak voxels in the left medial superior frontal lobe, the left inferior temporal lobe (comprising the left parahippocampal gyrus), right supraorbital frontal gyrus, left middle temporal lobe, right insula, and one cluster each near the right precentral gyrus and near the left inferior parietal lobe. For NOF6 we found one significant right hemispheric cluster with peak voxel in the putamen at threshold  $p < .001$  and four significant clusters at threshold  $p < .01$  with peak voxels in the left medial superior frontal lobe, right precuneus, right putamen, and one cluster near the left pallidum. Finally, for NOF7 and %correct there was no significant cluster at threshold  $p < .001$ , but one at threshold  $p < .01$  in the left inferior temporal lobe (comprising the parahippocampal gyrus). Please see Table 3, for more details.

**Table 3**

*Significant Results of Brain–Behavioral Analyses for NOF Level and %Correct in the Pilot Study*

NOF level	Anatomical region	Side	MNI coordinates Peak voxel			Cluster size (kE)	$p$ (FWE-corr)
			$x$	$y$	$z$		
Threshold $p < .001$							
NOF2	Cerebellum crus 1	Right	32	-64	-36	3,804	.018
NOF5	Medial superior frontal lobe	Left	-14	55	6	8,873	<.001
NOF5	Supraorbital frontal gyrus	Right	16	61	-3	6,333	.001
NOF5	Insula	Right	34	-8	13	5,048	.004
NOF6	Putamen	Right	27	9	9	3,541	.025
Threshold $p < .01$							
NOF2	Undefined voxel near the middle frontal gyrus	Right	31	39	18	19,934	.001
NOF2	Cerebellum	Left	-10	-43	-9	24,997	<.001
NOF2	Superior frontal regions	Left	-20	12	47	14,246	.009
NOF2	Cerebellum	Right	18	-41	-14	10,414	.050
NOF2	Cerebellum crus 1	Right	32	-64	-36	19,412	.001
NOF2	Superior frontal regions	Right	19	4	66	12,966	.016
NOF5	Medial superior frontal lobe	Left	-14	55	6	33,183	<.001
NOF5	Inferior temporal lobe	Left	-44	5	-32	13,942	.010
NOF5	Supraorbital frontal gyrus	Right	16	61	-3	19,942	.001
NOF5	Insula	Right	34	-8	13	17,305	.002
NOF5	Undefined voxel near the precentral gyrus	Right	27	-3	44	15,713	.005
NOF5	Undefined voxel near the inferior parietal lobe	Left	-24	-44	48	12,755	.017
NOF5	Middle temporal lobe	Left	-46	-42	11	11,548	.029
NOF6	Medial superior frontal lobe	Left	-13	58	3	13,567	.012
NOF6	Undefined voxel near pallidum	Left	-11	3	-10	16,306	.004
NOF6	Precuneus	Right	14	-48	57	11,295	.033
NOF6	Putamen	Right	27	9	9	18,557	.002
NOF7	Inferior temporal lobe	Left	-52	-30	-21	18,536	.001

*Note.* MNI = Montreal Neurological Institute and Hospital; FWE-corr = family-wise-error corrected; NOF = number of features.

Our analyses for %commissions did not reveal any significant cluster at threshold  $p < .001$  for NOF2 but one at threshold  $p < .01$  in the right cerebellum crus 1 (MNI peak voxel coordinates:  $x = 27$ ,  $y = -66$ ,  $z = -35$ ; cluster size = 11,410 kE,  $p$  [FWE-corr] = .031). For NOF3, NOF4, NOF5, NOF6, and NOF7, we did not find any significant cluster at any threshold level for %commissions.

## Discussion of the Pilot Study

We aimed to develop a measure to assess the functioning of the PRC, a brain structure affected very early in AD pathology (Braak & Braak, 1991; Krumm et al., 2016). Based on models of PRC functioning, our study introduces a novel nonmnemonic visual oddity detection task, designed to assess the capacity to form an integrated and complex perceptual representation from separate visual features. Neuropsychological testing and MRI were applied in samples of older adults. In a pilot study, we investigated which stimuli components differentiated best between healthy older adults and patients in very early stages of AD. Results revealed that the ratio of NOF comprising the figures to the NODF of the target figure had a significant impact on performance. Furthermore, items with 5 or 6 NOF and 1 NODF as well as items with 7 NOF and either 1 or 2 NODF were found to be most promising in differentiating between diagnostic groups. Items with a single feature variation (i.e., spatial or feature variation) were significantly more difficult than items that combine both feature variations (i.e., spatial and feature variation). For items with spatial variation of the distinct feature, the VBM showed a significant cluster in the left MTL, comprising the parahippocampal gyrus. Feature variation on the other hand was correlated with other regions, such as the right precuneus and right putamen. Since neurofibrillary tangle accumulation in typical AD starts in the mPRC and ERC of the parahippocampal gyrus (Braak & Braak, 1991), the subsequently built test (i.e., the test used in the validation study) only used a spatial variation of the distinct feature. Furthermore, because the AD group showed similar results for items with NOF levels 2, 3, and 4, the test was further modified to only include items with NOF levels 5, 6, and 7.

As mentioned above, successful PRC recruitment depends on visual discrimination tasks with common features between stimuli, thereby processing them at the level of conjunctions or even more integrated object representations. AD patients, which typically show very early PRC degeneration, are expected to exhibit greater difficulties to make successful distinctions based on those representations, as they may have to resort on simpler features supported by the posterior ventral visual stream. In our pilot study, the latter approach might have been sufficient to successfully solve the task when NOF was low. Therefore, we decided to only include items with NOF levels 5, 6, and 7 for the test subsequently used in the validation study. In the same vein, results of the pilot study regarding spatial versus feature variation of items might also be contributed to less shared features between stimuli leading to decreased difficulty of items when one of the features was different. In comparison to spatial variation of items, the results of the VBM for items with feature variation in the pilot study did not show a significant cluster in the MTL. It is possible, that feature variations disrupted the similarity of the stimuli to the extent that recruitment of the PRC was no longer necessary to successfully discriminate between stimuli. Thus, we decided to only use spatial variation of the distinct feature in the test used in the validation study.

## The Validation Study

### Hypotheses of the Validation Study

The results of the pilot study as described above were used to inform revisions of neuroanatomical hypotheses. First, the VBM was not run for each NOF level (e.g., 5, 6, and 7) separately, but rather conducted for an aggregated score of correct answers in the discrimination task. Second, as proof of concept that cortical thinning in MTL subregions (e.g., mPRC, ERC) is specific to the AD group, cortical thickness of four a priori defined ROIs (mPRC, IPRC, ERC, and PHC) were compared between groups. Third, task performance was related to the cortical thickness of the four ROIs to disentangle their individual contributions. Informed by the results of the pilot study primary analysis focused on cortical thickness values from the left hemisphere of the four ROIs (left mPRC, left IPRC, left ERC, and left PHC). Secondary analysis included all cortical thickness values from the right hemisphere as well as cortical volumes of all ROIs from both hemispheres.

### Method of the Validation Study

#### Participants

The validation study collected data from 78 native Swiss-German or German-speaking adults including 25 NCs, 27 patients with AD, and 26 patients with MD. Cognitively healthy NCs were recruited from the "Registry of Healthy Individuals Interested to Participate in Research" of the Memory Clinic University Department of Geriatric Medicine FELIX PLATTER Basel, Switzerland. Written informed consent was obtained from all individuals prior to participation and the study was approved by the local ethics committee (EKNZ: Ethikkommission Nordwest- und Zentralschweiz). Thorough medical screening ensured their neurologic and psychiatric health (exclusion criteria: severe sensory or motor deficits; severe auditory, visual or speech deficits; severe systemic disease; diseases with severe or probable impact on the central nervous system [e.g., neurologic disorders including cerebral-vascular disease, generalized atherosclerosis, and psychiatric problems]; continuous mild-to-intense pain; and intake of potent psychoactive substances except minor tranquilizers). NCs were allowed no more than one out of normal range score in the MMSE (Folstein et al., 1975), BVL (Delis et al., 1987), Trail Making Test B (Reitan, 1958), or the 16-item version of the Informant Questionnaire on Cognitive Decline in the Elderly (Jorm et al., 1989). All tests were administered in German. Eight participants were diagnosed with aMCI (Albert et al., 2011) according to *DSM-IV* (American Psychiatric Association, 1994) and Winblad et al. (2004) criteria and 19 participants were diagnosed with early Alzheimer's dementia according to *DSM-IV* criteria (American Psychiatric Association, 1994), and NINCDS-ADRDA (McKhann et al., 2011) were also recruited from the Memory Clinic FELIX PLATTER. Participants diagnosed with aMCI and Alzheimer's dementia were combined to one group as the progression from aMCI to early stages of Alzheimer's dementia is gradual and time of diagnosis can vary (Brooks & Loewenstein, 2010). All patients had received a comprehensive neuropsychological assessment, MRI, and medical and neurological examinations including blood analyses (Monsch & Kressig, 2010), based on which a consensus diagnosis was made for each patient by an interdisciplinary team at the Memory Clinic FELIX PLATTER.

Twenty-six participants were diagnosed with MD, including 14 participants recruited from the Memory Clinic FELIX PLATTER and 12 recruited from the University Psychiatric Clinics Basel, Switzerland. MD patients had to score 6 or more points on the Geriatric Depression Scale (Galik et al., 2013), 10 or more points on the Becks Depression Inventory (Beck et al., 1961), or 13 or more on Becks Depression Inventory-II (Beck et al., 2011).

All study participants underwent an MRI scan and performed the adapted oddity detection task that had been established based on the results of the pilot study. It was confirmed that all NCs responded to at least 50% of all trials. In order to detect unlikely fast responses that suggest accidental key presses, a lower reaction time limit of 238 ms was set based on previous literature on the human average simple reaction time (see Woods et al., 2015). Only one single response was given below this cut-off and excluded from analyses. One patient in the AD group ended the oddity detection task prematurely and the data were excluded from further analyses.

Although the NC group was not demographically matched to the patient groups, they only significantly differed with respect to their mean age. MD patients were youngest (mean age = 60.4 years,  $SD = 9.92$  years), AD patients were oldest (mean age = 76.6 years,  $SD = 5.94$  years), and NCs were in between (mean age = 68.5 years,  $SD = 10.82$  years). As expected, there were significant differences in the MMSE, indicating mildly affected cognitive impairment of the AD patient group relative to both other groups (Monsch et al., 1995). Crucially, although the MD group had similar MMSE scores to the NC group, their lower  $z$  scores of the BVLTL indicated difficulties in episodic memory performance. Sample characteristics can be found in Table 4.

### Neuropsychological Testing

Based on the results of the pilot study, the test was optimized by including existing and newly created items comprised of features that caused the greatest performance differences. Subsequently, the test was then validated as part of the validation study. The neuropsychological testing took place at the Memory Clinic University Department of Geriatric Medicine FELIX PLATTER, Basel, Switzerland on research dedicated computers and was conducted by trained psychology student interns according to standard procedures. All participants were also administered, among others, the MMSE (Folstein et al., 1975), the BVLTL (Delis et al., 1987), and Trail Making Test B (Reitan, 1958). Each testing session lasted

approximately 2 hr. The oddity detection task itself lasted approximately 20 min. The task consisted of 58 trial-unique items, including four practice items followed by six motivational items intermixed between 48 test items. The latter were further analyzed. The six motivational items are simple stimuli that were included to keep those participants motivated who have substantial difficulties to solve the task. Accuracy feedback was only given in the test items. Using the E-prime 2.0 software, each trial started with 1,000 ms silence, after which an array of six self-drawn Kanji-like figures was presented in a  $3 \times 2$  grid on a computer screen until participants gave an answer (max. 20,000 ms). A keyboard with six buttons arranged in the same way as the  $3 \times 2$  grid was used. Participants had to press the corresponding button as fast as possible to identify the odd item. In each trial, all six figures consisted of five, six, or seven features. The target figure had either one or two features that were spatially different from the other figures. There were eight stimuli each for every combination of NOF and NODF (5-1, 5-2, 6-1, 6-2, 7-1, 7-2). Results of 48 trials of the oddity detection task were aggregated within each combination of NOFs and NODFs (6 combinations consisting of 8 stimuli each). For the eight stimuli of each combination, the %correct was calculated. Item analysis of the six combinations revealed that the six means for %correct can be summarized in an overall mean (Cronbach's  $\alpha$  .90), which is the %correct that was analyzed in the sequel.

### MRI Measures

**Acquisition and Preprocessing.** The average time interval between neuropsychological testing and MRI was 50 days ( $SD = 54$ ). All participants received MRI scanning on the same 3-Tesla scanner (MAGNETOM Skyra fit, Siemens) at the University Hospital in Basel (12 channel headcoil; T1-weighted 3D magnetization-prepared rapid gradient echo imaging; inversion time = 900 ms, repetition time 2,300 ms, echo time 2.92 ms, flip angle = 9°; acquisition matrix =  $256 \times 256$  mm, voxel size = 1 mm isotropic). MRI scans were preprocessed using FreeSurfer 5 (Massachusetts General Hospital, Boston, Massachusetts; <http://surfer.nmr.mgh.harvard.edu>; Dale et al., 1999; Fischl & Dale, 2000). Semiautomatic segmentation was formed of magnetization-prepared rapid acquisition gradient echo volumes into gray and white matter and the pial and gray/white matter surfaces (Dale et al., 1999). Tissue adjoining the anteromedial temporal lobe that interfered with the cortical surface reconstructions was removed by hand. TIV and

**Table 4**  
Sample Characteristics of the Validation Study

Variable	NCs		AD		MD	
	(N = 25)		(N = 27)		(N = 26)	
	14/11		12/15		14/12	
Gender (m/f)	M	SD	M	SD	M	SD
Age (years)	68.5	10.82	76.6	5.94	60.4	9.92
Education (years)	14.3	3.91	13.3	2.92	13.2	3.10
MMSE score	29.0	1.04	26.3	1.98	28.7	1.34
BVLTL z-score long-delay free recall	-0.07	1.01	-3.03	0.72	-0.57	1.22
TMT B z score	0.88	1.00	-0.34	1.14	0.10	1.43

*Note.* NCs = normal controls; AD = Alzheimer's disease; MD = major depression; m = male; f = female; MMSE = Mini-Mental State Examination; BVLTL = Basel version of the California Verbal Learning Test; TMT B = Trail Making Test B.

cortical thickness estimates, defined as the distance between vertices on the gray/white matter and pial surfaces, were obtained using FreeSurfer 5.

**VBM.** Whole-brain VBM analysis was conducted according to the pilot study as described earlier. Additionally, we included age as a covariate in the validation study, because groups significantly differed in age.

**ROIs.** Based on the results of the VBM analyses in the pilot study, a primary analysis investigated whether, after adjustment for age, education, and sex, the cortical thickness of the four ROIs (left mPRC, left IPRC, left ERC, and left PHC) predicted %correct responses. A Bonferroni adjustment for these four multiple tests with an experimentwise error rate of 5% was planned, however, discarded finally because none of the unadjusted  $p$  values was below 5%. Secondary analyses then included all cortical thickness values from the right hemisphere as well as cortical volumes of the ROIs from both hemispheres. Primary and secondary analyses are reported with unadjusted  $p$  values where  $p \leq 0.05$  is considered as distinct effect. Data were analyzed using R, Version 3.6.3 (R Core Team, 2020) and the packages ggplot2, Version 3.2.1 (Wickham, 2016), psych, Version 1.9.12.31 (Revelle, 2020) were used. Existing software for mPRC and IPRC segmentation are not yet accurate and reliable enough (e.g., Xie et al., 2019). Therefore, all ROIs were manually drawn by a blinded rater (SK) on coronal slices of the native space cortical surface reconstructions generated by FreeSurfer 5. ROIs were drawn for each hemisphere according to anatomic landmarks described in Kivisaari et al. (2013) and the manual segmentation protocol described in Krumm et al. (2016). The means of corresponding left and right cortical thickness values of the ROIs were corrected for TIV by the formula:

$$\begin{aligned} \text{corrected thickness}_{\text{participant}} \\ = \text{cortical thickness}_{\text{participant}} * \frac{\sqrt[3]{\text{mean TIV}_{\text{all participants}}}}{\sqrt[3]{\text{TIV}_{\text{participant}}}}. \end{aligned} \quad (1)$$

To correct cortical thickness values (one-dimensional; mm) by TIV (volumetric values;  $\text{mm}^3$ ), the third root of TIV was taken. Multiplication by the mean of these roots transforms the corrected values to the original scale. Similarly, volumes were corrected for TIV by the formula:

$$\text{corrected volume}_{\text{participant}} = \text{volume}_{\text{participant}} * \frac{\text{mean TIV}_{\text{all participants}}}{\text{TIV}_{\text{participant}}}. \quad (2)$$

All subsequent analyses within the validation study were done with corrected thicknesses and/or corrected volumes.

## Analyses

Based on the results of the pilot study, the validation study focused on %correct as the measurement of the oddity detection task. First, logistic regression models with covariates age, education, and sex were conducted to investigate the discriminative ability of the oddity detection task measure (%correct) to predict group membership between AD and both other participant groups. Second, the task performance was then related to whole-brain gray matter integrity by VBM analyses with TIV and age as covariates using a general linear model approach in SPM8 (Wellcome Institute of

Cognitive Neurology, www.fil.ion.ucl.ac.uk). No masking was applied, and groups were examined in the same model. All mappings were thresholded at  $p < .001$  uncorrected at the voxel level and clusters surviving a random-field corrected  $p < .05$  are reported in MNI space. Third, cortical thickness values and volumes of four ROIs within the MTL were compared between AD and both other participant groups for both hemispheres separately with analysis of covariance adjusting for age. Fourth, it was investigated whether the oddity detection task measure (%correct) is associated with cortical thickness or volumes of both hemispheres of the four ROIs using linear models with additional covariates age, sex, and education.

Since %correct was often close to 100 in the NC group, an arcsine transform of this value was applied:

$$\text{transformed \%correct} = \sin^{-1}\left(\sqrt{\frac{\%correct}{100}}\right). \quad (3)$$

The arcsine transformation takes account of skewness of proportions close to 0 (i.e., 0%) and 1 (i.e., 100%). Transformed values are approximately normally distributed and their variance is independent of the proportion (Warton & Hui, 2011). All analyses within the validation study were done with transformed %correct responses.

## Transparency and Openness

Data were analyzed using R, Version 4.0.0 (R Core Team, 2020) and the package lme4, Version 1.1-23. This study's design and its analyses were not preregistered. All analyses code and research materials as well as metadata and/or full data are available upon request.

## Results of the Validation Study

### Neuropsychological Test Results and Diagnostic Groups

Group membership was predicted by covariates age, education, sex, and %correct responses in the oddity detection task: The log-odds ratio of NC versus AD for %correct is  $-9.00$  ( $SE = 3.7$ ,  $p = .015$ ) yielding an area under the receiver operator characteristic curve (AUC) of 0.796, 95% CI [0.675, 0.918]. The log-odds ratio of AD versus MD for %correct is 4.81 ( $SE = 3.42$ ,  $p = .16$ ) with an AUC of 0.689, 95% CI [0.545, 0.833]. For an overview on task performance, see Figure 2.

### VBM

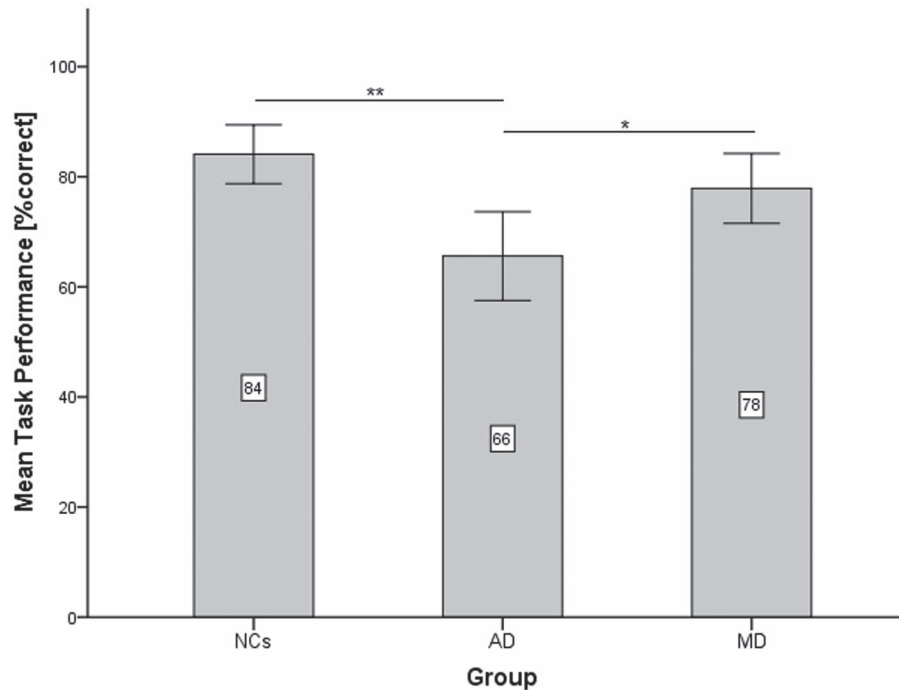
We found four significant clusters for %correct at threshold  $p < .001$  with peak voxels in the right superior and inferior temporal pole, left parahippocampal region, and left inferior temporal lobe (see Table 5). Clusters comprise the left and right entorhinal and PRC (see Figure 3).

### Cortical Thickness in Regions of Interest Across Diagnostic Groups

Age-adjusted cortical thickness of all four ROIs were compared between the three groups. Cortical thickness in both hemispheres was distinctly reduced in the AD group compared to both other groups for the mPRC (left mPRC:  $F[3, 74] = 13.42$ ; AD vs. NC:



**Figure 2**  
Performance in the Oddity Detection Task in the Validation Study by Group



Note. Mean task performance is shown as percentage correct out of 48 trials per group. Error bars show 95% confidence interval. NCs = normal controls; AD = Alzheimer's disease; MD = major depression.  
\* Significant differences at  $p < 0.05$ . \*\* Significant differences at  $p < 0.001$ .

$p = .006$ ; AD vs. MD:  $p = .01$ ; right mPRC:  $F[3, 74] = 14.9$ ; AD vs. NC:  $p < .001$ ; AD vs. MD:  $p = .003$ ) as well as the ERC (left ERC:  $F[3, 74] = 11.29$ ; AD vs. NC:  $p = .003$ ; AD vs. MD:  $p < .001$ ; right ERC:  $F[3, 74] = 10.71$ ; AD vs. NC:  $p = .001$ ; AD vs. MD:  $p = .001$ ). Further, distinct differences between the AD group and both other groups in cortical thickness were found for the left PHC,  $F(3, 74) = 4.81$ ; AD vs. NC:  $p = .020$ , AD vs. MD  $p = 0.23$ . There was no distinct difference between the groups in cortical thickness of the right PHC,  $F(3, 74) = 6.165$ ; AD vs. NC:  $p = .202$ , AD vs. MD:  $p = .232$ , and the IPRC in both hemispheres (left IPRC:  $F[3, 74] = 2.343$ ; AD vs. NC:  $p = .386$ , AD vs. MD:  $p = .135$ ; right IPRC:  $F[3, 74] = 4.884$ ; AD vs. NC  $p = .076$ , AD vs. MD  $p = .074$ ). An overview of cortical thickness and TIV in the validation study for the three participant groups is displayed in Table 6.

### Cortical Thickness in Regions of Interest and Neuropsychological Test Results

Residual diagrams revealed acceptable fulfilling of the model assumptions despite some nonlinearity and smaller residual variance at certain boundaries. Results of the primary analysis are shown in Tables 7 and 8. Results of the secondary analyses, including all cortical thickness values from the right hemisphere as well as cortical volumes of the ROIs from both hemispheres, can be found in Appendix B (Tables B1–B4). None of the ROI analyses achieved small  $p$  values.

### Discussion of the Validation Study

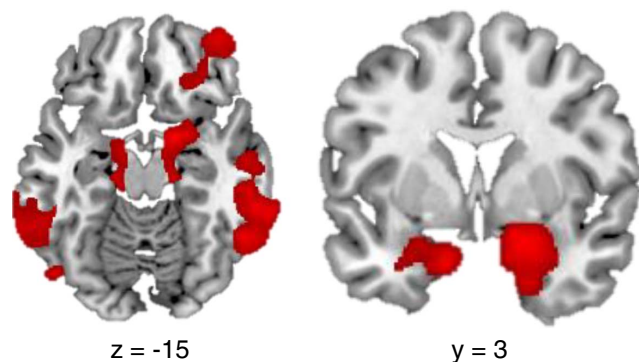
We aimed to develop a measure to assess the functioning of the PRC, a brain structure affected very early in AD pathology

**Table 5**  
Significant Results of Brain–Behavioral Analyses for %Correct With Covariates TIV and Age in the Validation Study

Anatomical region	Side	MNI coordinates Peak voxel			Cluster size (kE)	$p$ (FWE-corr)
		$x$	$y$	$z$		
Threshold $p < .001$						
Superior temporal pole	Right	24	6	–22	18,917	<.001
Parahippocampal gyrus	Left	–14	4	–26	6,648	.035
Inferior temporal lobe	Left	–56	–48	–18	9,211	.009
Inferior temporal lobe	Right	55	–53	–12	15,284	.001

Note. TIV = total intracranial volume; MNI = Montreal Neurological Institute and Hospital; FWE-corr = family-wise-error corrected.

**Figure 3**  
Significant Clusters for %Correct in the Validation Study



*Note.* Significant clusters for %correct with threshold  $p < .001$  in the validation study. Coordinates in Montreal Neurological Institute and Hospital (MNI) space. See the online article for the color version of this figure.

(Braak & Braak, 1991; Krumm et al., 2016). Specifically, AD patients' capacity to form an integrated perceptual figure representation from separate visual features was tested (Barens et al., 2012; Bussey et al., 2005). Our study introduces a novel nonmnemonic visual oddity detection task that successfully detects deficits in the early stages of AD. This aligns with results of previous studies showing AD patients to evidence greater impairment of object discrimination as the number of shared features between objects increases (i.e., Barens et al., 2012; Lawrence et al., 2020; Newsome et al., 2012). However, these previous studies compared behavioral differences between low and high ambiguity trials, whereas in the present study all trials were highly ambiguous. Specifically, we presented more figures simultaneously and the figures were comprised of more individual features than in previous studies. Further, we linked performance to brain integrity through neuroimaging while specifically investigating the earliest neurofibrillary pathology sites (i.e., the mPRC and ERC).

Results of the pilot study were used to inform adaptation of test stimuli and neuroanatomical hypotheses that were then applied in the ensuing validation study. Results of the validation study revealed that the present oddity detection task showed good diagnostic discriminative ability between patients in the early stages of AD and NCs. As such, fewer correct responses in the visual oddity detection

task predicted very early AD, including its prodromal stage aMCI, compared to cognitively healthy adults. Our findings align with a growing body of work suggesting that subjects at risk for AD, individuals with aMCI, and patients with Alzheimer's dementia have difficulties in nonmnemonic object discrimination tasks, particularly when the presented objects share many features (Gaynor et al., 2019; Mason et al., 2017; Newsome et al., 2012). Regarding the discriminative ability of the task to differentiate between patients in early stages of AD and patients with MD in our sample, results did not show a distinction when corrected for age. Possible explanations and limitations are discussed below and highlight the need for age-matched participant groups for further validation of the task.

As proof of concept, we compared cortical thickness of four ROIs within the MTL between the three groups. In comparison to MD and NC, the AD group showed distinctly reduced cortical thickness bilaterally in the mPRC and ERC as well as the left PHC. These findings are in line with cortical thinning in the respective regions in typical early-stage AD (Braak & Braak, 1991; Sone et al., 2017). Importantly, the IPRC was not atrophied in the AD group compared to both other groups, which is comparable to one of our earlier findings (Krumm et al., 2016) and suggests that AD patients in our sample were at a relatively early stage of disease progression. As depicted in Table 6, the MD group had thickest cortices for all ROIs in both hemispheres, even thicker than NC participants, likely due to the significant younger age of the MD group. This again underscores the importance of the adjustment for age in all analyses of the validation study. Further, these results bolster our assumption that patients with early-stage AD show degenerated mPRCs and ERCs while there is no atrophy in MD patients in these regions. Thus, the present results support previous findings suggesting the use of mPRC and ERC thinning as part of the diagnostic process of early-stage AD in clinical and research settings (Krumm et al., 2016) and furthermore propose that this approach may also differentiate between AD and other etiologies of cognitive impairment, such as MD.

In a next step, it was investigated which brain regions were related to the performance in the novel oddity detection task. For %correct responses whole-brain analyses revealed four significant clusters with peak voxels in the right and left parahippocampal region, inferior temporal lobe, and near the right midfrontal lobe. Notably, the cluster of the right and left parahippocampal region comprised the entorhinal and PRC. Taken together, these findings are in line with typical tau pathology progression in AD (Braak & Braak, 1991)

**Table 6**  
Cortical Thickness and TIV From Structural MRI Scans in the Validation Study

Anatomical region	NCs (N = 25)				AD (N = 27)				MD (N = 26)			
	Left hemisphere		Right hemisphere		Left hemisphere		Right hemisphere		Left hemisphere		Right hemisphere	
	M	SD	M	SD	M	SD	M	SD	M	SD	M	SD
mPRC (mm)	2.81	0.55	3.08	0.61	2.25	0.42	2.28	0.48	2.96	0.49	3.08	0.51
IPRC (mm)	2.95	0.49	3.04	0.39	2.76	0.55	2.70	0.48	3.10	0.45	3.12	0.46
ERC (mm)	3.04	0.59	3.30	0.53	2.68	0.50	2.61	0.58	3.46	0.40	3.42	0.61
PHC (mm)	2.62	0.45	2.53	0.26	2.30	0.30	2.33	0.30	2.66	0.33	2.59	0.27
TIV (cm <sup>3</sup> )	1,521	185	1,521	185	1,492	136	1,492	136	1,471	210	1,471	210

*Note.* NCs = normal controls; AD = Alzheimer's disease; MD = major depression; mPRC = medial perirhinal cortex; IPRC = lateral perirhinal cortex; ERC = entorhinal cortex; PHC = parahippocampal cortex; TIV = total intracranial volume.

**Table 7**

*Results of the Linear Regression of %Correct Responses in the Oddity Detection Task Modeled Separately by Left mPRC and Left IPRC Thickness Values and Covariates in the Validation Study*

Variable	Left mPRC				Left IPRC			
	Estimate	SE	<i>t</i>	<i>p</i>	Estimate	SE	<i>t</i>	<i>p</i>
(Intercept)	1.084	0.287	3.775	<.001	1.100	0.266	4.129	<.001
Age	-0.0056	0.0025	-2.205	.031	-0.0058	0.0022	-2.639	.010
Education	0.026	0.008	3.249	.002	0.026	0.008	3.291	.002
Female	-0.004	0.054	-0.072	.942	-0.002	0.053	-0.029	.977
Thickness	0.012	0.046	0.259	.796	0.009	0.045	0.214	.831
<i>R</i> <sup>2</sup>	.298				.297			

*Note.* This table demonstrates linear regression results of task performance modeled by cortical thickness of the left medial perirhinal cortex (mPRC),  $F(4, 73) = 7.665$ ,  $p < .001$ , and left lateral perirhinal cortex (IPRC),  $F(4, 73) = 7.658$ ,  $p < .001$ .

and suggest the task as a promising measurement to diagnose very early stages of AD.

Against our assumption based on the hierarchical-representational account of PRC functioning, we did not find performance on the oddity task to be associated with cortical thickness or volume of the mPRC or ERC nor any of the other MTL subregions in our ROI-based analyses. These results may reflect that due to the anatomical proximity of the investigated ROIs, functional overlap is most likely, complicating the prediction of task performance by an individual ROI. Such discrepancies between VBM and ROI analyses are not uncommon in the neuroimaging literature (e.g., Giuliani et al., 2005; Seyedi et al., 2020; Testa et al., 2004). For example, Testa et al. (2004) showed that the detection of MTL atrophy in AD patients was more precise when using VBM compared to ROI analysis. Furthermore, several methodological considerations are needed in order to interpret these results. First, the sample size might have been too small to detect significant correlations between ROI-based atrophy and test performance, since the interindividual variance of ROI-based approaches is often very large. Second, the covariate age already accounted for a high proportion of variance in the ROI models, likely leading to a nonsignificant improvement of the model when task performance was added. A recent review by Hyatt et al. (2020) concludes that inference about the statistical significance of associations between MRI measures and psychological variables can be extremely altered by the addition of covariates. Thus, researchers should be cautious when using  $p$  values to determine significance in the presence of covariates (Hyatt et al., 2020). According to large-scale comparisons of imaging methods

for measuring AD severity, there is a concerning variety of procedures regarding variable adjustment for individual and group analyses that makes comparison across studies difficult (Barnes et al., 2010; Schwarz et al., 2016). Taken together, these methodological considerations might partially account for the fact that performance on the present oddity detection task was not significantly associated with ROI-based cortical thickness within the MTL. Procedures such as data transformation and covariate adjustment should be carefully considered in future studies. The use of more uniform methodology should permit a more accurate insight into the relationship of cortical thinning and associated cognitive impairments in the earliest stages of AD.

Nonetheless, the possibility needs to be considered that despite the conformity of our visual stimuli with important classical principles of Gestalt theory (e.g., proximity, connectedness), the novel oddity detection task did not primarily assess the ability to form integrated perceptual figure representations from separate visual features—a function that has been ascribed to the PRC (Barens et al., 2007; Lee et al., 2006). Furthermore, shape perception might not be solely determined by the computations mediated by the ventral visual stream. More recent studies found object representation to be influenced by the dorsal pathway, regardless of whether any visuomotor response is required (Freud et al., 2017). However, many questions remain regarding the nature of visual properties encoded in dorsal object representation as well as their topographical organization (Freud et al., 2017). At present, it remains unclear whether these areas compensate for a reduced PRC functionality in the early stages of AD.

**Table 8**

*Results of the Linear Regression of %Correct Responses in the Oddity Detection Task Modeled Separately by Left ERC and Left PHC Thickness Values and Covariates in the Validation Study*

Variable	Left ERC				Left PHC			
	Estimate	SE	<i>t</i>	<i>p</i>	Estimate	SE	<i>t</i>	<i>p</i>
(Intercept)	1.042	0.270	3.863	<.001	1.246	0.277	4.503	<.001
Age	-0.0055	0.0023	-2.437	.017	-0.0064	0.0022	-2.855	.006
Education	0.026	0.008	3.283	.002	0.026	0.008	3.304	.001
Female	-0.002	0.052	-0.034	.973	0.005	0.052	0.089	.929
Thickness	0.022	0.041	0.539	.592	-0.033	0.056	-0.593	.555
<i>R</i> <sup>2</sup>	.298				.296			

*Note.* This table demonstrates linear regression results of task performance modeled by cortical thickness of the left entorhinal cortex (ERC),  $F(4, 73) = 7.745$ ,  $p < .001$ , and left parahippocampal cortex (PHC),  $F(4, 73) = 7.766$ ,  $p < .001$ .

In addition, it is possible that several other cognitive subprocesses might have been necessary to complete the task. A visual object discrimination task involves a shift of attention between objects, which most likely also engages working memory, since objects or at least higher conjunctions of features must be maintained to compare the stimulus with others (Barens et al., 2012; Warren et al., 2011). As we presented six figures simultaneously, subjects had to guide their eye movements and selectively attend to individual features and figures (Agam et al., 2010; Reddy et al., 2009). Thus, the performance deficits of AD patients that we observed might be alternatively explained by general cognitive deficits in visual attention and working memory. Patients with aMCI and Alzheimer's dementia have indeed been shown to gradually lose control of their eye movements and attention (Crawford et al., 2013; Wilcockson et al., 2019). Functional imaging could specifically investigate which brain areas are actively engaged during task completion. Moreover, it will be important to explore how the PRC and its connections to other task-relevant structures affect performance. This would shed more light onto how cognitive, structural, and connectivity changes within the MTL subregions are interrelated and could serve as biomarkers for early AD. Other regions (i.e., parietal cortex) also seem to support early cognitive functions associated with visual perception that contribute as building blocks of memory (Staresina & Davachi, 2010) and appear to be affected in very early stages of AD (Jacobs et al., 2012). Even more, studies applying tasks that include feature binding across visual streams (e.g., motion, luminance) with greater demands on cross-cortical interaction found AD-related cortical pathology to be associated with neocortical functional dysconnectivity (e.g., Festa et al., 2005; Korthauer et al., 2020). Thus, future research could zoom out to investigate those neural correlates outside of the MTL subregions and possible underlying cortico-cortical disconnections (Korthauer et al., 2020; Parra, 2022).

Further limitations of the present study are the inclusion of only two different patient groups with a limited sample size to compare with cognitively healthy participants. Additionally, aMCI patients in the present sample were thought to be in the prodromal phases of AD; however, AD pathology was not confirmed by biomarkers. To further evaluate the discriminative ability of the novel oddity detection task, future studies should include demographically match groups as well as other etiologies than AD and MD with an overall bigger sample size and confirm AD pathology with respective biomarkers. In addition, especially when investigating early-stage AD, a follow-up examination in order to ensure the cognitive health of the control group would be beneficial because PRC functionality might already be affected before for example, episodic memory impairment occurs.

In conclusion, this study provides evidence that the novel complex visual oddity detection task is a sensitive measure to differentiate adults in early stages of AD from cognitively healthy adults. Results further demonstrate that early AD patients show cortical atrophy within the mPRC and ERC, but not the lPRC. VBM whole-brain analyses showed significant correlation of task performance and several cortical regions including the mPRC and ERC. However, when using an ROI-based approach, we did not find a distinct association of cortical thickness of any individual ROI within the MTL subregion and performance on the task. Further validation of this cognitive measure with appropriate methodological adjustments (e.g., age-matched participant groups) is needed. Additionally,

applying the task to other patient groups could further assess its ability to differentiate patients in early stages of AD from patients with other neurocognitive disorders. This would contribute to the development of more specific biomarkers that take advantage of the progress made in structural and functional measurements of the PRC, and neuroscientific models of its functioning. Ultimately, this would refine the detection of AD early on in disease progression and expand opportunities for targeted therapeutic intervention.

## References

- Agam, Y., Liu, H., Papanastassiou, A., Buia, C., Golby, A. J., Madsen, J. R., & Kreiman, G. (2010). Robust selectivity to two-object images in human visual cortex. *Current Biology*, *20*(9), 872–879. <https://doi.org/10.1016/j.cub.2010.03.050>
- Albert, M. S., DeKosky, S. T., Dickson, D., Dubois, B., Feldman, H. H., Fox, N. C., Gamst, A., Holtzman, D. M., Jagust, W. J., Petersen, R. C., Snyder, P. J., Carrillo, M. C., Thies, B., & Phelps, C. H. (2011). The diagnosis of mild cognitive impairment due to Alzheimer's disease: Recommendations from the National Institute on Aging-Alzheimer's Association work-groups on diagnostic guidelines for Alzheimer's disease. *Alzheimer's & Dementia*, *7*(3), 270–279. <https://doi.org/10.1016/j.jalz.2011.03.008>
- American Psychiatric Association. (1994). *DSM-IV: Diagnostic and statistical manual of mental disorders*.
- Ashburner, J. (2007). A fast diffeomorphic image registration algorithm. *NeuroImage*, *38*(1), 95–113. <https://doi.org/10.1016/j.neuroimage.2007.07.007>
- Barens, M. D., Bussey, T. J., Lee, A. C. H., Rogers, T. T., Davies, R. R., Saksida, L. M., Murray, E. A., & Graham, K. S. (2005). Functional specialization in the human medial temporal lobe. *Journal of Neuroscience*, *25*(44), 10239–10246. <https://doi.org/10.1523/JNEUROSCI.2704-05.2005>
- Barens, M. D., Gaffan, D., & Graham, K. S. (2007). The human medial temporal lobe processes online representations of complex objects. *Neuropsychologia*, *45*(13), 2963–2974. <https://doi.org/10.1016/j.neuropsychologia.2007.05.023>
- Barens, M. D., Groen, I. I. A., Lee, A. C. H., Yeung, L.-K., Brady, S. M., Gregori, M., Kapur, N., Bussey, T. J., Saksida, L. M., & Henson, R. N. A. (2012). Intact memory for irrelevant information impairs perception in amnesia. *Neuron*, *75*(1), 157–167. <https://doi.org/10.1016/j.neuron.2012.05.014>
- Barens, M. D., Henson, R. N. A., & Graham, K. S. (2011). Perception and conception: Temporal lobe activity during complex discriminations of familiar and novel faces and objects. *Journal of Cognitive Neuroscience*, *23*(10), 3052–3067. [https://doi.org/10.1162/jocn\\_a\\_00010](https://doi.org/10.1162/jocn_a_00010)
- Barnes, J., Ridgway, G. R., Bartlett, J., Henley, S. M. D., Lehmann, M., Hobbs, N., Clarkson, M. J., MacManus, D. G., Ourselin, S., & Fox, N. C. (2010). Head size, age and gender adjustment in MRI studies: A necessary nuisance? *NeuroImage*, *53*(4), 1244–1255. <https://doi.org/10.1016/j.neuroimage.2010.06.025>
- Bartko, S. J., Winters, B. D., Cowell, R. A., Saksida, L. M., & Bussey, T. J. (2007). Perceptual functions of perirhinal cortex in rats: Zero-delay object recognition and simultaneous oddity discriminations. *Journal of Neuroscience*, *27*(10), 2548–2559. <https://doi.org/10.1523/JNEUROSCI.5171-06.2007>
- Beck, A. T., Steer, R. A., & Brown, G. (2011). *Beck Depression Inventory—II* [Data set]. American Psychological Association. <https://doi.org/10.1037/100742-000>
- Beck, A. T., Ward, C. H., Mendelson, M., Mock, J., & Erbaugh, J. (1961). An inventory for measuring depression. *Archives of General Psychiatry*, *4*(6), 561–571. <https://doi.org/10.1001/archpsyc.1961.01710120031004>
- Boccia, M., Acierno, M., & Piccardi, L. (2015). Neuroanatomy of Alzheimer's disease and late-life depression: A coordinate-based meta-analysis of MRI



- studies. *Journal of Alzheimer's Disease: JAD*, 46(4), 963–970. <https://doi.org/10.3233/JAD-142955>
- Braak, H., Alafuzoff, I., Arzberger, T., Kretschmar, H., & Del Tredici, K. (2006). Staging of Alzheimer disease-associated neurofibrillary pathology using paraffin sections and immunocytochemistry. *Acta Neuropathologica*, 112(4), 389–404. <https://doi.org/10.1007/s00401-006-0127-z>
- Braak, H., & Braak, E. (1991). Neuropathological staging of Alzheimer-related changes. *Acta Neuropathologica*, 82(4), 239–259. <https://doi.org/10.1007/BF00308809>
- Braak, H., & Braak, E. (1995). Staging of Alzheimer's disease-related neurofibrillary changes. *Neurobiology of Aging*, 16(3), 271–278. [https://doi.org/10.1016/0197-4580\(95\)00021-6](https://doi.org/10.1016/0197-4580(95)00021-6)
- Brooks, L. G., & Loewenstein, D. A. (2010). Assessing the progression of mild cognitive impairment to Alzheimer's disease: Current trends and future directions. *Alzheimer's Research & Therapy*, 2(5), Article 28. <https://doi.org/10.1186/alzrt52>
- Burger, K., Zinkowski, R., Teipel, S. J., Arai, H., DeBernardis, J., Kerkman, D., McCulloch, C., Padberg, F., Faltraco, F., Goernitz, A., Tapiola, T., Rapoport, S. I., Pirttilä, T., Möller, H.-J., & Hampel, H. (2003). Differentiation of geriatric major depression from Alzheimer's disease with CSF tau protein phosphorylated at threonine 231. *The American Journal of Psychiatry*, 160(2), 376–379. <https://doi.org/10.1176/appi.ajp.160.2.376>
- Bussey, T. J., & Saksida, L. M. (2002). The organization of visual object representations: A connectionist model of effects of lesions in perirhinal cortex. *European Journal of Neuroscience*, 15(2), 355–364. <https://doi.org/10.1046/j.0953-816x.2001.01850.x>
- Bussey, T. J., & Saksida, L. M. (2007). Memory, perception, and the ventral visual–perirhinal–hippocampal stream: Thinking outside of the boxes. *Hippocampus*, 17(9), 898–908. <https://doi.org/10.1002/hipo.20320>
- Bussey, T. J., Saksida, L. M., & Murray, E. A. (2002). Perirhinal cortex resolves feature ambiguity in complex visual discriminations. *European Journal of Neuroscience*, 15(2), 365–374. <https://doi.org/10.1046/j.0953-816x.2001.01851.x>
- Bussey, T. J., Saksida, L. M., & Murray, E. A. (2005). The perceptual-mnemonic/feature conjunction model of perirhinal cortex function. *The Quarterly Journal of Experimental Psychology Section B*, 58(3–4b), 269–282. <https://doi.org/10.1080/02724990544000004>
- Cate, A. D., & Köhler, S. (2006). The missing whole in perceptual models of perirhinal cortex. *Trends in Cognitive Sciences*, 10(9), 396–397. <https://doi.org/10.1016/j.tics.2006.07.004>
- Christensen, H., Griffiths, K., Mackinnon, A., & Jacomb, P. (1997). A quantitative review of cognitive deficits in depression and Alzheimer-type dementia. *Journal of the International Neuropsychological Society*, 3(6), 631–651. <https://doi.org/10.1017/S1355617797006310>
- Cowell, R. A., Bussey, T. J., & Saksida, L. M. (2010). Components of recognition memory: Dissociable cognitive processes or just differences in representational complexity? *Hippocampus*, 20(11), 1245–1262. <https://doi.org/10.1002/hipo.20865>
- Crawford, T. J., Higham, S., Mayes, J., Dale, M., Shaunak, S., & Lekwuwa, G. (2013). The role of working memory and attentional disengagement on inhibitory control: Effects of aging and Alzheimer's disease. *AGE*, 35(5), 1637–1650. <https://doi.org/10.1007/s11357-012-9466-y>
- Dale, A. M., Fischl, B., & Sereno, M. I. (1999). Cortical surface-based analysis. *NeuroImage*, 9(2), 179–194. <https://doi.org/10.1006/nimg.1998.0395>
- Delhaye, E., Bahri, M. A., Salmon, E., & Bastin, C. (2019). Impaired perceptual integration and memory for unitized representations are associated with perirhinal cortex atrophy in Alzheimer's disease. *Neurobiology of Aging*, 73, 135–144. <https://doi.org/10.1016/j.neurobiolaging.2018.09.021>
- Delis, D. C., Kramer, J. H., Kaplan, E., & Ober, B. A. (1987). *California verbal learning test*. Psychological Corporation.
- Erez, J., Cusack, R., Kendall, W., & Barense, M. D. (2016). Conjunctive coding of complex object features. *Cerebral Cortex*, 26(5), 2271–2282. <https://doi.org/10.1093/cercor/bhv081>
- Festa, E. K., Insler, R. Z., Salmon, D. P., Paxton, J., Hamilton, J. M., & Heindel, W. C. (2005). Neocortical disconnectivity disrupts sensory integration in Alzheimer's disease. *Neuropsychology*, 19(6), 728–738. <https://doi.org/10.1037/0894-4105.19.6.728>
- Fischl, B., & Dale, A. M. (2000). Measuring the thickness of the human cerebral cortex from magnetic resonance images. *Proceedings of the National Academy of Sciences*, 97(20), 11050–11055. <https://doi.org/10.1073/pnas.200033797>
- Folstein, M. F., Folstein, S. E., & McHugh, P. R. (1975). “Mini-mental state.” A practical method for grading the cognitive state of patients for the clinician. *Journal of Psychiatric Research*, 12(3), 189–198. [https://doi.org/10.1016/0022-3956\(75\)90026-6](https://doi.org/10.1016/0022-3956(75)90026-6)
- Freud, E., Culham, J. C., Plaut, D. C., & Behrmann, M. (2017). Correction: The large-scale organization of shape processing in the ventral and dorsal pathways. *eLife*, 6, Article e34464. <https://doi.org/10.7554/eLife.34464>
- Galik, E., Fukudo, S., Tanaka, Y., Gidron, Y., Campbell, T. S., Johnson, J. A., Zernicke, K. A., Pellowski, J., García, L. I., Mitchell, J. W., Esausquin, J. T., Salem, R. M., Rodriguez-Murillo, L., Chiba-Falek, O., Jiang, R., Jiang, R., Campbell, T. S., Johnson, J. A., Zernicke, K. A., ... Anderson, G. M. (2013). Geriatric depression scale. In M. D. Gellman & J. R. Turner (Eds.), *Encyclopedia of behavioral medicine* (pp. 857–858). Springer. [https://doi.org/10.1007/978-1-4419-1005-9\\_194](https://doi.org/10.1007/978-1-4419-1005-9_194)
- Gaynor, L. S., Curiel Cid, R. E., Penate, A., Rosselli, M., Burke, S. N., Wicklund, M., Loewenstein, D. A., & Bauer, R. M. (2019). Visual object discrimination impairment as an early predictor of mild cognitive impairment and Alzheimer's disease. *Journal of the International Neuropsychological Society*, 25(7), 688–698. <https://doi.org/10.1017/S1355617719000316>
- Giuliani, N. R., Calhoun, V. D., Pearlson, G. D., Francis, A., & Buchanan, R. W. (2005). Voxel-based morphometry versus region of interest: A comparison of two methods for analyzing gray matter differences in schizophrenia. *Schizophrenia Research*, 74(2–3), 135–147. <https://doi.org/10.1016/j.schres.2004.08.019>
- Hartmann, F., Reinhardt, J., Stippich, C., & Krumm, S. (2021). Manual correction of voxel misclassifications in mesiotemporal structures does not alter brain–behavioral results in an Episodic Memory Task. *Journal of Clinical Medicine*, 10(21), 4869. <https://doi.org/10.3390/jcm10214869>
- Hyatt, C. S., Owens, M. M., Crowe, M. L., Carter, N. T., Lynam, D. R., & Miller, J. D. (2020). The quandary of covarying: A brief review and empirical examination of covariate use in structural neuroimaging studies on psychological variables. *NeuroImage*, 205, Article 16225. <https://doi.org/10.1016/j.neuroimage.2019.116225>
- Insausti, R., Juottonen, K., Soininen, H., Insausti, A. M., Partanen, K., Vainio, P., Laakso, M. P., & Pitkänen, A. (1998). MR volumetric analysis of the human entorhinal, perirhinal, and temporopolar cortices. *AJNR. American Journal of Neuroradiology*, 19(4), 659–671.
- Jacobs, H. I. L., Van Boxtel, M. P. J., Jolles, J., Verhey, F. R. J., & Uylings, H. B. M. (2012). Parietal cortex matters in Alzheimer's disease: An overview of structural, functional and metabolic findings. *Neuroscience and Biobehavioral Reviews*, 36(1), 297–309. <https://doi.org/10.1016/j.neubiorev.2011.06.009>
- Jorm, A. F., Scott, R., & Jacomb, P. A. (1989). Assessment of cognitive decline in dementia by informant questionnaire. *International Journal of Geriatric Psychiatry*, 4(1), 35–39. <https://doi.org/10.1002/gps.930040109>
- Kaplan, E. F., Goodglass, H., & Weintraub, S. (1978). *The Boston naming test*. Veterans Administration Medical Center.
- Kivisaari, S. L., Probst, A., & Taylor, K. I. (2013). The perirhinal, entorhinal, and parahippocampal cortices and hippocampus: An overview of functional anatomy and protocol for their segmentation in MR images. In S. Ulmer & O. Jansen (Eds.), *FMRI: Basics and clinical applications* (pp. 239–267). Springer. [https://doi.org/10.1007/978-3-642-34342-1\\_19](https://doi.org/10.1007/978-3-642-34342-1_19)
- Kivisaari, S. L., & Taylor, K. I. (2012). *Transentorhinal cortex function and structure in preclinical Alzheimer's disease* [Unpublished raw data].

- Knierim, J. J., Neunuebel, J. P., & Deshmukh, S. S. (2014). Functional correlates of the lateral and medial entorhinal cortex: Objects, path integration and local–global reference frames. *Philosophical Transactions of the Royal Society of London, Series B: Biological Sciences*, 369(1635), Article 20130369. <https://doi.org/10.1098/rstb.2013.0369>
- Korthauer, L. E., Heindel, W. C., Lai, L. Y., Tremont, G., Ott, B. R., & Festa, E. K. (2020). Impaired integration of object feature knowledge in amnesic mild cognitive impairment. *Neuropsychology*, 34(6), 699–712. <https://doi.org/10.1037/neu0000670>
- Krumm, S., Kivisaari, S. L., Probst, A., Monsch, A. U., Reinhardt, J., Ulmer, S., Stippich, C., Kressig, R. W., & Taylor, K. I. (2016). Cortical thinning of parahippocampal subregions in very early Alzheimer's disease. *Neurobiology of Aging*, 38, 188–196. <https://doi.org/10.1016/j.neurobiolaging.2015.11.001>
- Lawrence, A. V., Cardoza, J., & Ryan, L. (2020). Medial temporal lobe regions mediate complex visual discriminations for both objects and scenes: A process-based view. *Hippocampus*, 30(8), 879–891. <https://doi.org/10.1002/hipo.23203>
- Lee, A. C. H., Buckley, M. J., Gaffan, D., Emery, T., Hodges, J. R., & Graham, K. S. (2006). Differentiating the roles of the hippocampus and perirhinal cortex in processes beyond long-term declarative memory: A double dissociation in dementia. *Journal of Neuroscience*, 26(19), 5198–5203. <https://doi.org/10.1523/JNEUROSCI.3157-05.2006>
- Lee, A. C. H., & Rudebeck, S. R. (2010). Human medial temporal lobe damage can disrupt the perception of single objects. *Journal of Neuroscience*, 30(19), 6588–6594. <https://doi.org/10.1523/JNEUROSCI.0116-10.2010>
- Mason, E. J., Hussey, E. P., Molitor, R. J., Ko, P. C., Donahue, M. J., & Ally, B. A. (2017). Family history of Alzheimer's disease is associated with impaired perceptual discrimination of novel objects. *Journal of Alzheimer's Disease*, 57(3), 735–745. <https://doi.org/10.3233/JAD-160772>
- McKhann, G. M., Knopman, D. S., Chertkow, H., Hyman, B. T., Jack, C. R., Jr., Kawas, C. H., Klunk, W. E., Koroshetz, W. J., Manly, J. J., Mayeux, R., Mohs, R. C., Morris, J. C., Rossor, M. N., Scheltens, P., Carrillo, M. C., Thies, B., Weintraub, S., & Phelps, C. H. (2011). The diagnosis of dementia due to Alzheimer's disease: Recommendations from the National Institute on Aging–Alzheimer's Association workgroups on diagnostic guidelines for Alzheimer's disease. *Alzheimer's & Dementia*, 7(3), 263–269. <https://doi.org/10.1016/j.jalz.2011.03.005>
- McTighe, S. M., Cowell, R. A., Winters, B. D., Bussey, T. J., & Saksida, L. M. (2010). Paradoxical false memory for objects after brain damage. *Science*, 330(6009), 1408–1410. <https://doi.org/10.1126/science.1194780>
- Monsch, A., & Kressig, R. (2010). Specific care program for the older adults: Memory clinics. *European Geriatric Medicine*, 1(2), 128–131. <https://doi.org/10.1016/j.eurger.2010.03.006>
- Monsch, A. U., Foldi, N. S., Ermini-Fünfschilling, D. E., Berres, M., Taylor, K. I., Seifritz, E., Stähelin, H. B., & Spiegel, R. (1995). Improving the diagnostic accuracy of the Mini-Mental State Examination. *Acta Neurologica Scandinavica*, 92(2), 145–150. <https://doi.org/10.1111/j.1600-0404.1995.tb01029.x>
- Murray, E. A., Bussey, T. J., & Saksida, L. M. (2007). Visual perception and memory: A new view of medial temporal lobe function in primates and rodents. *Annual Review of Neuroscience*, 30(1), 99–122. <https://doi.org/10.1146/annurev.neuro.29.051605.113046>
- Naylor, M. D., Karlawish, J. H., Arnold, S. E., Khachaturian, A. S., Khachaturian, Z. S., Lee, V. M.-Y., Baumgart, M., Banerjee, S., Beck, C., Blennow, K., Brookmeyer, R., Brunden, K. R., Buckwalter, K. C., Comer, M., Covinsky, K., Feinberg, L. F., Frisoni, G., Green, C., Guimaraes, R. M., ... Trojanowski, J. Q. (2012). Advancing Alzheimer's disease diagnosis, treatment, and care: Recommendations from the Ware Invitational Summit. *Alzheimer's & Dementia*, 8(5), 445–452. <https://doi.org/10.1016/j.jalz.2012.08.001>
- Newsome, R. N., Duarte, A., & Barense, M. D. (2012). Reducing perceptual interference improves visual discrimination in mild cognitive impairment: Implications for a model of perirhinal cortex function. *Hippocampus*, 22(10), 1990–1999. <https://doi.org/10.1002/hipo.22071>
- O'Neil, E. B., Barkley, V. A., & Köhler, S. (2013). Representational demands modulate involvement of perirhinal cortex in face processing. *Hippocampus*, 23(7), 592–605. <https://doi.org/10.1002/hipo.22117>
- O'Neil, E. B., Cate, A. D., & Köhler, S. (2009). Perirhinal cortex contributes to accuracy in recognition memory and perceptual discriminations. *Journal of Neuroscience*, 29(26), 8329–8334. <https://doi.org/10.1523/JNEUROSCI.0374-09.2009>
- Palmer, S., & Rock, I. (1994). Rethinking perceptual organization: The role of uniform connectedness. *Psychonomic Bulletin & Review*, 1(1), 29–55. <https://doi.org/10.3758/BF03200760>
- Parra, M. A. (2022). Barriers to effective memory assessments for Alzheimer's disease. *PsyArXiv*. <https://doi.org/10.3233/JAD-215445>
- Perri, R., Serra, L., Carlesimo, G. A., Caltagirone, C., & the Early Diagnosis Group of Italian Interdisciplinary Network on Alzheimer's Disease. (2007). Preclinical dementia: An Italian multicentre study on amnesic mild cognitive impairment. *Dementia and Geriatric Cognitive Disorders*, 23(5), 289–300. <https://doi.org/10.1159/000100871>
- Petersen, R. C., Parisi, J. E., Dickson, D. W., Johnson, K. A., Knopman, D. S., Boeve, B. F., Jicha, G. A., Ivnik, R. J., Smith, G. E., Tangalos, E. G., Braak, H., & Kokmen, E. (2006). Neuropathologic features of amnesic mild cognitive impairment. *Archives of Neurology*, 63(5), 665–672. <https://doi.org/10.1001/archneur.63.5.665>
- R Core Team. (2020). *R: A language and environment for statistical computing*. R Foundation for Statistical Computing. <https://www.R-project.org/>
- Reddy, L., Kanwisher, N. G., & VanRullen, R. (2009). Attention and biased competition in multi-voxel object representations. *Proceedings of the National Academy of Sciences*, 106(50), 21447–21452. <https://doi.org/10.1073/pnas.0907330106>
- Reitan, R. M. (1958). Validity of the trail making test as an indicator of organic brain damage. *Perceptual and Motor Skills*, 8(3), 271–276. <https://doi.org/10.2466/pms.1958.8.3.271>
- Revelle, W. (2020). *psych: Procedures for psychological, psychometric, and personality research* (R package Version 1.9.12 31). Northwestern University.
- Rotomskis, A., Margevičiūtė, R., Germanavičius, A., Kaubrys, G., Budrys, V., & Bagdonas, A. (2015). Differential diagnosis of depression and Alzheimer's disease with the Addenbrooke's Cognitive Examination-Revised (ACE-R). *BMC Neurology*, 15(1), Article 57. <https://doi.org/10.1186/s12883-015-0315-3>
- Ryan, L., Cardoza, J. A., Barense, M. D., Kawa, K. H., Wallentin-Flores, J., Arnold, W. T., & Alexander, G. E. (2012). Age-related impairment in a complex object discrimination task that engages perirhinal cortex. *Hippocampus*, 22(10), 1978–1989. <https://doi.org/10.1002/hipo.22069>
- Sarazin, M., Berr, C., De Rotrou, J., Fabrigoule, C., Pasquier, F., Legrain, S., Michel, B., Puel, M., Volteau, M., Touchon, J., Verny, M., & Dubois, B. (2007). Amnesic syndrome of the medialtemporal type identifies prodromal AD: A longitudinal study. *Neurology*, 69(19), 1859–1867. <https://doi.org/10.1212/01.wnl.0000279336.36610.f7>
- Schwarz, C. G., Gunter, J. L., Wiste, H. J., Przybelski, S. A., Weigand, S. D., Ward, C. P., Senjem, M. L., Vemuri, P., Murray, M. E., Dickson, D. W., Parisi, J. E., Kantarci, K., Weiner, M. W., Petersen, R. C., & Jack, C. R. (2016). A large-scale comparison of cortical thickness and volume methods for measuring Alzheimer's disease severity. *NeuroImage: Clinical*, 11, 802–812. <https://doi.org/10.1016/j.nicl.2016.05.017>
- Seyedi, S., Jafari, R., Talaei, A., Naseri, S., Momennezhad, M., Moghaddam, M. D., & Akbari-Lalimi, H. (2020). Comparing VBM and ROI analyses for detection of gray matter abnormalities in patients with bipolar disorder using MRI. *Middle East Current Psychiatry*, 27(1), Article 69. <https://doi.org/10.1186/s43045-020-00076-3>
- Sone, D., Imabayashi, E., Maikusa, N., Okamura, N., Furumoto, S., Kudo, Y., Ogawa, M., Takano, H., Yokoi, Y., Sakata, M., Tsukamoto, T.,

- Kato, K., & Matsuda, H. (2017). Regional tau deposition and subregion atrophy of medial temporal structures in early Alzheimer's disease: A combined positron emission tomography/magnetic resonance imaging study. *Alzheimer's & Dementia: Diagnosis, Assessment & Disease Monitoring*, 9(1), 35–40. <https://doi.org/10.1016/j.dadm.2017.07.001>
- Staresina, B. P., & Davachi, L. (2010). Object unitization and associative memory formation are supported by distinct brain regions. *Journal of Neuroscience*, 30(29), 9890–9897. <https://doi.org/10.1523/JNEUROSCI.0826-10.2010>
- Taylor, K. I., & Probst, A. (2008). Anatomic localization of the transentorhinal region of the perirhinal cortex. *Neurobiology of Aging*, 29(10), 1591–1596. <https://doi.org/10.1016/j.neurobiolaging.2007.03.024>
- Testa, C., Laakso, M. P., Sabbatoli, F., Rossi, R., Beltramello, A., Soinen, H., & Frisoni, G. B. (2004). A comparison between the accuracy of voxel-based morphometry and hippocampal volumetry in Alzheimer's disease. *Journal of Magnetic Resonance Imaging*, 19(3), 274–282. <https://doi.org/10.1002/jmri.20001>
- Thalman, B., Spiegel, R., Stähelin, H. B., Brubacher, D., Ermini-Fünfschilling, D., Bläsi, S., & Monsch, A. U. (2002). Dementia screening in general practice: Optimized scoring for the Clock Drawing Test. *Brain Aging*, 2, 36–43. <https://doi.org/10.1093/ageing/afu157>
- Tsopelas, C., Stewart, R., Savva, G. M., Brayne, C., Ince, P., Thomas, A., & Matthews, F. E. (2011). Neuropathological correlates of late-life depression in older people. *The British Journal of Psychiatry*, 198(2), 109–114. <https://doi.org/10.1192/bjp.bp.110.078816>
- Van Hoesen, G. W. (1995). Anatomy of the medial temporal lobe. *Magnetic Resonance Imaging*, 13(8), 1047–1055. [https://doi.org/10.1016/0730-725X\(95\)02012-1](https://doi.org/10.1016/0730-725X(95)02012-1)
- Wagemans, J., Elder, J. H., Kubovy, M., Palmer, S. E., Peterson, M. A., Singh, M., von der Heydt, R., & the Perceptual Grouping and Figure-Ground Organization. (2012). A century of Gestalt psychology in visual perception: I. Perceptual grouping and figure-ground organization. *Psychological Bulletin*, 138(6), 1172–1217. <https://doi.org/10.1037/a0029333>
- Warren, D. E., Duff, M. C., Tranel, D., & Cohen, N. J. (2011). Observing degradation of visual representations over short intervals when medial temporal lobe is damaged. *Journal of Cognitive Neuroscience*, 23(12), 3862–3873. [https://doi.org/10.1162/jocn\\_a\\_00089](https://doi.org/10.1162/jocn_a_00089)
- Warton, D. I., & Hui, F. K. C. (2011). The arcsine is asinine: The analysis of proportions in ecology. *Ecology*, 92(1), 3–10. <https://doi.org/10.1890/10-0340.1>
- Wickham, H. (2016). *Ggplot2: Elegant graphics for data analysis* (2nd ed.). Springer International Publishing. <https://doi.org/10.1007/978-3-319-24277-4>
- Wilcockson, T. D. W., Mardanbegi, D., Xia, B., Taylor, S., Sawyer, P., Gellersen, H. W., Leroy, I., Killick, R., & Crawford, T. J. (2019). Abnormalities of saccadic eye movements in dementia due to Alzheimer's disease and mild cognitive impairment. *Aging (Albany NY)*, 11(15), 5389–5398. <https://doi.org/10.18632/aging.102118>
- Winblad, B., Palmer, K., Kivipelto, M., Jelic, V., Fratiglioni, L., Wahlund, L.-O., Nordberg, A., Bäckman, L., Albert, M., Almkvist, O., Arai, H., Basun, H., Blennow, K., de Leon, M., DeCarli, C., Erkinjuntti, T., Giacobini, E., Graff, C., Hardy, J., ... Petersen, R. C. (2004). Mild cognitive impairment—beyond controversies, towards a consensus: Report of the International Working Group on mild cognitive impairment. *Journal of Internal Medicine*, 256(3), 240–246. <https://doi.org/10.1111/j.1365-2796.2004.01380.x>
- Woods, D. L., Wyma, J. M., Yund, E. W., Herron, T. J., & Reed, B. (2015). Factors influencing the latency of simple reaction time. *Frontiers in Human Neuroscience*, 9, Article 131. <https://doi.org/10.3389/fnhum.2015.00131>
- Xie, L., Wisse, L. E. M., Pluta, J., de Flores, R., Piskin, V., Manjón, J. V., Wang, H., Das, S. R., Ding, S.-L., Wolk, D. A., & Yushkevich, P. A. (2019). Automated segmentation of medial temporal lobe subregions on in vivo T1-weighted MRI in early stages of Alzheimer's disease. *Human Brain Mapping*, 40(12), 3431–3451. <https://doi.org/10.1002/hbm.24607>
- Yeung, L.-K., Olsen, R. K., Bild-Enkin, H. E. P., D'Angelo, M. C., Kacollja, A., McQuiggan, D. A., Keshabyan, A., Ryan, J. D., & Barense, M. D. (2017). Anterolateral entorhinal cortex volume predicted by altered intra-item configural processing. *The Journal of Neuroscience*, 37(22), 5527–5538. <https://doi.org/10.1523/JNEUROSCI.3664-16.2017>

(Appendices follow)

## Appendix A

## Detailed Results of the Pilot study

## Interpretation of Table A1 and Figure A1

Participants diagnosed with aMCI as well as participants diagnosed with Alzheimer's dementia performed significantly worse than NCs. Compared to font type "AD," participants achieved higher scores of %correct when the odd-one was written in the "Air" font, while they performed lower for fonts "Chi," "Pap," and "Vin." There was a significant interaction between aMCI participants and font "Air." These

**Table A1**

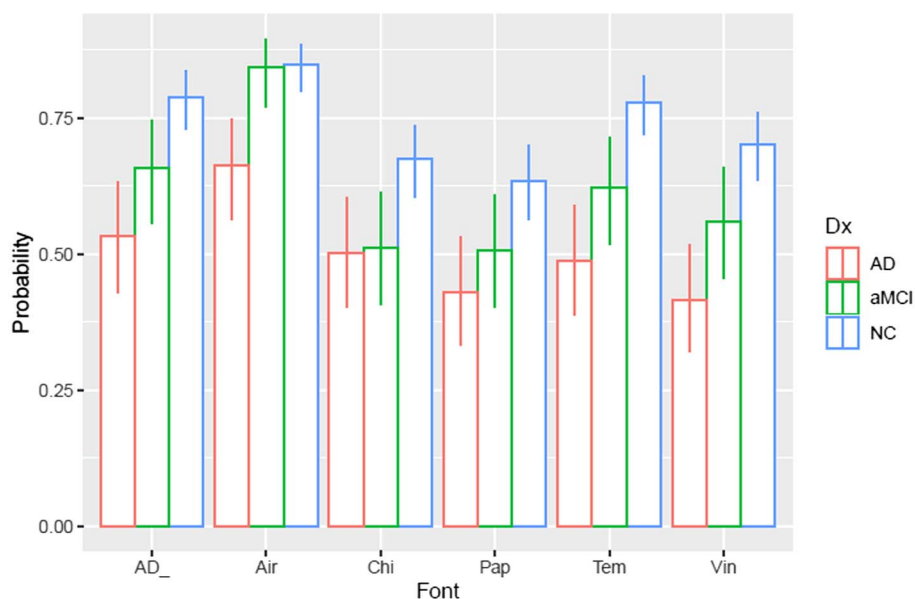
Results of Mixed-Effects Logistic Regressions of %Correct for Font Type and Diagnostic Group in the Pilot Study

Variable	Estimate	SD	z value	Pr(> z )
(Intercept)	1.3099	0.1622	8.07	6.80e <sup>-16</sup> ***
DxaMCI	-0.6605	0.2712	-2.44	0.01488*
DxAD	-1.1820	0.2654	-4.45	8.40e <sup>-06</sup> ***
fontAir	0.3992	0.1753	2.28	0.02276*
fontChi	-0.5832	0.1583	-3.68	0.00023***
fontPap	-0.7591	0.1569	-4.84	1.30e <sup>-06</sup> ***
fontTem	-0.0551	0.1653	-0.33	0.73865
fontVin	-0.4570	0.1595	-2.86	0.00417**
DxaMCI: fontAir	0.6277	0.2934	2.14	0.03240*
DxAD: fontAir	0.1458	0.2673	0.55	0.58560
DxaMCI: fontChi	-0.0202	0.2618	-0.08	0.93839
DxAD: fontChi	0.4661	0.2530	1.84	0.06537
DxaMCI: fontPap	0.1347	0.2609	0.52	0.60562
DxAD: fontPap	0.3483	0.2527	1.38	0.16821
DxaMCI: fontTem	-0.1003	0.2675	-0.38	0.70757
DxAD: fontTem	-0.1204	0.2574	-0.47	0.64007
DxaMCI: fontVin	0.0434	0.2628	0.17	0.86885
DxAD: fontVin	-0.0134	0.2547	-0.05	0.95819

Note. Reference for the font is font type called "AD," reference for the diagnostic group is the normal control group. SD = standard error; Dx = diagnosis; aMCI = amnesic mild cognitive impairment; AD = Alzheimer's dementia; Air, Chi, Pap, Tem, and Vin are the names of the font.  $p < .1$ . \* $p < .05$ . \*\* $p < .01$ . \*\*\* $p < .001$ .

**Figure A1**

Percentage Correct for Font Types and Diagnostic Groups in the Pilot Study



Note. See the online article for the color version of this figure.

(Appendices continue)



results suggest that participants were more likely to detect the odd-one when it was written in font “Air” compared to the other fonts. However, since this was the case for all groups, we did not make any adjustments to the fonts.

### Interpretation of Table A2 and Figure A2

As expected, NCs had the best rate of accuracy, AD showed worst performance and aMCI were in the middle. This was the same for all locations. Most errors were performed by all groups on location 4.

**Table A2**

*Results of Mixed-Effects Logistic Regressions of %Correct for Location of the Odd-One and Diagnostic Group in the Pilot Study*

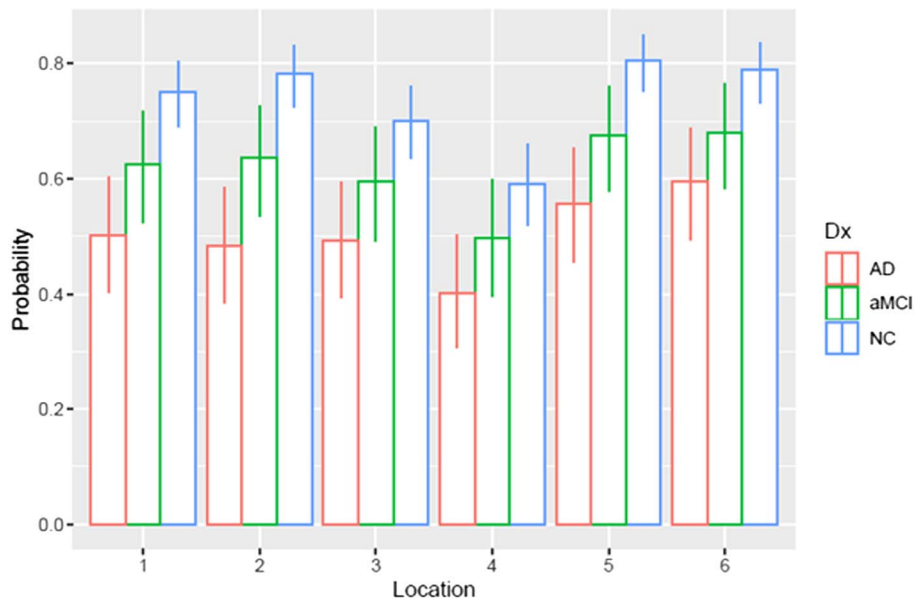
Variable	Estimate	SD	z value	Pr(> z )
(Intercept)	1.1083	0.1570	7.06	1.70e <sup>-12***</sup>
DxaMCI	-0.5957	0.2648	-2.25	0.024*
DxAD	-1.0975	0.2603	-4.22	2.50e <sup>-05***</sup>
location2	0.1724	0.1622	1.06	0.288
location3	-0.2561	0.1558	-1.64	0.100
location4	-0.7370	0.1519	-4.85	1.20e <sup>-06***</sup>
location5	0.3145	0.1651	1.91	0.057
location6	0.2141	0.1630	1.31	0.189
DxaMCI: location2	-0.1288	0.2641	-0.49	0.626
DxAD: location2	-0.2502	0.2552	-0.98	0.327
DxaMCI: location3	0.1270	0.2591	0.49	0.624
DxAD: location3	0.2172	0.2511	0.86	0.387
DxaMCI: location4	0.2097	0.2559	0.82	0.412
DxAD: location4	0.3244	0.2501	1.30	0.195
DxaMCI: location5	-0.0923	0.2675	-0.35	0.730
DxAD: location5	-0.0999	0.2574	-0.39	0.698
DxaMCI: location6	0.0310	0.2665	0.12	0.907
DxAD: location6	0.1589	0.2568	0.62	0.536

*Note.* Reference for location is location 1, reference for the diagnostic group is the normal control group. SD = standard error; Dx = diagnosis; aMCI = amnesic mild cognitive impairment; AD = Alzheimer’s dementia.

$p < .1$ . \* $p < .05$ . \*\* $p < .01$ . \*\*\* $p < .001$ .

**Figure A2**

*%Correct for Location of the Odd-One and Diagnostic Groups in the Pilot Study*



*Note.* Dx = diagnosis; aMCI = amnesic mild cognitive impairment; AD = Alzheimer’s dementia; NC = normal control. See the online article for the color version of this figure.

(Appendices continue)

### Interpretation of Table A3 and Figure A3

There is no specific difference between NODF levels 1 and 2.

**Table A3**

*Results of Mixed-Effects Logistic Regressions of %Correct for Number of Distinctive Features Within the Odd-One and Diagnostic Group in the Pilot Study*

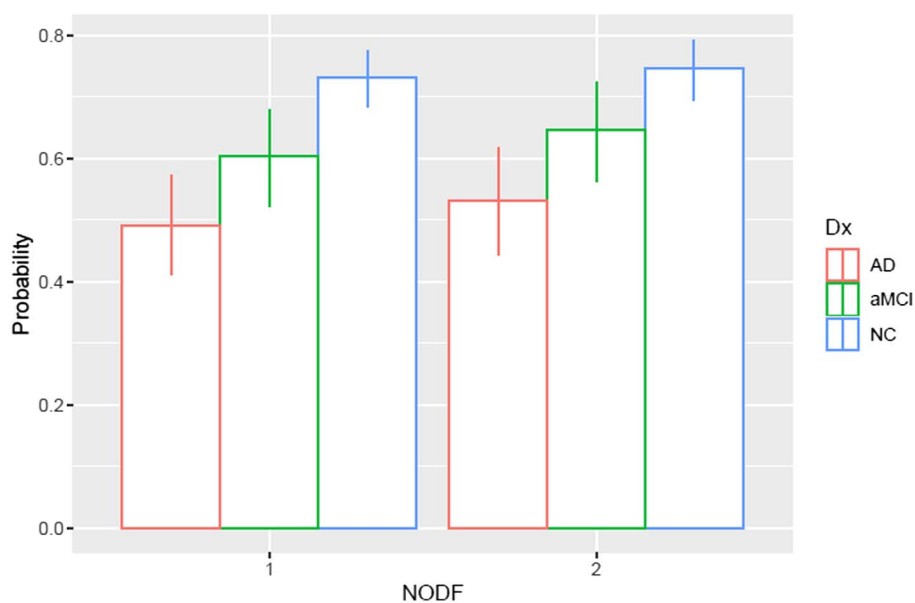
Variable	Estimate	SD	z value	Pr(> z )
(Intercept)	1.0070	0.1203	8.37	<2e <sup>-16</sup> ***
DxaMCI	-0.5879	0.2064	-2.85	0.0044**
DxAD	-1.0399	0.2050	-5.07	3.9e <sup>-07</sup> ***
NODF2	0.0777	0.0964	0.81	0.4199
DxaMCI: NODF2	0.1119	0.1600	0.70	0.4840
DxAD: NODF2	0.0825	0.1544	0.53	0.5934

*Note.* Reference for number of distinctive features is one distinctive feature (NODF1), reference for the diagnostic group is the normal control group. SD = standard error; Dx = diagnosis; aMCI = amnesic mild cognitive impairment; AD = Alzheimer's dementia; NODF = number of distinctive features.

\*  $p < .05$ . \*\*  $p < .01$ . \*\*\*  $p < .001$ .

**Figure A3**

*%Correct for Number of Distinctive Features Within the Odd-One and Diagnostic Groups in the Pilot Study*



*Note.* Dx = diagnosis; aMCI = amnesic mild cognitive impairment; AD = Alzheimer's dementia; NC = normal control. See the online article for the color version of this figure.

(Appendices continue)

### Interpretation of Table A4 and Figure A4

For items with NOF levels 2, 3, and 4, aMCI and Alzheimer's dementia groups performed relatively similar, indicating that items with NOF levels 5, 6, and 7 might differentiate better between groups.

**Table A4**

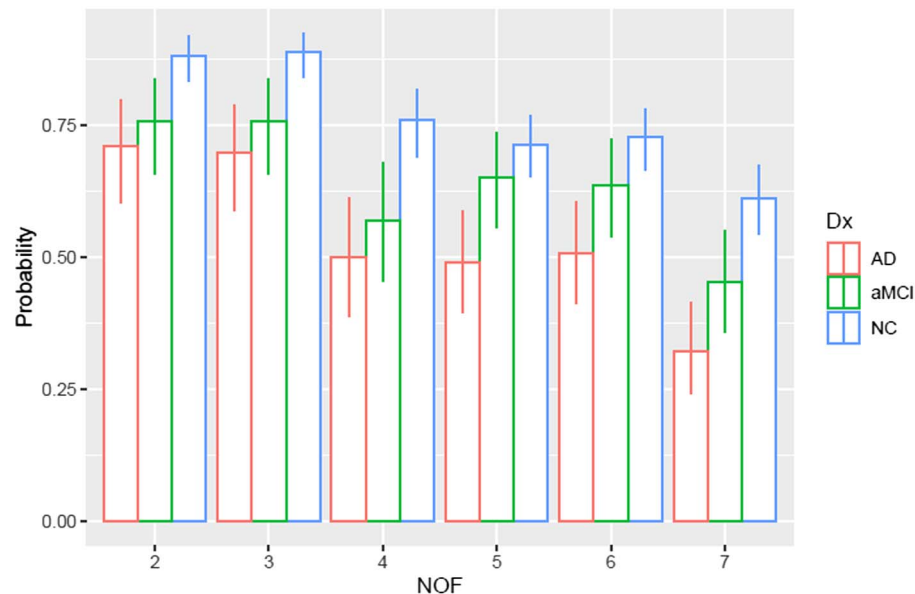
*Results of Mixed-Effects Logistic Regressions of Number of Feature of the Odd-One and Diagnostic Group in the Pilot Study*

Variable	Estimate	SD	z value	Pr(> z )
(Intercept)	2.00355	0.20783	9.64	<2e <sup>-16</sup> ***
DxaMCI	-0.86239	0.32789	-2.63	0.00853**
DxAD	-1.10686	0.32041	-3.45	0.00055***
NOF3	0.06192	0.24745	0.25	0.80240
NOF4	-0.85837	0.22268	-3.85	0.00012***
NOF5	-1.09241	0.19794	-5.52	3.40E <sup>-08</sup> ***
NOF6	-1.02888	0.19836	-5.19	2.10E <sup>-07</sup> ***
NOF7	-1.55382	0.19593	-7.93	2.20E <sup>-15</sup> ***
DxaMCI: NOF3	-0.06194	0.37224	-0.17	0.86784
DxAD: NOF3	-0.12953	0.35876	-0.36	0.71806
DxaMCI: NOF4	-0.00348	0.34670	-0.01	0.99200
DxAD: NOF4	-0.0372	0.33636	-0.11	0.91194
DxaMCI: NOF5	0.57285	0.30758	1.86	0.06254.
DxAD: NOF5	0.15275	0.29679	0.51	0.60678
DxaMCI: NOF6	0.44265	0.30754	1.44	0.15006
DxAD: NOF6	0.16268	0.29702	0.55	0.58389
DxaMCI: NOF7	0.21892	0.30545	0.72	0.47355
DxAD: NOF7	-0.08725	0.29872	-0.29	0.77023

*Note.* Reference for number of features is two features (NOF2), reference for the diagnostic group is the normal control group. SD = standard error; Dx = diagnosis; aMCI = amnesic mild cognitive impairment; AD = Alzheimer's dementia; NOF = number of features.  $p < .1$ . \*  $p < .05$ . \*\*  $p < .01$ . \*\*\*  $p < .001$ .

**Figure A4**

*%Correct for Number of Features Within the Odd-One and Diagnostic Groups in the Pilot Study*



*Note.* Dx = diagnosis; aMCI = amnesic mild cognitive impairment; AD = Alzheimer's dementia; NC = normal control. See the online article for the color version of this figure.

(Appendices continue)

### Interpretation of Table A5 and Figure A5

There seems to be a ceiling effect for NOF2 and 3. Further, the performance of aMCI and Alzheimer's dementia groups are rather similar for items with NOF4. Most promising to differentiate between all three groups are items with NOF5 and NODF1, NOF6 and NODF1, and NOF7 with either NODF1 or NODF2.

**Table A5**

*Results of Mixed-Effects Logistic Regressions of Number of Feature Combined With Number of Different Features of the Odd-One and Diagnostic Group in the Pilot Study*

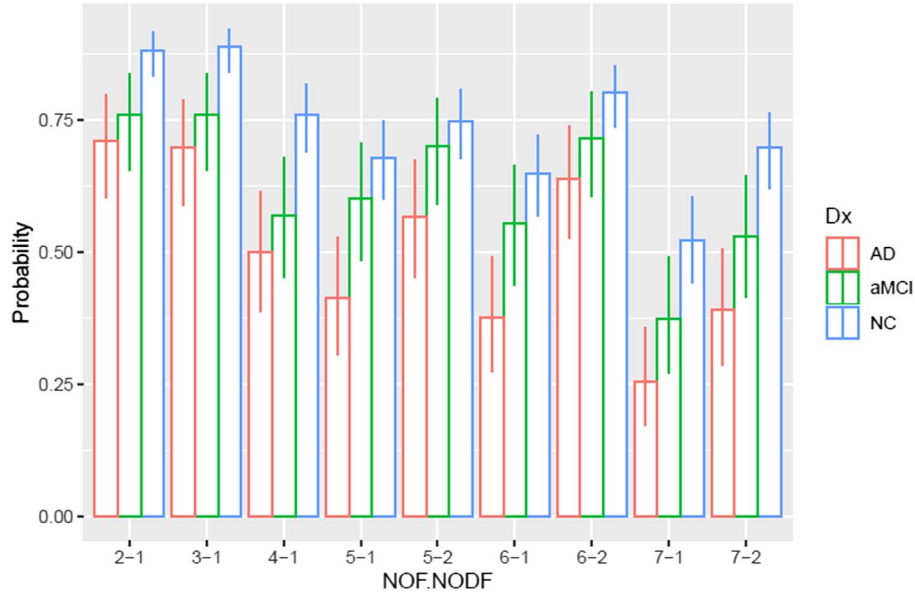
Variable	Estimate	SD	z value	Pr(> z )
(Intercept)	2.01055	0.20932	9.61	<2e <sup>-16</sup> ***
DxaMCI	-0.86469	0.33058	-2.62	0.00889**
DxAD	-1.11024	0.32307	-3.44	0.00059***
NOF.NODF3-1	0.06215	0.24794	0.25	0.80206
NOF.NODF4-1	-0.86202	0.22321	-3.86	0.00011***
NOF.NODF5-1	-1.26377	0.21797	-5.80	6.60E <sup>-09</sup> ***
NOF.NODF6-1	-1.39819	0.21675	-6.45	1.10E <sup>-10</sup> ***
NOF.NODF7-1	-1.91709	0.21452	-8.94	<2e <sup>-16</sup> ***
NOF.NODF5-2	-0.92035	0.22225	-4.14	3.50E <sup>-05</sup> ***
NOF.NODF6-2	-0.61329	0.22797	-2.69	0.00714**
NOF.NODF7-2	-1.17711	0.21882	-5.38	7.50E <sup>-08</sup> ***
DxaMCI: NOF.NODF3-1	-0.06218	0.37299	-0.17	0.86761
DxAD: NOF.NODF3-1	-0.13001	0.35947	-0.36	0.71759
DxaMCI: NOF.NODF4-1	-0.00343	0.34755	-0.01	0.99211
DxAD: NOF.NODF4-1	-0.03708	0.33713	-0.11	0.91242
DxaMCI: NOF.NODF5-1	0.52727	0.34467	1.53	0.12607
DxAD: NOF.NODF5-1	0.00774	0.33493	0.02	0.98156
DxaMCI: NOF.NODF6-1	0.46889	0.34317	1.37	0.17183
DxAD: NOF.NODF6-1	-0.01077	0.33544	-0.03	0.97439
DxaMCI: NOF.NODF7-1	0.25471	0.34415	0.74	0.45923
DxAD: NOF.NODF7-1	-0.05839	0.34279	-0.17	0.86475
DxaMCI: NOF.NODF5-2	0.62326	0.35157	1.77	0.07626
DxAD: NOF.NODF5-2	0.28799	0.33696	0.85	0.39274
DxaMCI: NOF.NODF6-2	0.38797	0.35624	1.09	0.27612
DxAD: NOF.NODF6-2	0.28634	0.34283	0.84	0.40359
DxaMCI: NOF.NODF7-2	0.15258	0.34431	0.44	0.65766
DxAD: NOF.NODF7-2	-0.17021	0.33622	-0.51	0.61268

*Note.* Reference for number of features combined with number of different features is two features with one different feature (NOF.NODF2-1), reference for the diagnostic group is the normal control group. SD = standard error; Dx = diagnosis; aMCI = amnesic mild cognitive impairment; AD = Alzheimer's dementia; NOF = number of features; NODF = number of different features.  
 $p < .1$ . \*  $p < .05$ . \*\*  $p < .01$ . \*\*\*  $p < .001$ .

(Appendices continue)



**Figure A5**  
 %Correct for Number of Features Combining Number of Different Features of the Odd-One and Diagnostic Groups in the Pilot Study



*Note.* Dx = diagnosis; aMCI = amnesic mild cognitive impairment; AD = Alzheimer’s dementia; NC = normal control. See the online article for the color version of this figure.

**Appendix B**

**Results of Secondary Analyses of the Validation Study**

**Interpretation of Appendix B**

None of the linear regressions of %correct responses in the oddity detection task modeled by cortical thickness values of MTL subregions of the right hemisphere (right mPRC, right IPRC, right ERC, and right PHC), as well as their volume estimates for each hemisphere, achieved small *p* values.

**Table B1**

*Results of the Linear Regression of %Correct Responses in the Oddity Detection Task Modeled Separately by Right mPRC and Right IPRC Thickness Values and Covariates in the Validation Study*

Variable	Right mPRC				Right IPRC			
	Estimate	SE	<i>t</i>	<i>p</i>	Estimate	SE	<i>t</i>	<i>p</i>
(Intercept)	1.063	0.277	3.837	<.001	1.153	0.284	4.052	<.001
Age	-0.0055	0.0025	-2.230	.029	-0.0060	0.0023	-2.624	.011
Education	0.026	0.008	3.280	.002	0.026	0.008	3.292	.002
Remale	-0.005	0.053	-0.086	.932	-0.001	0.053	0.024	.981
Thickness	0.016	0.039	0.394	.695	-0.004	0.049	-0.084	.934
<i>R</i> <sup>2</sup>	.297				.295			

*Note.* This table demonstrates linear regression results of task performance modeled by cortical thickness of the right medial perirhinal cortex (mPRC),  $F(4, 73) = 7.697, p < .001$ , and the right lateral perirhinal cortex (IPRC),  $F(4, 73) = 7.644, p < .001$ .

(Appendices continue)

**Table B2**

Results of the Linear Regression of %Correct Responses in the Oddity Detection Task Modeled Separately by Right ERC and Right PHC Thickness Values and Covariates in the Validation Study

Variable	Right ERC				Right PHC			
	Estimate	SD	<i>t</i>	<i>p</i>	Estimate	SD	<i>t</i>	<i>p</i>
(Intercept)	1.188	0.278	4.269	<.001	1.025	0.338	3.036	.003
Age	-0.0062	0.0023	-2.667	.009	-0.0055	0.0024	-2.324	.023
Education	0.026	0.008	3.254	.002	0.026	0.008	3.304	.001
Female	0.001	0.052	0.018	.985	-0.003	0.052	-0.058	.954
Thickness	-0.010	0.036	-0.279	.781	0.033	0.079	0.416	.679
<i>R</i> <sup>2</sup>	.296							

Note. This table demonstrates linear regression results of task performance modeled by cortical thickness of the right entorhinal cortex (ERC),  $F(4, 73) = 7.669$ ,  $p < .001$ , and the right parahippocampal cortex (PHC),  $F(4, 73) = 7.703$ ,  $p < .001$ .

**Table B3**

Results of the Linear Regression of %Correct Responses in the Oddity Detection Task Modeled by mPRC Volume and Covariates in the Validation Study

Variable	Left mPRC				Right mPRC			
	Estimate	SD	<i>t</i>	<i>p</i>	Estimate	SD	<i>t</i>	<i>p</i>
(Intercept)	1.044	0.262	3.984	<.001	0.937	0.246	3.812	<.001
Age	-0.0053	0.0024	-2.245	.028	-0.0048	0.0022	-2.145	.035
Education	0.027	0.008	3.323	.001	0.026	0.008	3.254	.002
Female	0.002	0.052	0.034	.097	-0.005	0.051	-0.097	.097
Thickness	0.0001	0.001	0.571	.569	0.0002	0.001	1.437	.155
<i>R</i> <sup>2</sup>	.298				.315			

Note. This table demonstrates linear regression results of task performance modeled by volume of the medial perirhinal cortex (mPRC) for the left,  $F(4, 73) = 7.757$ ,  $p < .001$ , and right,  $F(4, 73) = 8.374$ ,  $p < .001$ , hemisphere.

**Table B4**

Results of the Linear Regression of %Correct Responses in the Oddity Detection Task Modeled by ERC Volume and Covariates in the Validation Study

Variable	Left ERC				Right ERC			
	Estimate	SD	<i>t</i>	<i>p</i>	Estimate	SD	<i>t</i>	<i>p</i>
(Intercept)	1.089	0.266	4.085	<.001	1.089	0.256	4.215	<.001
Age	-0.0055	0.0026	-2.098	.039	-0.0055	0.0025	-2.146	.035
Education	0.026	0.008	3.298	.002	0.026	0.008	3.281	.002
Female	-0.001	0.052	-0.027	.979	-0.002	0.052	-0.047	.963
Thickness	0.00002	0.0001	0.280	.780	0.00002	0.0001	0.363	.718
<i>R</i> <sup>2</sup>	.296				.296			

Note. This table demonstrates linear regression results of task performance modeled by volume of the entorhinal cortex (ERC) for the left,  $F(4, 73) = 7.669$ ,  $p < .001$ , and right,  $F(4, 73) = 8.374$ ,  $p < .001$ , hemisphere.

(Appendices continue)

**Table B5**

*Results of the Linear Regression of %Correct Responses in the Oddity Detection Task Modeled by IPRC Volume and Covariates in the Validation Study*

Variable	Left IPRC				Right IPRC			
	Estimate	SD	<i>t</i>	<i>P</i>	Estimate	SD	<i>t</i>	<i>p</i>
(Intercept)	0.911	0.246	3.708	<.001	1.019	0.251	4.066	<.001
Age	-0.0045	0.0023	-2.000	.049	-0.0054	0.0022	-2.418	.018
Education	0.026	0.008	3.253	.002	0.027	0.008	3.339	.001
Female	0.001	0.051	0.013	.989	0.003	0.052	0.050	.960
Thickness	0.0002	0.0001	1.614	.111	0.0001	0.0001	0.815	.418
<i>R</i> <sup>2</sup>	.319				.302			

*Note.* This table demonstrates linear regression results of task performance modeled by volume of the lateral perirhinal cortex (IPRC) for the left,  $F(4, 73) = 7.658$ ,  $p < .001$ , and right,  $F(4, 73) = 7.877$ ,  $p < .001$ , hemisphere.

**Table B6**

*Results of the Linear Regression of %Correct Responses in the Oddity Detection Task Modeled by PHC Volume and Covariates in the Validation Study*

Variable	Left PHC				Right PHC			
	Estimate	SD	<i>t</i>	<i>p</i>	Estimate	SD	<i>t</i>	<i>p</i>
(Intercept)	1.039	0.261	3.986	<.001	1.057	0.278	4.103	<.001
Age	-0.0056	0.0023	-2.441	.017	-0.0056	0.0022	-2.531	.014
Education	0.027	0.008	3.334	.001	0.027	0.008	3.329	.001
Female	-0.004	0.052	-0.075	.940	0.005	0.053	0.092	.927
Thickness	0.00005	0.0001	0.609	.545	0.00004	0.0001	0.512	.610
<i>R</i> <sup>2</sup>	.299				.298			

*Note.* This table demonstrates linear regression results of task performance modeled by volume of the parahippocampal cortex (PHC) for the left,  $F(4, 73) = 7.773$ ,  $p < .001$ , and right,  $F(4, 73) = 7.734$ ,  $p < .001$ , hemisphere.

Received February 1, 2022  
 Revision received July 24, 2022  
 Accepted August 3, 2022 ■

## 2.2. Studie II

Excellent Interrater Reliability for Manual Segmentation of the Medial Perirhinal Cortex

## Article

# Excellent Interrater Reliability for Manual Segmentation of the Medial Perirhinal Cortex

Nicolas A. Henzen<sup>1,2,\*</sup>, Julia Reinhardt<sup>3,4,5</sup>, Maria Blatow<sup>6</sup>, Reto W. Kressig<sup>1,7</sup> and Sabine Krumm<sup>1,7</sup> <sup>1</sup> University Department of Geriatric Medicine FELIX PLATTER, 4055 Basel, Switzerland<sup>2</sup> Faculty of Psychology, University of Basel, 4001 Basel, Switzerland<sup>3</sup> Division of Diagnostic and Interventional Neuroradiology, Department of Radiology, University Hospital Basel, University of Basel, 4031 Basel, Switzerland<sup>4</sup> Department of Cardiology and Cardiovascular Research Institute Basel (CRIB), University Hospital Basel, University of Basel, 4031 Basel, Switzerland<sup>5</sup> Department of Orthopedic Surgery and Traumatology, University Hospital of Basel, University of Basel, 4031 Basel, Switzerland<sup>6</sup> Section of Neuroradiology, Department of Radiology and Nuclear Medicine, Neurocenter, Cantonal Hospital Lucerne, University of Lucerne, 6000 Lucerne, Switzerland<sup>7</sup> Faculty of Medicine, University of Basel, 4056 Basel, Switzerland

\* Correspondence: nicolas.henzen@felixplatter.ch; Tel.: +41-61-326-47-83

**Abstract:** *Objective:* Evaluation of interrater reliability for manual segmentation of brain structures that are affected first by neurofibrillary tau pathology in Alzheimer's disease. *Method:* Medial perirhinal cortex, lateral perirhinal cortex, and entorhinal cortex were manually segmented by two raters on structural magnetic resonance images of 44 adults (20 men; mean age = 69.2 ± 10.4 years). Intraclass correlation coefficients (ICC) of cortical thickness and volumes were calculated. *Results:* Very high ICC values of manual segmentation for the cortical thickness of all regions (0.953–0.986) and consistently lower ICC values for volume estimates of the medial and lateral perirhinal cortex (0.705–0.874). *Conclusions:* The applied manual segmentation protocol allows different raters to achieve remarkably similar cortical thickness estimates for regions of the parahippocampal gyrus. In addition, the results suggest a preference for cortical thickness over volume as a reliable measure of atrophy, especially for regions affected by collateral sulcus variability (i.e., medial and lateral perirhinal cortex). The results provide a basis for future automated segmentation and collection of normative data.

**Keywords:** Alzheimer's disease; perirhinal cortex; entorhinal cortex; segmentation; structural MRI



**Citation:** Henzen, N.A.; Reinhardt, J.; Blatow, M.; Kressig, R.W.; Krumm, S. Excellent Interrater Reliability for Manual Segmentation of the Medial Perirhinal Cortex. *Brain Sci.* **2023**, *13*, 850. <https://doi.org/10.3390/brainsci13060850>

Academic Editors: Anna Kozłowska, Andrew Chih Wei Huang, Seong Soo A. An, Bai Chuang Shyu and Muh-Shi Lin

Received: 7 April 2023  
Revised: 15 May 2023  
Accepted: 18 May 2023  
Published: 24 May 2023



**Copyright:** © 2023 by the authors. Licensee MDPI, Basel, Switzerland. This article is an open access article distributed under the terms and conditions of the Creative Commons Attribution (CC BY) license (<https://creativecommons.org/licenses/by/4.0/>).

## 1. Introduction

Detecting the earliest signs of Alzheimer's disease (AD) is a great challenge since the progressive neurodegenerative disease usually remains unnoticed until difficulties in daily living activities emerge [1]. At this stage, neuropathological brain changes in domains such as memory, language, executive processing, or visuospatial functioning are objectified with standard neuropsychological assessments [2,3]. However, neuropathological brain changes associated with AD are thought to begin years before the onset of clinical symptoms. The main neuropathological markers of AD are  $\beta$ -amyloid plaques and neurofibrillary tangles (NFT) of pathological tau protein [4]. In comparison to the extracellular amyloid plaques, intracellular NFT occur more numerous and in a more hierarchical pattern in the temporal lobe [5]. NFT disturb neuronal functioning and are thought to be more strongly correlated to cognitive impairment than amyloid plaques [5–7]. The continuous deposition of NFT in AD is closely associated with neuron loss [4,8] and is believed to be causally linked to cerebral atrophy [9]. NFT density is indirectly reflected by grey matter atrophy in structural magnetic resonance imaging (MRI) [10]. Against this background, the present study focuses on NFT. In typical AD, this neurofibrillary tau pathology starts in the medial part of the

perirhinal cortex (mPRC), also referred to as the transentorhinal cortex [4,11]. As the disease progresses, NFT spread to the entorhinal cortex (ERC) and eventually to hippocampal subfields and throughout the brain [4,12]. In support of this notion, Sone et al. [13] found regional NFT accumulation in early-stage AD to be associated with cortical thinning in the perirhinal cortex and ERC. Hippocampal atrophy, on the other hand, was more strongly associated with a higher number of  $\beta$ -amyloid plaques [13]. Accordingly, sensitive preclinical structural imaging biomarkers enable the earliest diagnosis and, thus, treatment with current symptomatic as well as future disease-modifying drugs when as little damage as possible has been done [2,14]. Furthermore, the earliest neuropathological predictors allow the tracking of disease progression and are of significant interest in AD research as well as the clinical setting [15].

Regions of the parahippocampal gyrus (e.g., ERC, mPRC) of the medial temporal lobe are associated with atrophy in the early stages of AD. As mentioned before, in typical AD, the neurofibrillary tau pathology starts in the mPRC before spreading to the ERC and hippocampus [4,11]. Nonetheless, in clinical settings, AD diagnosis commonly relies on atrophy scores of the ERC [16] as well as on medial temporal lobe atrophy scores rating the hippocampus, the choroid fissure, and the lateral ventricle [17]. The mPRC is mostly neglected. Since the mPRC is a fairly small structure (e.g., length of 2.1 cm anterior-posterior and mean width of 0.95 cm in one random cognitively healthy participant segmented by NAH), visual, quantitative evaluation is difficult. However, the assessment of the mPRC integrity in clinical settings could be improved by a computed atrophy value (e.g., cortical thickness). Recent studies support the potential of the mPRC's integrity in clinical settings. For example, Kulason et al. [18] detected significant differences in mPRC but not ERC thickness between individuals with mild cognitive impairment (MCI) and normal controls. Further results revealed cortical thinning in the mPRC 9–14 years prior to an MCI diagnosis, while ERC thinning was measurable 8–11 years prior to diagnosis [19]. In comparison, hippocampus atrophy was found 2–4 years before the clinical symptom onset of AD [20]. Moreover, a study published by Krumm et al. [21] reported patients with amnesic MCI, the presumed prodromal stage of Alzheimer's dementia, to show atrophy of the mPRC before the lateral part of the perirhinal cortex (IPRC). Specifically, the IPRC was only atrophied in patients with Alzheimer's dementia. These findings are in line with the proposed staging of NFT accumulation [4,12] and suggest mPRC integrity as a promising marker to detect the earliest signs of AD. Furthermore, the evaluation of mPRC integrity allows a differentiation to other neurodegenerative diseases in which NFT neuropathology plays a key role but does not primarily affect the mPRC, such as corticobasal degeneration with prominent NFT in the cerebral cortex, specifically in frontoparietal regions [22]. Interpretation of the literature on the perirhinal cortex is harmed by the use of different nomenclature and several changes in the definition of neuroanatomic localization [23]. Braak and Braak first described a transitional area between the ERC and neocortex, namely the transentorhinal region. This region is characterized by a distinct layer of oblique pyramidal cells in layer II, which are highly vulnerable to neurofibrillary changes and are the first to be affected in typical AD [4,24]. According to Taylor and Probst [11], the mPRC coincides with the transentorhinal area by Braak and Braak [24]. Further, the anterior and posterior borders of the mPRC correspond to Brodmann's cytoarchitectonic field 35 [25]. The highly variable nomenclature and differences in defining the areas boundaries make comparison between studies difficult.

As mentioned above, cortical NFT begin in the mPRC, while the IPRC is only affected in a later stage [4]. This reflects the importance of separately segmenting these structures. Otherwise, disease progression may be underestimated in early-stage AD. Anatomically, the collateral sulcus of the medial temporal lobe defines the transition from mPRC to IPRC and is characterized by high inter- and intraindividual differences (e.g., length and form of the sulcus). This collateral sulcus variability represents a significant obstacle to the accurate segmentation of the mPRC and IPRC, as it substantially influences the delimitation of the borders of these regions [11,26]. Specifically, the lack of software that accurately

and automatically segments the mPRC might be the main reason why imaging studies have hardly ever investigated the mPRC separately from the IPRC. A reliable manual segmentation protocol as the basis for future development and validation of an automated segmentation protocol is of significant importance [27].

Comparable to the focus of structural assessment in AD, neuropsychological testing routinely focuses on hippocampal function (e.g., episodic memory tests). As the site of the first NFT, perirhinal functioning might reflect a promising neuropsychological marker in incipient AD. However, specific tasks for perirhinal cortex measurement are not yet readily available. The majority of our current knowledge about the perirhinal cortex results from animal studies. These indicate that the perirhinal cortex is located at the apex of the ventral stream and is associated with visual object processing [28–30]. Originating from the primary visual cortex, the complexity of represented features increases along the ventral visual stream leading to the perirhinal cortex, which is in charge of the most complex visual analyses [28,31,32]. In addition, the perirhinal cortex is connected to various other brain regions and further receives and processes auditory and somatosensory information [33]. A promising oddity detection task testing the ability to form an integrated perceptual representation from similar low-level visual features, a function assigned to the perirhinal cortex, was recently published by Frei et al. [34]. The task reflects a sensitive measure to differentiate early-stage AD patients from cognitively healthy adults. Further, based on the conceptual structure account by Taylor et al. [35], the perirhinal cortex is crucial in the discrimination of highly confusable (e.g., living things) in comparison to less confusable (e.g., non-living things) stimuli. Accordingly, AD patients are expected to show more difficulty processing living than non-living things. This is based on the fact that living things share more similar features, making them easier to confuse than non-living things. Such function of semantic object processing can be assessed by fluency tests. A study by Hirni et al. [36] showed that semantic fluency tests can monitor mPRC integrity. Another study by Krumm et al. [37] demonstrated that the combined measurement of two fluency tests of living things (animals and fruits) best differentiated AD patients and cognitively healthy participants. Overall, these results are very promising and reflect the relevance of further research addressing the perirhinal cortex/mPRC on the challenging path to detect the earliest signs of AD.

In summary, the present study aimed to evaluate the interrater reliability of a manual segmentation protocol, which takes collateral sulcus variability into account (depicted in [21]). Regions of interest (ROIs) for the manual segmentation comprised mPRC, IPRC, and ERC, which are affected in different stages of classic AD and might allow an evaluation of disease progression [4]. High interrater reliability would indicate that the applied manual segmentation protocol allows different raters to achieve highly similar results. In addition, the manual segmentation was carried out by an experienced (SK) and an inexperienced (NAH) rater to assess the practicability of the applied segmentation protocol. Furthermore, we contrasted the interrater reliability of cortical thickness and volume estimates. In comparison to three-dimensional measurements of atrophy (i.e., volumes), cortical thickness of the perirhinal cortex is independent of the form and length of the collateral sulcus [38–40]. Therefore, we expect differences in manual segmentation between the two raters to be more pronounced for volume estimates.

The main object of this study was to: (1) evaluate the interrater reliability of a manual segmentation protocol for the mPRC, IPRC, and ERC between two raters with different levels of experience and (2) compare two measurements of atrophy estimates (cortical thickness vs. volume).

## 2. Materials and Methods

### 2.1. Participants

In a clinical setting, a potential future automated segmentation protocol would be applied to patients with different diseases. To satisfy this circumstance, data from 44 native Swiss-German or German-speaking adults (20 men; mean age = 69.2 years,

SD = 10.42 years) were randomly selected from a larger study (N = 131) at the Memory Clinic FELIX PLATTER, University Department of Geriatric Medicine FELIX PLATTER, Basel, Switzerland. The random selection process was performed by NAH while fully blinded to participant information (i.e., diagnosis, age, gender, and education). Only after manual segmentation was NAH unblinded, and participants were assigned to 1 of 4 groups, namely cognitively healthy normal controls (NCs), Major Depression (MD), MCI or dementia due to AD, and MCI or dementia due to other etiologies than AD (non-AD; e.g., due to Lewy body disease). See Table 1 for a more detailed overview. Cognitively healthy NCs were recruited from the “Registry of Healthy Individuals Interested to Participate in Research” of the Memory Clinic University Department of Geriatric Medicine FELIX PLATTER Basel, Switzerland. Thorough medical screening ensured their neurologic and psychiatric health (exclusion criteria: severe sensory or motor deficits; severe visual, auditory or speech deficits; severe systemic disease; diseases with severe or probable impact on the central nervous system [e.g., neurologic disorders including cerebral-vascular diseases, generalized atherosclerosis, and psychiatric problems]; continuous mild-to intense pain; and intake of potent psychoactive substances, except minor tranquilizers). In addition, they were not allowed to have more than 1 score out of the normal range on the Mini-Mental State Examination (MMSE; [41]), the Basel Verbal Learning Test (BVL, the German equivalent to the California Verbal Learning Test; [42]), Trail Making Test B [43], or the 16-items version of the Informant Questionnaire on Cognitive Decline in the Elderly [44]. All tests were administered in Swiss German or German. The AD group consisted of nine patients diagnosed with Alzheimer’s dementia according to DSM-IV [45] and NINCDS-ADRDA criteria [46] and nine patients diagnosed with amnesic MCI [47] according to DSM-IV [45] and Winblad et al. [48] criteria. The non-AD group contained three patients diagnosed with dementia due to other etiologies than AD (two due to Lewy body disease and one due to Parkinson’s disease) and six patients diagnosed with non-amnesic MCI (five with unknown etiology and one due to vascular disease). AD and non-AD patients were recruited from the Memory Clinic FELIX PLATTER, University Department of Geriatric Medicine FELIX PLATTER, Basel, Switzerland, where they received a neuropsychological assessment, MRI, medical and neurological examinations including blood analyses, and gait analysis.

**Table 1.** Sample characteristics.

	NCs (n = 9)		AD (n = 18)		non-AD (n = 9)		MD (n = 8)	
Gender (m/f)	5/4		7/11		6/3		2/6	
	Mean	SD	Mean	SD	Mean	SD	Mean	SD
Age (years)	70.89	11.41	71.56	10.61	71.56	7.09	59.13	6.40
Education (years)	13.33	4.03	14.50	3.24	12.89	2.42	13.63	2.88
MMSE score	29.00	1.00	26.72	2.42	25.89	1.54	29.00	1.41

Note. NCs = normal controls; AD = Alzheimer’s disease; non-AD = cognitive impairment due to other etiologies than Alzheimer’s disease; MD = Major Depression; m = male; f = female; MMSE = Mini-Mental State Examination.

Some patients additionally received cerebrospinal fluid testing and/or positron emission tomography scans. AD and non-AD patients were diagnosed by an interdisciplinary team at the University Department of Geriatric Medicine FELIX PLATTER, Basel, Switzerland [49]. Six patients were diagnosed with MD by the same interdisciplinary team mentioned above, and 2 were recruited from the University Psychiatric Clinics Basel, Switzerland. MDs were diagnosed according to ICD-10 criteria [50] and evaluated in an interview and with standardized questionnaires. MD patients had to score at least 6 points on the Geriatric Depression Scale [51], 10 or more points on the Becks Depression Inventory [52], or at least 13 points on the Becks Depression Inventory-II [53]. The study was approved by the local ethics committee and performed in compliance with relevant laws and institutional guidelines. Written informed consent was obtained from all participants prior to participation.



## 2.2. MRI Acquisition

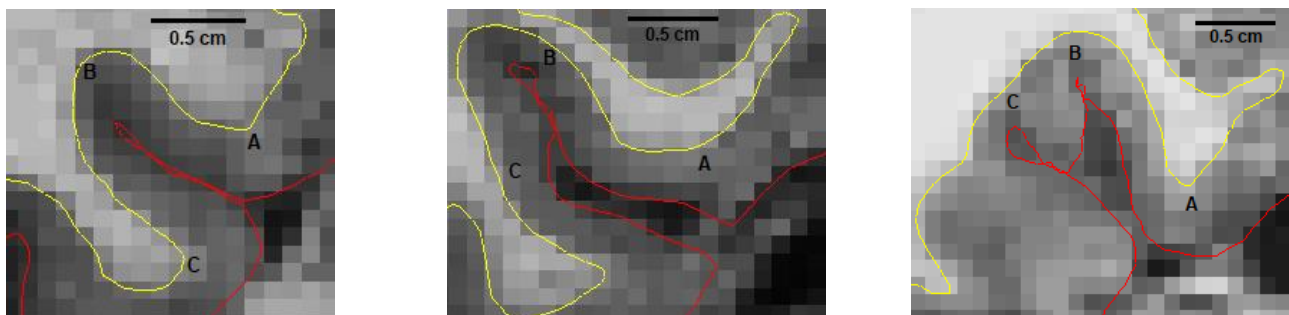
All participants received T1-weighted 3D magnetization-prepared rapid acquisition gradient echo (MPRAGE) structural MRI using the same 3-Tesla scanner (MAGNETOM Skyra fit, Siemens (Erlangen, Germany); 12 channel headcoil; inversion time = 900 ms, repetition time 2300 ms, echo time 2.92 ms, flip angle = 9°; acquisition matrix = 256 × 256 mm, voxel size = 1 mm isotropic) at the University Hospital Basel, Switzerland.

## 2.3. Preprocessing of Structural MR Images

MRI scans were preprocessed using FreeSurfer (Massachusetts General Hospital, Boston, MA, USA; <http://surfer.nmr.mgh.harvard.edu> (accessed on 8 January 2022); [38,39]). In a semi-automated processing stream, FreeSurfer segmented the T1-weighted 3D magnetization-prepared rapid acquisition gradient echo (MPRAGE) volumes into the grey and white matter. Then, the surface of white matter, represented by the transition area from white to grey matter, and the pial surface were modeled [38]. Finally, tissue classification was visually verified, and, if necessary, manual correction was carried out for all subjects.

## 2.4. Manual Segmentation

ROIs (i.e., mPRC, IPRC, and ERC) for both hemispheres were manually drawn by 2 raters blinded for diagnosis, including 1 experienced rater (SK) and 1 inexperienced rater (NAH). Introduction to the manual segmentation for the inexperienced rater included the demonstration of landmarks for all ROIs in FreeSurfer by SK according to the protocol depicted in Krumm et al. [21] (for example, the anterior-posterior borders of manual segmentation, see Supplementary Materials). Afterward, manual segmentation was performed autonomously using the manual segmentation protocol on coronal slices of native-space reconstructions of the cortical surface provided by FreeSurfer (see Figures 1 and 2 for examples). Mean cortical thickness and volumes for each ROI were acquired using FreeSurfer (Massachusetts General Hospital, Boston, MA, USA; <http://surfer.nmr.mgh.harvard.edu>).

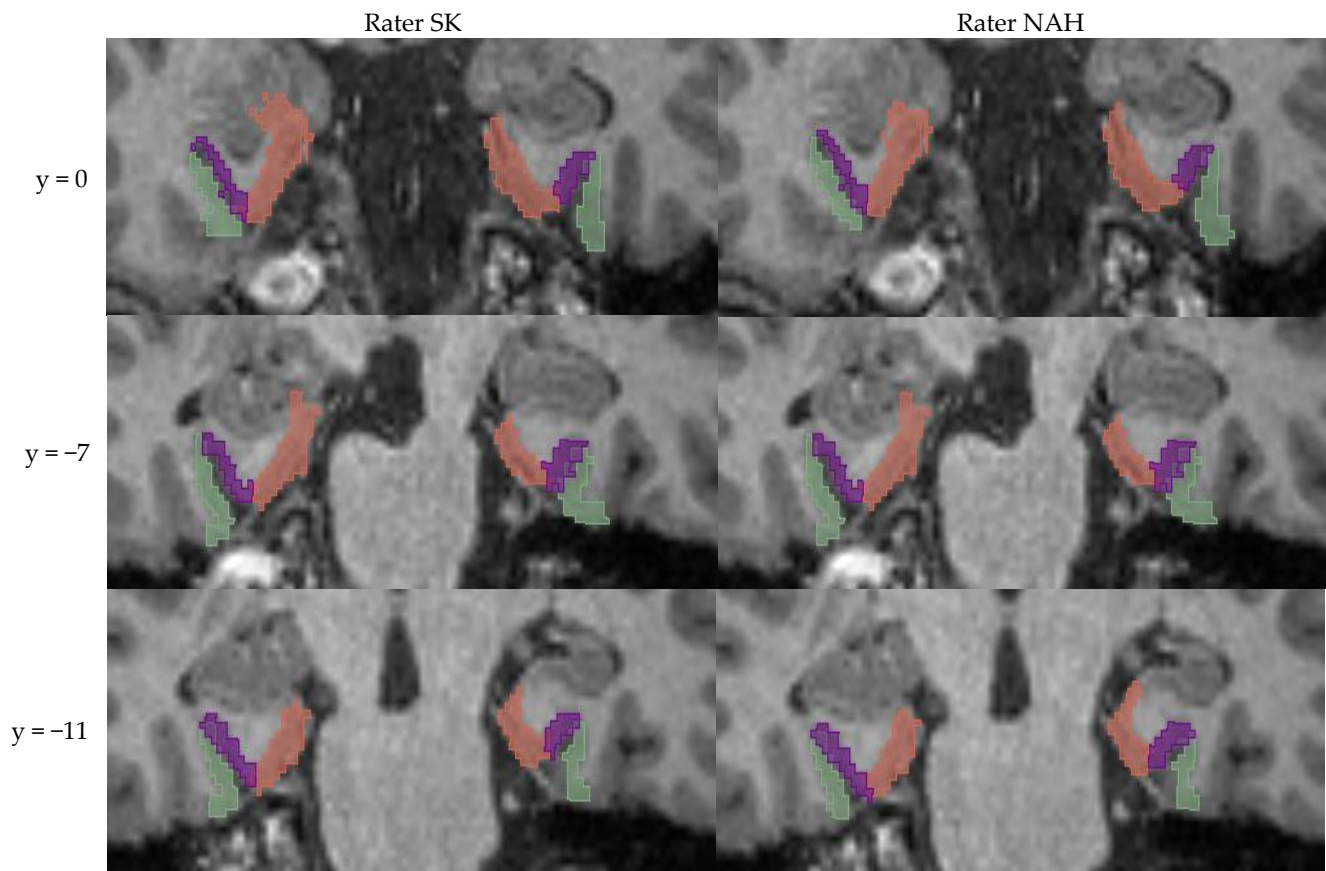


**Figure 1.** Example of three different appearances of the collateral sulcus on the right hemisphere in random participants and their effects on borders of medial and lateral perirhinal cortex; left: normal collateral sulcus length (<1.5 cm), middle: deep collateral sulcus length (>1.5 cm), and right: bifurcated collateral sulcus. A. medial border of mPRC, B. lateral border of mPRC/medial border of IPRC, C. lateral border of IPRC. The yellow line represents the grey matter's surface, and the red line represents the pial surface as generated by FreeSurfer. Abbreviations: mPRC = medial perirhinal cortex; IPRC = lateral perirhinal cortex.

## 2.5. Statistical Analyses

To evaluate the interrater reliability between both raters, ROI cortical thickness and volume estimates from all participants were compared between the 2 raters. Thus, we did not differentiate between diagnostic groups. Intraclass correlation coefficient (ICC) estimates and their 95% confidence intervals were calculated using SPSS 22 (IBM Corp. Released 2013. IBM SPSS Statistics for Windows, Version 22.0. Armonk, NY, USA) based

on a single-rating, absolute-agreement, and a 2-way mixed-effects model according to the guidelines of Koo and Li [54].



**Figure 2.** Examples of manual segmentation (using FreeSurfer) for three different coronal slices (MNI y-coordinates are shown) of the same random participant. Green = lateral perirhinal cortex; lila = medial perirhinal cortex; orange = entorhinal cortex.

### 3. Results

The results of the ICC analyses for cortical thickness estimates are summarized in Table 2. Analogous results for volume estimates are depicted in Table 3.

**Table 2.** ICC calculation for cortical thickness estimates using single-rating, absolute-agreement, two-way mixed-effects model.

Variable	Cronbach's Alpha	ICC	95% Confidence Interval		F Test		
			Lower Bound	Upper Bound	Value	df1/df2	<i>p</i>
mPRC lh	0.993	0.986	0.974	0.992	136.618	43/43	$4.81 \times 10^{-35}$
mPRC rh	0.994	0.985	0.967	0.992	154.670	43/43	$3.46 \times 10^{-36}$
IPRC lh	0.992	0.984	0.970	0.991	118.834	43/43	$9.23 \times 10^{-34}$
IPRC rh	0.975	0.953	0.915	0.974	40.344	43/43	$5.82 \times 10^{-24}$
ERC lh	0.984	0.969	0.944	0.983	62.657	43/43	$6.44 \times 10^{-28}$
ERC rh	0.980	0.961	0.930	0.979	49.390	43/43	$9.02 \times 10^{-26}$

Note. ICC = intraclass correlation coefficient; mPRC = medial perirhinal cortex; IPRC = lateral perirhinal cortex; ERC = entorhinal cortex; lh = left hemisphere; rh = right hemisphere.

**Table 3.** ICC calculation for volume estimates using single-rating, absolute-agreement, two-way mixed-effects model.

Variable	Cronbach's Alpha	ICC	95% Confidence Interval		F Test		
			Lower Bound	Upper Bound	Value	df1/df2	<i>p</i>
mPRC lh	0.932	0.874	0.781	0.929	14.647	43/43	$3.06 \times 10^{-15}$
mPRC rh	0.864	0.757	0.597	0.859	7.363	43/43	$6.58 \times 10^{-10}$
IPRC lh	0.909	0.831	0.712	0.904	10.960	43/43	$6.53 \times 10^{-13}$
IPRC rh	0.825	0.705	0.518	0.827	5.703	43/43	$3.96 \times 10^{-8}$
ERC lh	0.978	0.948	0.887	0.974	44.603	43/43	$7.40 \times 10^{-25}$
ERC rh	0.951	0.908	0.838	0.949	20.326	43/43	$5.58 \times 10^{-18}$

Note. ICC = intraclass correlation coefficient; mPRC = medial perirhinal cortex; IPRC = lateral perirhinal cortex; ERC = entorhinal cortex; lh = left hemisphere; rh = right hemisphere.

#### 4. Discussion

We aimed to evaluate the interrater reliability of a manual segmentation protocol for regions of the medial temporal lobe, including the mPRC, IPRC, and ERC. Especially the mPRC is of great interest because this brain structure is the first region affected by neurofibrillary tau pathology in typical AD [4]. The ICC analyses for cortical thickness estimates showed very high interrater reliability for manual mPRC segmentation as well as for IPRC and ERC. The results provide evidence that the applied segmentation protocol, which considers collateral sulcus variability, allows different raters to achieve strikingly similar results. Furthermore, after only a brief introduction to the landmarks of all ROIs, the inexperienced rater (NAH) was able to follow the segmentation protocol as depicted in Krumm et al. [21], reflecting remarkable practicability.

As mentioned before, the collateral sulcus of the medial temporal lobe defines the boundaries between the mPRC and IPRC and is characterized by high anatomical variability (e.g., length and form of the sulcus). Therefore, the difficulty in segmentation is most likely associated with the variable shape of the collateral sulci [11,26]. In addition, the collateral sulcus variability mostly affects the volume and much less the cortical thickness of adjacent areas [38–40]. For the mPRC and IPRC, the ICC analysis for volume compared to cortical thickness estimates revealed a consistently lower degree of reliability between both raters. This difference was not found for the ERC, whose borders are not as strongly determined by the collateral sulcus. These results are in line with previous findings describing the effect of the collateral sulcus variability on volumes of its adjacent regions [40,55]. In summary, the lower ICC results for volume estimates suggest cortical thickness to be a more reliable and, thus, preferable measurement of atrophy, particularly for regions affected by the collateral sulcus variability (e.g., mPRC and IPRC).

Nonetheless, there are limitations to our study. We did not aim to reflect the general population but rather to illustrate the clinical routine, where most of the individuals are patients with different etiologies, and only a few are healthy. Participants were randomly selected from a larger study. This led to a heterogeneous sample with a sufficient total number of investigated subjects but rather low sample sizes per diagnostic group (e.g., NCs, MD). Furthermore, the random selection of participants resulted in a sample of predominantly well-educated individuals who were rather young compared to the usual age of individuals suffering from dementia. However, as can be seen from the mean MMSE scores in Table 1, they were in very early disease stages. Future studies could increase the sizes of diagnostic groups to differentially investigate them. In addition, a sample that represents the general population in terms of age, ethnicity, multimorbidity, and educational background should be aimed for. Further, we renounced investigating the intrarater agreement because we do not expect significant intrarater differences since our interrater reliability is very high. However, future studies might still want to include outcomes of more than two raters and analyze the intrarater reliability to improve the generalizability of the results. Further, we used isotropic 1 mm<sup>3</sup> T1-weighted images for our analysis. Since the cortical thickness is automatically generated after manual segmentation, tissue

misclassification during the preprocessing steps (e.g., the border between white matter and grey matter) is possible. This could lead to inaccurate values of cortical thickness, which may hinder research and application in the clinical setting. Recent findings suggest the use of higher-resolution images for hippocampus subfields, which may also apply to our parahippocampal regions and could improve results [27].

Manual segmentation is time-consuming and unfeasible for clinical settings, let alone for larger data. Software that accurately and automatically segments mPRC would be of great interest. Xie et al. [56] proposed a promising, automated segmentation based on a multiatlas segmentation software for Brodmann area 35, which corresponds to the mPRC. The comparison between the manual and automated segmentation showed a Dice similarity coefficient of 0.77 [56]. This result reflects room for improvement for automated segmentation of the mPRC, which could possibly be achieved using the manual segmentation protocol applied in our study (depicted in [21]) as ground truth. As mentioned before, a reliable manual segmentation protocol is of utmost importance for the development and validation of an automated segmentation protocol [27]. In combination with commonly used atrophy scores in clinical settings (e.g., ERC and medial temporal lobe atrophy [16,17]), mPRC integrity has the potential to add valuable information, especially in early-stage AD, for follow-up examinations as well as for differential diagnostics. To achieve this, a proof of concept needs to be stated that the mPRC is atrophied in AD individuals only but intact in patients suffering from other diseases. Since the collateral sulcus has a pronounced effect on borders of adjacent regions (e.g., mPRC) and shows very different appearances not only between subjects but also within the same individual, the next step is the collection of normative data from healthy individuals as well as different diagnostic groups. This allows not only to capture the interindividual variability of healthy individuals but also to determine pathological values of atrophy (e.g., cortical thickness) for individualized patient evaluation in clinical routine. This would suggest mPRC's integrity to be used as an early biomarker for AD and provide additional information for differential diagnostics in clinical settings. In addition, as the site of the first NFT, a broader focus on the assessment of perirhinal cortex function for the early diagnosis of AD in clinical settings would be worthwhile. The combined evaluation of structural and functional changes in clinical settings and research represents a promising approach to detecting the earliest signs of AD. Furthermore, future functional anatomical studies may provide more insight into these early changes in AD.

## 5. Conclusions

This study provides evidence that the applied manual segmentation protocol for cortical regions first affected by neurofibrillary tau pathology in AD (e.g., the mPRC and ERC) allows different raters to achieve remarkably similar cortical thickness estimates. In addition, we confirmed the practicability for an inexperienced rater and finally provided evidence to prefer cortical thickness to volume as a reliable measure of atrophy, especially for regions affected by the collateral sulcus variability (e.g., the mPRC and IPRC). Future studies are encouraged to develop time-saving automated segmentation on the basis of the provided results and compare the accuracy with the manual segmentation. Further, the present study recommends a manual segmentation protocol to be used in future proof of concept studies. Such studies should prove the hypothesis that the mPRC is affected early by atrophy in AD but not in the early stages of other neurodegenerative diseases. It is essential to apply the segmentation to a broad range of diseases using appropriate sample sizes to allow the generalization of results. Moreover, for individualized patient evaluation in clinical routine, the collection of normative data from healthy individuals as well as different diagnostic groups is needed.

**Supplementary Materials:** The following supporting information can be downloaded at: <https://www.mdpi.com/article/10.3390/brainsci13060850/s1>, Figures S1–S8: Visualization of the borders of mPRC, IPRC, and ERC in coronal slices.



**Author Contributions:** Conceptualization, N.A.H. and S.K.; Data curation, J.R., M.B. and S.K.; Formal analysis, N.A.H.; Funding acquisition, S.K.; Investigation, S.K.; Methodology, N.A.H. and S.K.; Project administration, S.K.; Resources, J.R., M.B., R.W.K. and S.K.; Software, J.R., M.B. and S.K.; Supervision, S.K.; Validation, S.K.; Visualization, N.A.H.; Writing—original draft, N.A.H. and S.K.; Writing—review & editing, N.A.H., J.R., M.B., R.W.K. and S.K. All authors have read and agreed to the published version of the manuscript.

**Funding:** This research was funded by grants from the Alfred and Anneliese Sutter-Stöttner Foundation and The APC was funded by the FELIX PLATTER Foundation for Research and Innovation.

**Institutional Review Board Statement:** The study was conducted in accordance with the local ethics committee (Ethikkommission Nordwest- und Zentralschweiz [EKNZ]; protocol code EKNZ 2014-297, approved 1 June 2016, further amendments approved 15 June 2016 and 2 December 2016).

**Informed Consent Statement:** Informed consent was obtained from all subjects involved in the study.

**Data Availability Statement:** All analysis code and research materials, as well as metadata and/or full data, are available upon request.

**Acknowledgments:** We thank Andreas U. Monsch as the facilitator of this project.

**Conflicts of Interest:** The authors declare no conflict of interest.

## References

- Graham, N.; Emery, T.; Hodges, J. Distinctive cognitive profiles in Alzheimer's disease and subcortical vascular dementia. *J. Neurol. Neurosurg. Psychiatry* **2004**, *75*, 61–71. [[PubMed](#)]
- Morris, J.C.; Kimberly, A.; Quaid, K.; Holtzman, D.M.; Kantarci, K.; Kaye, J.; Reiman, E.M.; Klunk, W.E.; Siemers, E.R. Role of biomarkers in studies of presymptomatic Alzheimer's disease. *Alzheimer's Dement.* **2005**, *1*, 145–151. [[CrossRef](#)] [[PubMed](#)]
- Schultz, C.; Del Tredici, K.; Braak, H. Neuropathology of Alzheimer's Disease. In *Alzheimer's Disease: A Physician's Guide to Practical Management*; Richter, R.W., Richter, B.Z., Eds.; Humana Press: Totowa, NJ, USA, 2004; pp. 21–31. [[CrossRef](#)]
- Braak, H.; Braak, E. Neuropathological staging of Alzheimer-related changes. *Acta Neuropathol.* **1991**, *82*, 239–259. [[CrossRef](#)] [[PubMed](#)]
- Guillozet, A.L.; Weintraub, S.; Mash, D.C.; Mesulam, M.M. Neurofibrillary Tangles, Amyloid, and Memory in Aging and Mild Cognitive Impairment. *Arch. Neurol.* **2003**, *60*, 729–736. [[CrossRef](#)] [[PubMed](#)]
- Goedert, M.; Spillantini, M.G.; Crowther, R.A. Tau Proteins and Neurofibrillary Degeneration. *Brain Pathol.* **1991**, *1*, 279–286. [[CrossRef](#)]
- Kimura, T.; Yamashita, S.; Fukuda, T.; Park, J.-M.; Murayama, M.; Mizoroki, T.; Yoshiike, Y.; Sahara, N.; Takashima, A. Hyperphosphorylated tau in parahippocampal cortex impairs place learning in aged mice expressing wild-type human tau. *EMBO J.* **2007**, *26*, 5143–5152. [[CrossRef](#)]
- Bobinski, M.; Wegiel, J.; Tarnawski, M.; Bobinski, M.; Reisberg, B.; de Leon, M.J.; Miller, D.C.; Wisniewski, H.M. Relationships between Regional Neuronal Loss and Neurofibrillary Changes in the Hippocampal Formation and Duration and Severity of Alzheimer Disease. *J. Neuropathol. Exp. Neurol.* **1997**, *56*, 414–420. [[CrossRef](#)]
- Gómez-Isla, T.; Hollister, R.; West, H.; Mui, S.; Growdon, J.H.; Petersen, R.C.; Parisi, J.E.; Hyman, B.T. Neuronal loss correlates with but exceeds neurofibrillary tangles in Alzheimer's disease. *Ann. Neurol.* **1997**, *41*, 17–24. [[CrossRef](#)]
- Vemuri, P.; Jack, C.R. Role of structural MRI in Alzheimer's disease. *Alzheimer's Res. Ther.* **2010**, *2*, 23. [[CrossRef](#)]
- Taylor, K.I.; Probst, A. Anatomic localization of the transentorhinal region of the perirhinal cortex. *Neurobiol. Aging* **2008**, *29*, 1591–1596. [[CrossRef](#)]
- Braak, H.; Del Tredici, K. Staging of cortical neurofibrillary inclusions of the Alzheimer's type. In *Alzheimer: 100 Years and Beyond*; Jucker, M., Beyreuther, K., Haass, C., Nitsch, R.M., Christen, Y., Eds.; Springer: Berlin/Heidelberg, Germany, 2006; pp. 97–106. [[CrossRef](#)]
- Sone, D.; Imabayashi, E.; Maikusa, N.; Okamura, N.; Furumoto, S.; Kudo, Y.; Ogawa, M.; Takano, H.; Yokoi, Y.; Sakata, M.; et al. Regional tau deposition and subregion atrophy of medial temporal structures in early Alzheimer's disease: A combined positron emission tomography/magnetic resonance imaging study. *Alzheimer's Dement. Diagn. Assess. Dis. Monit.* **2017**, *9*, 35–40. [[CrossRef](#)] [[PubMed](#)]
- Sperling, R.A.; Aisen, P.S.; Beckett, L.A.; Bennett, D.A.; Craft, S.; Fagan, A.M.; Iwatsubo, T.; Jack, C.R.; Kaye, J.; Montine, T.J.; et al. Toward defining the preclinical stages of Alzheimer's disease: Recommendations from the National Institute on Aging-Alzheimer's Association workgroups on diagnostic guidelines for Alzheimer's disease. *Alzheimer's Dement. J. Alzheimer's Assoc.* **2011**, *7*, 280–292. [[CrossRef](#)] [[PubMed](#)]
- Talwar, P.; Kushwaha, S.; Chaturvedi, M.; Mahajan, V. Systematic Review of Different Neuroimaging Correlates in Mild Cognitive Impairment and Alzheimer's Disease. *Clin. Neuroradiol.* **2021**, *31*, 953–967. [[CrossRef](#)] [[PubMed](#)]

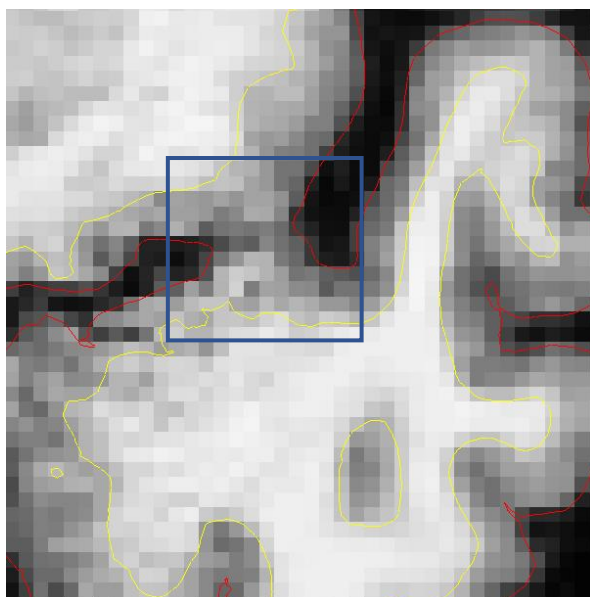
16. Enkirch, S.J.; Träschütz, A.; Müller, A.; Widmann, C.N.; Gielen, G.H.; Heneka, M.T.; Jurcoane, A.; Schild, H.H.; Hattingen, E. The ERICA Score: An MR Imaging–based Visual Scoring System for the Assessment of Entorhinal Cortex Atrophy in Alzheimer Disease. *Radiology* **2018**, *288*, 226–333. [[CrossRef](#)]
17. Scheltens, P.; van de Pol, L. Impact commentaries. Atrophy of medial temporal lobes on MRI in “probable” Alzheimer’s disease and normal ageing: Diagnostic value and neuropsychological correlates. *J. Neurol. Neurosurg. Psychiatry* **2012**, *83*, 1038–1040. [[CrossRef](#)]
18. Kulason, S.; Tward, D.J.; Brown, T.; Sicut, C.S.; Liu, C.-F.; Ratnanather, J.T.; Younes, L.; Bakker, A.; Gallagher, M.; Albert, M.; et al. Cortical thickness atrophy in the transentorhinal cortex in mild cognitive impairment. *NeuroImage Clin.* **2019**, *21*, 101617. [[CrossRef](#)]
19. Kulason, S.; Xu, E.; Tward, D.J.; Bakker, A.; Albert, M.; Younes, L.; Miller, M.I. Entorhinal and Transentorhinal Atrophy in Preclinical Alzheimer’s Disease. *Front. Neurosci.* **2020**, *14*, 804. [[CrossRef](#)]
20. Younes, L.; Albert, M.; Miller, M.I. Inferring changepoint times of medial temporal lobe morphometric change in preclinical Alzheimer’s disease. *NeuroImage Clin.* **2014**, *5*, 178–187. [[CrossRef](#)]
21. Krumm, S.; Kivisaari, S.L.; Probst, A.; Monsch, A.U.; Reinhardt, J.; Ulmer, S.; Stippich, C.; Kressig, R.W.; Taylor, K.I. Cortical thinning of parahippocampal subregions in very early Alzheimer’s disease. *Neurobiol. Aging* **2016**, *38*, 188–196. [[CrossRef](#)]
22. Kouri, N.; Murray, M.E.; Hassan, A.; Rademakers, R.; Uitti, R.J.; Boeve, B.F.; Graff-Radford, N.R.; Wszolek, Z.K.; Litvan, I.; Josephs, K.A.; et al. Neuropathological features of corticobasal degeneration presenting as corticobasal syndrome or Richardson syndrome. *Brain* **2011**, *134*, 3264–3275. [[CrossRef](#)]
23. Augustinack, J.C.; Huber, K.E.; Stevens, A.A.; Roy, M.; Frosch, M.P.; van der Kouwe, A.J.W.; Wald, L.L.; Van Leemput, K.; McKee, A.C.; Fischl, B. Alzheimer’s Disease Neuroimaging Initiative. Predicting the location of human perirhinal cortex, Brodmann’s area 35, from MRI. *NeuroImage* **2013**, *64*, 32–42. [[CrossRef](#)] [[PubMed](#)]
24. Braak, H.; Braak, E. On areas of transition between entorhinal allocortex and temporal isocortex in the human brain. Normal morphology and lamina-specific pathology in Alzheimer’s disease. *Acta Neuropathol.* **1985**, *68*, 325–332. [[CrossRef](#)] [[PubMed](#)]
25. Brodmann, K.; Garey, L. *Brodmann’s Localisation in the Cerebral Cortex: The Principles of Comparative Localisation in the Cerebral Cortex Based on the Cytoarchitectonics*; Springer: Berlin/Heidelberg, Germany, 2006. [[CrossRef](#)]
26. Kivisaari, S.L.; Probst, A.; Taylor, K.I. The Perirhinal, Entorhinal, and Parahippocampal Cortices and Hippocampus: An Overview of Functional Anatomy and Protocol for Their Segmentation in MR Images. In *FMRI: Basics and Clinical Applications*; Ulme, S., Jansen, O., Eds.; Springer: Berlin/Heidelberg, Germany, 2013; pp. 239–267. [[CrossRef](#)]
27. Wisse, L.E.M.; Chételat, G.; Daugherty, A.M.; de Flores, R.; la Joie, R.; Mueller, S.G.; Stark, C.E.L.; Wang, L.; Yushkevich, P.A.; Berron, D.; et al. Hippocampal subfield volumetry from structural isotropic 1 mm<sup>3</sup> MRI scans: A note of caution. *Hum. Brain Mapp.* **2021**, *42*, 539–550. [[CrossRef](#)] [[PubMed](#)]
28. Bussey, T.J.; Saksida, L.M.; Murray, E.A. Perirhinal cortex resolves feature ambiguity in complex visual discriminations. *Eur. J. Neurosci.* **2002**, *15*, 365–374. [[CrossRef](#)]
29. Cowell, R.A. Computational models of perirhinal cortex function. *Hippocampus* **2012**, *22*, 1952–1964. [[CrossRef](#)]
30. Desimone, R.; Ungerleider, L.G. Multiple visual areas in the caudal superior temporal sulcus of the macaque. *J. Comp. Neurol.* **1986**, *248*, 164–189. [[CrossRef](#)]
31. Cowell, R.A.; Bussey, T.J.; Saksida, L.M. Components of recognition memory: Dissociable cognitive processes or just differences in representational complexity? *Hippocampus* **2010**, *20*, 1245–1262. [[CrossRef](#)]
32. Murray, E.A.; Richmond, B.J. Role of perirhinal cortex in object perception, memory, and associations. *Curr. Opin. Neurobiol.* **2001**, *11*, 188–193. [[CrossRef](#)]
33. Suzuki, W.L.; Amaral, D.G. Perirhinal and parahippocampal cortices of the macaque monkey: Cortical afferents. *J. Comp. Neurol.* **1994**, *350*, 497–533. [[CrossRef](#)]
34. Frei, M.; Berres, M.; Kivisaari, S.L.; Henzen, N.A.; Monsch, A.U.; Reinhardt, J.; Blatow, M.; Kressig, R.W.; Krumm, S. Can you find it? Novel oddity detection task for the early detection of Alzheimer’s disease. *Neuropsychology*, 2022, *advance online publication*. [[CrossRef](#)]
35. Taylor, K.I.; Moss, H.E.; Tyler, L.K. The Conceptual Structure Account: A cognitive model of semantic memory and its neural instantiation. In *Neural Basis of Semantic Memory*; Cambridge University Press: Cambridge, UK, 2007; pp. 265–301.
36. Hirni, D.I.; Kivisaari, S.L.; Monsch, A.U.; Taylor, K.I. Distinct neuroanatomical bases of episodic and semantic memory performance in Alzheimer’s disease. *Neuropsychologia* **2013**, *51*, 930–937. [[CrossRef](#)]
37. Krumm, S.; Berres, M.; Kivisaari, S.L.; Monsch, A.U.; Reinhardt, J.; Blatow, M.; Kressig, R.W.; Taylor, K.I. Cats and Apples: Semantic Fluency Performance for Living Things Identifies Patients with Very Early Alzheimer’s Disease. *Arch. Clin. Neuropsychol. Off. J. Natl. Acad. Neuropsychol.* **2021**, *36*, 838–843. [[CrossRef](#)] [[PubMed](#)]
38. Dale, A.M.; Fischl, B.; Sereno, M.I. Cortical Surface-Based Analysis: I. Segmentation and Surface Reconstruction. *NeuroImage* **1999**, *9*, 179–194. [[CrossRef](#)] [[PubMed](#)]
39. Fischl, B.; Sereno, M.I.; Dale, A.M. Cortical Surface-Based Analysis: II: Inflation, Flattening, and a Surface-Based Coordinate System. *NeuroImage* **1999**, *9*, 195–207. [[CrossRef](#)] [[PubMed](#)]
40. Insausti, R.; Juottonen, K.; Soininen, H.; Insausti, A.M.; Partanen, K.; Vainio, P.; Laakso, M.P.; Pitkänen, A. MR volumetric analysis of the human entorhinal, perirhinal, and temporopolar cortices. *Am. J. Neuroradiol.* **1998**, *19*, 659–671. [[PubMed](#)]

41. Folstein, M.F.; Folstein, S.E.; McHugh, P.R. “Mini-mental state”: A practical method for grading the cognitive state of patients for the clinician. *J. Psychiatr. Res.* **1975**, *12*, 189–198. [[CrossRef](#)] [[PubMed](#)]
42. Delis, D.C.; Kramer, J.H.; Kaplan, E.; Ober, B.A. *California Verbal Learning Test*; Psychological Corporation: New York, NY, USA, 1987.
43. Reitan, R.M. Validity of the Trail Making Test as an Indicator of Organic Brain Damage. *Percept. Mot. Ski.* **1958**, *8*, 271–276. [[CrossRef](#)]
44. Jorm, A.F.; Scott, R.; Jacomb, P.A. Assessment of cognitive decline in dementia by informant questionnaire. *Int. J. Geriatr. Psychiatry* **1989**, *4*, 35–39. [[CrossRef](#)]
45. American Psychiatric Association. *DSM-IV: Diagnostic and Statistical Manual of Mental Disorders*; American Psychiatric Press: Washington, DC, USA, 1994.
46. McKhann, G.M.; Knopman, D.S.; Chertkow, H.; Hyman, B.T.; Jack, C.R.; Kawas, C.H.; Klunk, W.E.; Koroshetz, W.J.; Manly, J.J.; Mayeux, R.; et al. The diagnosis of dementia due to Alzheimer’s disease: Recommendations from the National Institute on Aging-Alzheimer’s Association workgroups on diagnostic guidelines for Alzheimer’s disease. *Alzheimer’s Dement. J. Alzheimer’s Assoc.* **2011**, *7*, 263–269. [[CrossRef](#)] [[PubMed](#)]
47. Albert, M.S.; DeKosky, S.T.; Dickson, D.; Dubois, B.; Feldman, H.H.; Fox, N.C.; Gamst, A.; Holtzman, D.M.; Jagust, W.J.; Petersen, R.C.; et al. The diagnosis of mild cognitive impairment due to Alzheimer’s disease: Recommendations from the National Institute on Aging-Alzheimer’s Association workgroups on diagnostic guidelines for Alzheimer’s disease. *Alzheimer’s Dement. J. Alzheimer’s Assoc.* **2011**, *7*, 270–279. [[CrossRef](#)]
48. Winblad, B.; Palmer, K.; Kivipelto, M.; Jelic, V.; Fratiglioni, L.; Wahlund, L.-O.; Nordberg, A.; Bäckman, L.; Albert, M.; Almkvist, O.; et al. Mild cognitive impairment—beyond controversies, towards a consensus: Report of the International Working Group on Mild Cognitive Impairment. *J. Intern. Med.* **2004**, *256*, 240–246. [[CrossRef](#)]
49. Monsch, A.; Kressig, R. Specific care program for the older adults: Memory Clinics. *Eur. Geriatr. Med.* **2010**, *1*, 128–131. [[CrossRef](#)]
50. World Health Organization. *ICD-10: International Statistical Classification of Diseases and Related Health Problems: Tenth Revision*; World Health Organization: Geneva, Switzerland, 2004. Available online: <https://apps.who.int/iris/handle/10665/42980> (accessed on 1 July 2016).
51. Galik, E.; Fukudo, S.; Tanaka, Y.; Gidron, Y.; Campbell, T.S.; Johnson, J.A.; Zernicke, K.A.; Pellowski, J.; Garcia, L.I.; Mitchell, J.W.; et al. Geriatric Depression Scale. In *Encyclopedia of Behavioral Medicine*; Gellman, M.D., Turner, J.R., Eds.; Springer: New York, NY, USA, 2013; pp. 857–858. [[CrossRef](#)]
52. Beck, A.T. An Inventory for Measuring Depression. *Arch. Gen. Psychiatry* **1961**, *4*, 561. [[CrossRef](#)] [[PubMed](#)]
53. Beck, A.T.; Steer, R.A.; Brown, G. *Beck Depression Inventory–II*; American Psychological Association: Worcester, MA, USA, 2011. [[CrossRef](#)]
54. Koo, T.K.; Li, M.Y. A Guideline of Selecting and Reporting Intraclass Correlation Coefficients for Reliability Research. *J. Chiropr. Med.* **2016**, *15*, 155–163. [[CrossRef](#)] [[PubMed](#)]
55. Pruessner, J.C.; Köhler, S.; Crane, J.; Pruessner, M.; Lord, C.; Byrne, A.; Kabani, N.; Collins, D.L.; Evans, A.C. Volumetry of temporopolar, perirhinal, entorhinal and parahippocampal cortex from high-resolution MR images: Considering the variability of the collateral sulcus. *Cereb. Cortex* **2002**, *12*, 1342–1353. [[CrossRef](#)] [[PubMed](#)]
56. Xie, L.; Wisse, L.E.M.; Pluta, J.; Flores, R. de; Piskin, V.; Manjón, J.V.; Wang, H.; Das, S.R.; Ding, S.-L.; Wolk, D.A.; et al. Automated segmentation of medial temporal lobe subregions on in vivo T1-weighted MRI in early stages of Alzheimer’s disease. *Hum. Brain Mapp.* **2019**, *40*, 3431–3451. [[CrossRef](#)]

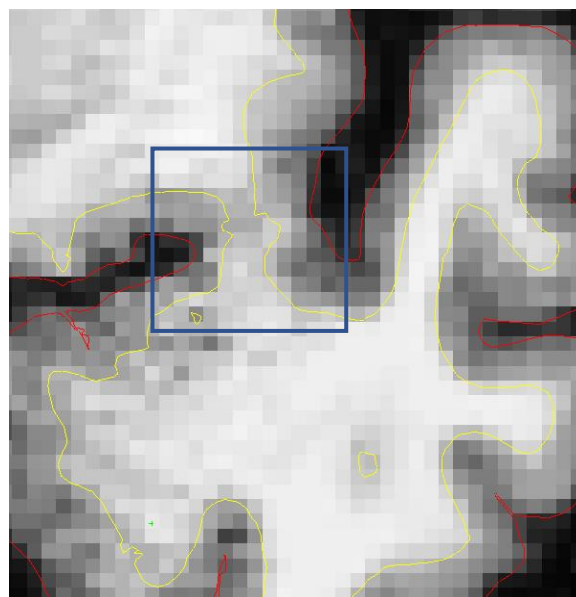
**Disclaimer/Publisher’s Note:** The statements, opinions and data contained in all publications are solely those of the individual author(s) and contributor(s) and not of MDPI and/or the editor(s). MDPI and/or the editor(s) disclaim responsibility for any injury to people or property resulting from any ideas, methods, instructions or products referred to in the content.

Supplementary materials

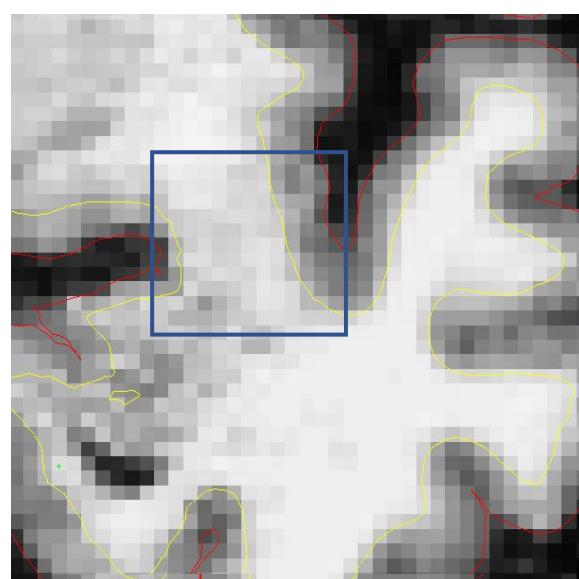
The following **Figures S1-8** visualize the borders of mPRC, IPRC, and ERC in coronal slices using FreeSurfer in one random participant. **A:** How to find the **anterior border** of the left hemisphere (**Figures S1-4**). Yellow line represents white matter surface and red line represents pial surface as generated by FreeSurfer. *Note: 1slice is equal to 1mm.*



**Figure S1.** Anterior border +3slices: Last slice, where the white matter of the limen insulae is not visible (blue mark).



**Figure S2.** Anterior border +2slices: First slice, where the white matter of the limen insulae is visible (blue mark).



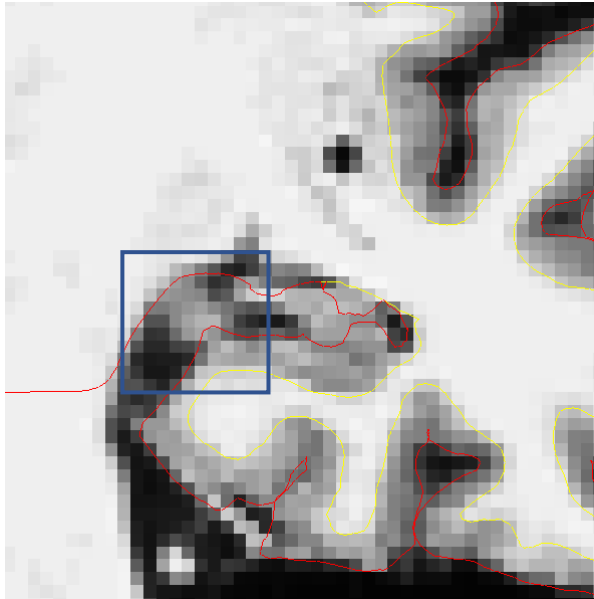
**Figure S3.** Anterior border: 2slices posterior to the first slice, where the white matter of the limen insulae is visible.

Structure	Anterior border
ERC	2 mm posterior to the first anterior slice where the white matter of the limen insulae is visible.
Medial PRC	Same coronal level as the anterior border of the ERC, i.e., 2 mm posterior to the first anterior slice where the white matter of the limen insulae is visible.
Lateral PRC	Same coronal level as the anterior border of the ERC, i.e., 2 mm posterior to the first anterior slice where the white matter of the limen insulae is visible.

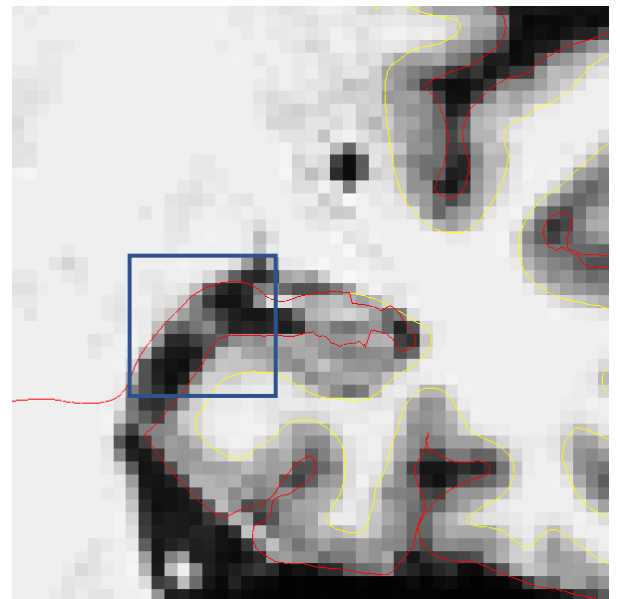
**Figure S4.** Anterior border: Adapted and modified from Krumm et al. (2016).



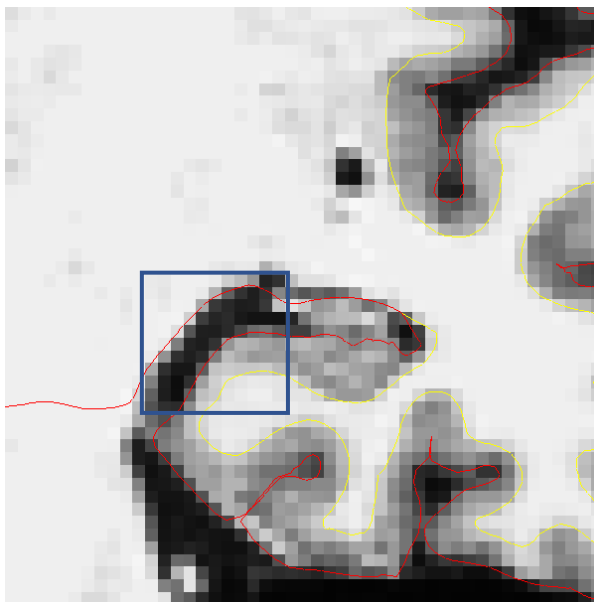
**B: How to find the posterior border of the left hemisphere (Figures S5-8).**



**Figure S5.** Posterior border +2slices: Apex of the intralimbic gyrus is still visible (blue mark).



**Figure S6.** Posterior border +1slice: Last slice still containing the apex of the intralimbic gyrus (blue mark).



**Figure S7.** Posterior border: 1slice posterior to the last slice still containing the apex of the intralimbic gyrus (blue mark).

Structure	Posterior border
ERC	1 mm posterior to the last slice still containing the apex of the intralimbic gyrus.
Medial PRC	1 mm posterior to the last slice still containing the apex of the intralimbic gyrus.
Lateral PRC	1 mm posterior to the last slice still containing the apex of the intralimbic gyrus.

**Figure S8.** Posterior border: Adapted and modified from Krumm et al. (2016).

### 2.3. Studie III

Automated segmentation for cortical thickness of the medial perirhinal cortex

## Automated segmentation for cortical thickness of the medial perirhinal cortex

Nicolas A. Henzen<sup>1,2\*</sup>, Ahmed Abdulkadir<sup>3,4\*</sup>, Julia Reinhardt<sup>5,6,7</sup>, Maria Blatow<sup>8</sup>, Reto W. Kressig<sup>1,9</sup>, and

Sabine Krumm<sup>1,9</sup>

<sup>1</sup>University Department of Geriatric Medicine FELIX PLATTER, Basel, Switzerland

<sup>2</sup>Faculty of Psychology, University of Basel, Basel, Switzerland

<sup>3</sup>Department of Clinical Neurosciences, Laboratory for Research in Neuroimaging LREN, Centre for Research in Neurosciences, Lausanne University Hospital and University of Lausanne, Lausanne, Switzerland

<sup>4</sup>Center for Artificial Intelligence, Zürich University of Applied Sciences, Winterthur, Switzerland

<sup>5</sup>Division of Diagnostic and Interventional Neuroradiology, Department of Radiology, University Hospital Basel, University of Basel, Basel, Switzerland

<sup>6</sup>Department of Cardiology and Cardiovascular Research Institute Basel (CRIB), University Hospital Basel, University of Basel, Switzerland

<sup>7</sup>Department of Orthopedic Surgery and Traumatology, University Hospital of Basel, University of Basel, Basel, Switzerland

<sup>8</sup>Section of Neuroradiology, Department of Radiology and Nuclear Medicine, Neurocenter, Cantonal Hospital Lucerne, University of Lucerne, Lucerne, Switzerland

<sup>9</sup>Faculty of Medicine, University of Basel, Basel, Switzerland

\* Nicolas A. Henzen and Ahmed Abdulkadir contributed equally to this study and share first authorship

**Correspondence:** Nicolas A. Henzen, University Department of Geriatric Medicine FELIX PLATTER, Basel, Switzerland. Email: [Nicolas.Henzen@felixplatter.ch](mailto:Nicolas.Henzen@felixplatter.ch)

Memory Clinic FELIX PLATTER

University Department of Geriatric Medicine FELIX PLATTER  
Burgfelderstrasse 101  
4055 Basel | Switzerland  
+41 61 326 47 68 | [felixplatter.ch](http://felixplatter.ch)

## **Abstract**

Alzheimer's disease (AD) is characterized by a progressive spread of neurofibrillary tangles (NFT), beginning in the medial perirhinal cortex (mPRC; also referred to as the transentorhinal cortex), advancing to the entorhinal cortex (ERC), and subsequently involving the hippocampus, lateral perirhinal cortex (IPRC), and the rest of the brain. Given the close relationship between NFT accumulation and neuronal loss, the mPRC reflects a promising structural marker for early diagnosis of AD. However, there are currently no tools available that automatically measure the cortical thickness of the mPRC. Utilizing the nnU-Net framework, we trained models on structural MRI of 126 adults, with manually segmented labels as ground truth. These models were then applied to an independent dataset of 103 adults (comprising patients with Alzheimer's dementia, amnesic mild cognitive impairment (aMCI), and healthy controls). High agreement was observed between manual and automated measurements of cortical thickness. Furthermore, we found significant atrophy in the Alzheimer's dementia group in the mPRC, ERC, and IPRC compared to healthy controls. Comparison of the aMCI group and healthy controls revealed significant differences in the ERC only. The results underscore the utility of our automated segmentation tool in advancing Alzheimer's research.

**Keywords:** Alzheimer's disease; perirhinal cortex; entorhinal cortex; structural MRI; deep learning; semantic segmentation

## 1. Introduction

Discovering the earliest signs of Alzheimer's disease (AD) and thereby starting treatment as early in the disease progression as possible is of great interest (Morris et al., 2005; Sperling et al., 2011). Neuropathological brain changes associated with AD, namely  $\beta$ -amyloid plaques and neurofibrillary tangles (NFT), are thought to begin years before clinical symptoms become evident. In contrast to  $\beta$ -amyloid plaques, NFT are more strongly correlated with cognitive deficits (Giannakopoulos et al., 2003) and progress in a hierarchical manner throughout the brain in typical AD (Braak & Braak, 1991). This continuous accumulation of NFT is strongly related to loss of neurons (Bobinski et al., 1997; Braak & Braak, 1991) and has been shown to be causally associated to cerebral atrophy in affected regions (Gómez-Isla et al., 1997). In regard to the sporadic AD (representing approximately 95% of all cases) the first region typically affected by neurofibrillary tau pathology is the medial perirhinal cortex (mPRC), also referred to as the transentorhinal cortex (Braak & Braak, 1991; Taylor & Probst, 2008). In later stages, this neurofibrillary tau pathology spreads to the medially located entorhinal cortex (ERC) and eventually to the hippocampus, and throughout the brain (Braak & Braak, 1991; Rullmann et al., 2022; Schwarz et al., 2016). In clinical settings, the diagnosis of AD often relies on visual assessment of atrophy, such as the ERC atrophy score (ERICA; Enkirch et al., 2018) along with the medial temporal lobe atrophy score that evaluates the hippocampus, the choroid fissure, and the lateral ventricle (MTA; Scheltens & Pol, 2012). In this context, the mPRC is often overlooked, and if considered, it is usually in form of the entire perirhinal cortex. Given its relatively small size, we believe that assessing mPRC integrity in clinical settings could be enhanced by using a computed measure of atrophy (e.g., cortical thickness). Recent studies are in line with this notion, reflecting the potential of the mPRC's integrity in clinical settings. For example, Sone et al. (2017) discovered that in early stages of AD, regional NFT accumulation is associated with cortical thinning in the perirhinal cortex and entorhinal cortex (ERC). As a result, brain structures that are initially impacted by NFT induced atrophy (e.g., mPRC) likely serve as sensitive preclinical structural imaging biomarkers. Indeed, more recent studies, with focus on mPRC atrophy, found promising results suggesting mPRC integrity as a sensitive and specific marker for early AD (e.g. Krumm et al., 2016; Kulason et al.,

2019; 2020). In addition, these findings further indicate, that the lateral part of the perirhinal cortex (IPRC) is only affected after the mPRC, which is in line with the proposed staging of NFT-related pathology (Braak & Braak, 1991; Braak & Del Tredici, 2006). Based on these results, we hypothesize that investigating the cortical thickness of mPRC and IPRC separately is more sensitive in early-stage AD than the cortical thickness of the entire PRC.

Anatomically, the transition from the mPRC to the IPRC is defined by the collateral sulcus of the medial temporal lobe, which exhibits considerable inter- and intraindividual variations (e.g., differences in length and form of the sulcus). This variability poses a significant challenge to accurately segment the mPRC and IPRC regions, as it profoundly influences the delimitation of their boundaries (for an insight into manual segmentation see Henzen et al., 2023). In a recent study we demonstrated an excellent inter-rater reliability between two rater using an existing manual segmentation protocol for the mPRC, IPRC, and ERC, which takes collateral sulcus variability into account (Henzen et al., 2023). Although manual segmentation for quantification of brain regions from MRI is the gold standard, it comes with the disadvantage of time-consuming implementation and is therefore not feasible for clinical and research setting (Morey et al., 2009). To address this, we employed advanced machine learning techniques in this study to enhance the applicability of mPRC measurements in AD diagnostics and research settings (Alzubaidi et al., 2021).

Advancements in algorithm and computation resources over time have significantly propelled the development of different segmentation techniques for neuroimaging, such as FreeSurfer (Reuter et al., 2012) or Statistical Parametric Mapping (SPM; Ashburner & Friston, 2005). Parallely, machine learning approaches based on convolutional neural network (CNN) architectures (e.g., U-Net) are experiencing a growing trend (Alzubaidi et al., 2021). Against this backdrop, we aimed to develop an automated segmentation tool based on U-Net, a generic deep-learning-based software package for cell detection and cell segmentation, which can be trained and applied to new data. In addition, it is customizable, which allows an adaption to specific challenges (Çiçek et al., 2016; Ronneberger et al., 2015). First, we aimed to replicate the results described by Krumm et al. (2016) to evaluate a potential clinical benefit. The study

found a significant atrophy in the mPRC and ERC when comparing both Alzheimer's dementia patients (dAD) as well as amnesic mild cognitive impairment (aMCI) patients with healthy controls. Notably, atrophy in the IPRC was observed exclusively in the dAD group, aligning with the NFT distribution pattern in early AD (Braak & Braak, 1991; Braak & Del Tredici, 2006; Krumm et al., 2016). While Krumm et al. (2016) used a manual segmentation protocol to extract cortical thickness, this study aimed to replicate the results using an automated segmentation method in the identical sample. Second, the automated segmentation is compared to the manual segmentation for the cortical thickness of brain regions first affected by atrophy in typical AD (e.g., mPRC, ERC). A reliable automated segmentation, especially of the mPRC, would facilitate the use in research and clinical settings to improve early detection of AD.

## **2. Materials and Methods**

### *2.1 Participants and MRI Acquisition*

#### 2.1.1 Training data set

The training data set (N=126, mean age=69.8 ± 10.8 years) consisted of 101 patients and 25 healthy control participants (NC). Written informed consent was obtained from all individuals prior to participation and the study was approved by the local ethics committee (EKNZ: Ethikkommission Nordwest- und Zentralschweiz). NCs were recruited from the "Registry of Healthy Individuals Interested to Participate in Research" of the Memory Clinic FELIX PLATTER Basel, Switzerland. They had undergone a thorough medical screening and neuropsychological testing to confirm their cognitive health. In particular, the exclusion criteria encompassed severe impairments in auditory, visual, or speech abilities; substantial sensory or motor deficits; severe systemic illnesses; persistent moderate to intense pain; conditions with significant or likely effects on the central nervous system (e.g., neurological disorders such as cerebral-vascular disease, generalized atherosclerosis, and psychiatric disorders); and the use of potent psychoactive substances, except for mild tranquilizers. In addition, all individuals classified NC obtained standard scores within the normal range on the Mini-Mental State Examination (MMSE) (Folstein et al., 1975), California Verbal Learning Task (Delis et al., 1988), Clock Drawing Test (Critchley, 1953), and the short version of the Boston Naming Test (Kaplan et al., 1983). Of the 101 patients, 29 participants were

diagnosed with mild cognitive disorder (MCI) according to DMS-IV (Bell, 1994). 26 participants were diagnosed with Major Depression (MD) including 14 participants recruited from the Memory Clinic FELIX PLATTER Basel, Switzerland, and 12 recruited from the University Psychiatric Clinics Basel, Switzerland. MDs had to score 10 or more points on the Becks Depression Inventory (Beck, 1961), 13 or more on Becks Depression Inventory-II (Beck et al., 2011), or 6 or more points on the Geriatric Depression Scale (Molton, 2013). 8 participants were diagnosed with aMCI (Albert et al., 2011) according to DSM-IV (American Psychiatric Association, 1994) and Winblad et al. (2004) criteria. 18 participants were diagnosed with dementia due to AD (dAD) according to DSM-IV criteria (American Psychiatric Association, 1994), and NINCDS-ADRDA (McKhann et al., 2011). aMCI and dAD were combined to one AD group (N=26) based on the assumption that the progression from aMCI to early dementia stage of AD is gradual and time of diagnosis can differ (Brooks & Loewenstein, 2010). Further, 20 patients were diagnosed with dementia due to other etiologies than AD (non-AD; e.g., due to Lewy body disease) according to DSM-IV. For an overview see Table 1. All patients had been recruited either from the Memory Clinic FELIX PLATTER Basel, Switzerland, where they had received neuropsychological testing, and medical and neurological examinations including blood analyses, or in the case of the 12 MDs from the University Psychiatric Clinics Basel, Switzerland. All participants were native Swiss-German or German-speaking adults.

Participants received T1-weighted 3D magnetization-prepared rapid acquisition gradient echo (MPRAGE) structural MRI using the same 3-Tesla scanner (MAGNETOM Skyra fit, Siemens; inversion time = 900 ms, repetition time 2300 ms, echo time 2.92 ms, flip angle = 9; acquisition matrix = 256 x 256 mm, voxel size = 1 mm isotropic) at the University Hospital Basel, Switzerland.



**Table 1***Training data set – sample characteristics*

	NCs (N = 25)		MCI (N = 29)		MD (N = 26)		AD (N = 26)		non-AD (N = 20)	
Gender (m/f)	11/14		16/13		14/12		14/12		8/12	
	<i>Mean</i>	<i>SD</i>	<i>Mean</i>	<i>SD</i>	<i>Mean</i>	<i>SD</i>	<i>Mean</i>	<i>SD</i>	<i>Mean</i>	<i>SD</i>
Age (yrs)	68.98	10.74	71.09	11.29	61.88	10.82	76.11	6.83	70.90	8.79
Education (yrs)	14.26	3.91	13.67	3.15	13.31	3.04	13.31	3.16	12.78	3.26
MMSE score	29.00	1.00	27.72	1.39	28.77	1.28	26.35	1.99	27.20	2.44

*Note.* NCs = normal controls; MCI = mild cognitive impairment; AD = Alzheimer's disease; nonAD = mild cognitive impairment or dementia not due to Alzheimer's disease (e.g. due to Lewy body); MD = Major Depression; m = male; f = female; MMSE = Mini-Mental State Examination; SD = standard deviation.

### 2.1.2 Test data set

The test data set (N=103, mean age=76.4 ± 7.0 years) is identical to the one used for group comparison in Krumm et al. (2016) and contained 46 healthy control participants (NC), 34 participants diagnosed with early Alzheimer's dementia (dAD) according to NINCDS-ADRDA and DSM-IV criteria (American Psychiatric Association, 1994) and 23 patients with amnesic mild cognitive disorder (aMCI) according to DSM-IV and Winblad et al. (2004) criteria (see Table 2). For a comprehensive overview of the inclusion and exclusion criteria, see Krumm et al. (2016). All patients had been recruited from the Memory Clinic FELIX PLATTER Basel, Switzerland, where they had received neuropsychological testing, and medical and neurological examinations including blood analyses. All participants were native Swiss-German or German-speaking adults.

Participants received T1-weighted 3D magnetization-prepared rapid acquisition gradient echo (MPRAGE) structural MRI using the same 3-Tesla scanner (MAGNETOM Verio, Siemens; inversion time = 1000 ms, repetition time 2000 ms, echo time 3.75 ms, flip angle = 8; acquisition matrix = 256 x 256 mm, voxel size = 1 mm isotropic) at the University Hospital Basel, Switzerland.

**Table 2***Test data set – sample characteristics*

Variable	NC versus aMCI				NC versus early dAD			
	NC (N = 46)		aMCI (N = 23)		NC (N = 31)		Early dAD (N = 34)	
Gender (m/f)	27/19		11/12		18/13		16/18	
	<i>Mean</i>	<i>SD</i>	<i>Mean</i>	<i>SD</i>	<i>Mean</i>	<i>SD</i>	<i>Mean</i>	<i>SD</i>
Age (yrs)	74.78	7.09	76.08	8.26	78.10	5.58	78.89	5.24
Education (yrs)	13.41	3.10	14.00	3.66	12.55	2.46	12.24	3.04
MMSE score	29.26	1.10	28.22	1.86	29.19	1.05	26.32	2.09

*Note.* NC = normal controls; aMCI= amnesic mild cognitive impairment; dAD = Alzheimer's dementia; m = male; f = female; MMSE = Mini-Mental State Examination; SD = standard deviation.

### 2.2 Preprocessing of structural MRI

MRI scans were preprocessed using FreeSurfer (Massachusetts General Hospital, Boston, MA, USA; <http://surfer.nmr.mgh.harvard.edu>; accessed on 7 January 2020; Dale et al., 1999; Fischl et al., 1999). In a semi-automated processing stream, FreeSurfer segmented the T1-weighted 3D magnetization-prepared rapid acquisition gradient echo (MPRAGE) volumes into grey and white matter. Next, the surface of white matter, represented by the transition area from white to grey matter, and the pial surface were modeled (Dale et al., 1999). Lastly, tissue classification was visually confirmed for all participants, and, if required, manual adjustments were performed.

### 2.3 Training and application of automated segmentation

The semi-automatic labels were mapped to the gray matter obtained by FreeSurfer and transformed to the 3D voxel space to create regional masks for mPRC, lPRC, ERC, and the parahippocampal cortex (PHC). Using each of the masks, we trained a separate network to segment the respective region as a voxel mask. The predicted voxel mask was then mapped back to the FreeSurfer space to compute morphological characteristics such as the average cortical thickness. We used the nnU-Net (Isensee et al., 2021) framework to train the networks. In two cases, the prediction of one of the masks failed and could not be projected to the FreeSurfer space to cortical thickness values (e.g., ERC right

hemisphere for one participant, IPRC right hemisphere for another participant). These measurements were excluded from further analyses.

#### *2.4 Statistical Analyses*

For each ROI, an aggregated bilateral cortical thickness value was used. Cortical thickness measurements were normalized for head size (as total intracranial volume [TIV]) as reported by Krumm et al. (2016) using the formula  $[(\text{cortical thickness})/(\text{TIV}) * 100]$ . For reporting in Table 3, normalized values were retransformed to mm using the mean TIV of the two comparing groups (e.g., dAD versus NC mean TIV = 1453 cm<sup>3</sup>; aMCI versus NC mean TIV = 1480 cm<sup>3</sup>). Group differences were examined conducting univariate analysis of covariance (ANCOVA), incorporating age, sex, and education level as covariates. To address multiple comparisons, significance thresholds were adapted using the Bonferroni correction (e.g.,  $p = 0.05/8 = 0.00625$ ). In addition, to evaluate the accuracy between the two methods (manual and automated segmentation), TIV corrected bilateral cortical thickness values of all participants of the test data set were compared using intraclass correlation coefficient (ICC) estimates and their 95% confidence intervals based on a single-rating, consistency, and a 2-way mixed-effects model according to the guidelines of Koo and Li (Koo & Li, 2016). All analyses were executed in SPSS software, and while Krumm et al. (2016) utilized SPSS 21.0, our replication utilized the subsequent version, SPSS 22.0 (IBM Corp. Released 2013. IBM SPSS Statistics for Windows, Version 22.0. Armonk, NY, USA).

### **3. Results**

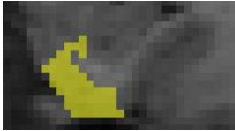

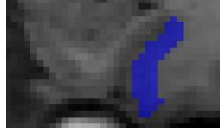

Two-tailed, univariate ANCOVAs with sex, age, and education as covariates were performed to determine whether each ROI (ERC, mPRC, IPRC, and PHC) was atrophied in the aMCI and dAD groups relative to their corresponding NC sample. Significance was tested with Bonferroni corrected p-values (i.e.,  $p = 0.05/8 = 0.00625$ ).

In comparison to the NC group, the dAD group showed significantly lower average cortical thickness of the ERC, mPRC, and IPRC, but not the PHC [ERC:  $F(1,60) = 39.820, p < 0.00625$ , mPRC:  $F(1,60)$

= 32.270,  $p < 0.00625$ , IPRC:  $F(1,60) = 10.907$ ,  $p < 0.00625$ , PHC:  $F(1,60) = 7.808$ ,  $p = 0.007 < 0.05$  i.e., did not survive Bonferroni correction of 0.00625]. In comparison to the NC group, only the ERC was significantly atrophied in the aMCI group [ERC:  $F(1,64) = 13.249$ ,  $p < 0.00625$ ], while the  $p$ -value of the mPRC, IPRC, and PHC did not survive Bonferroni correction of 0.00625 [mPRC:  $F(1,64) = 4.884$ ,  $p = 0.031$ ; IPRC:  $F(1,64) = 6.408$ ,  $p = 0.014$ ; PHC:  $F(1,64) = 6.716$ ,  $p = 0.012$ ]. The ICC analyses between manual and automated segmentation for TIV corrected cortical thickness estimates are summarized in Table 4.

**Table 3**

*Normalized and retransformed mean cortical thickness in each ROI over both hemispheres*

Group				
	ERC	mPRC	IPRC	PHC
	M (SD)	M (SD)	M (SD)	M (SD)
<b>NC versus aMCI</b>				
NC (n = 46)	3.55 (0.39)	2.82 (0.44)	3.09 (0.46)	2.42 (0.40)
aMCI (n = 23)	3.21 (0.44)	2.61 (0.53)	2.88 (0.42)	2.22 (0.25)
Relative differences (%)	11*	8	7	8
<b>NC versus dAD</b>				
NC (n=31)	3.54 (0.43)	2.72 (0.42)	3.06 (0.47)	2.35 (0.42)
dAD (n=34)	2.93 (0.41)	2.13 (0.53)	2.66 (0.61)	2.13 (0.48)
Relative differences (%)	20*	28*	15*	10

*Note.* M and SD are displayed in mm and represent TIV corrected bilateral cortical thickness values as described in Section 2.4. Key: dAD, Alzheimer's dementia; aMCI, amnesic mild cognitive impairment; ERC, entorhinal cortex; IPRC, lateral perirhinal cortex; M, mean; mPRC, medial perirhinal cortex; NC, normal controls; PHC, parahippocampal cortex; ROI, region of interest; SD, standard deviation. Each ROI of the left hemisphere in one random participant is shown in different color. ERC, mPRC, and IPRC are shown on the same coronal level, while PHC is shown 16 mm posterior. Significant differences ( $p < 0.00625$ ) are indicated with an asterisk (\*).

**Table 4**

*ICC calculation for TIV corrected cortical thickness estimates between manual and automated segmentation using single-rating, consistency, two-way mixed-effects model.*

Variable	Cronbach's Alpha	ICC	95% Confidence Interval		F Test		
			Lower Bound	Upper Bound	Value	df1/df2	<i>p</i>
mPRC	0.969	0.941	0.914	0.959	32.724	102/102	0.0× 10 <sup>0</sup>
IPRC	0.953	0.910	0.870	0.939	21.312	101/101	0.0× 10 <sup>0</sup>
ERC	0.941	0.889	0.841	0.924	17.091	101/101	0.0× 10 <sup>0</sup>
PHC	0.948	0.902	0.858	0.932	19.326	102/102	0.0× 10 <sup>0</sup>

*Note.* ICC = intraclass correlation coefficient; mPRC = medial perirhinal cortex; IPRC = lateral perirhinal cortex; ERC = entorhinal cortex; PHC = parahippocampal cortex.

#### 4. Discussion

Our goal was to replicate the findings of Krumm et al. (2016), who used a manual segmentation protocol to extract cortical thickness values of key regions within the parahippocampal gyrus (e.g., mPRC, IPRC, ERC, and PHC). Recognizing the labor-intensive nature of manual MRI-segmentation, we trained a deep convolutional network, specifically utilizing U-Net architecture, for the automated segmentation of the same regions and subsequently applied it to the identical sample as used in the group analysis in Krumm et al. (2016). In line with the findings of Krumm et al. (2016), our study found significant atrophy in the ERC, mPRC, and IPRC within the early dAD group when compared to the NC group. However, when comparing the aMCI group to the NC group, the null hypothesis of no difference could only be rejected in the ERC, while the null hypothesis of no difference in cortical thickness in the mPRC could not be rejected after applying strict correction for multiple comparisons, unlike the findings of Krumm et al. (2016). Nonetheless, the results are highly promising for future research in the early detection of AD, which will be discussed below. In addition, we compared the manual with the automated segmentation. The ICC analyses for cortical thickness estimates showed high ICC values between the manually and automatically generated cortical thickness values for all four ROIs (mPRC, IPRC, ERC, and PHC), suggesting manual and automatic segmentation to generate comparable outcomes.

As highlighted, the early involvement of the mPRC in NFT pathology in typical AD positions a specific mPRC-integrity score (e.g., cortical thickness) as a promising early and sensitive imaging biomarker. Building upon our initial aim to replicate the critical findings of Krumm et al. (2016) regarding atrophy in the ERC and mPRC as early markers of Alzheimer's disease, we have now bridged a significant gap in the field. The previously outlined very high reliability of a manual segmentation protocol, as detailed in the introduction, laid a solid foundation for accurate and detailed analysis of brain regions crucial for early detection of AD (Henzen et al., 2023). By integrating machine learning techniques, particularly through the training of a U-Net based deep convolutional network (Isensee et al., 2021), we have developed an automated segmentation tool that parallels the very high interrater reliability seen using the manual segmentation protocol. These findings establish a foundation for more efficient application in clinical and research settings, potentially improving the early diagnosis of AD.

In evaluating the early dAD group against the NC group using the identical sample, we replicated significant atrophy findings in the ERC, mPRC, and IPRC as reported by Krumm et al. (2016). Yet, in the aMCI vs. NC comparison, significant difference in cortical thickness was confined to the ERC. The results diverge from Krumm et al.'s (2016) findings regarding the mPRC, despite the same underlying sample. This discrepancy could reflect the limitations of our current methodological approach, especially regarding the accuracy of our automated segmentation tool mimicking manual segmentation results. Since the automated segmentation strives to replicate manual segmentation outcomes, its efficacy is inherently bounded by the precision of the manual segmentation technique. Although the manual segmentation served as the reference standard in our study, it still represents an estimation of the true cortical thickness, as all methodologies inherently possess limitations and potential biases. The results based on our sample suggest that the manual segmentation might be slightly more sensitive, but it lacks practicability in clinical or research setting. For example, manual segmentation for the mPRC requires about 20 minutes of labor per person, which is typically regarded as unfeasible in a clinical setting. The automated segmentation, on the other hand, runs unattended in the background in less than 5 minutes. Consequently, due to its high consistency with the manual segmentation, despite a potential bias, the automated method emerges as a promising alternative. Nonetheless, the future application and

validation of our new automated tool remain of utmost importance. Conducting a longitudinal study with initially healthy individuals would be particularly beneficial. This approach not only aims to collect essential normative data for the wider application of our tool in clinical settings but also enables the retrospective analysis of cortical changes in participants who later develop symptomatic AD. In addition, incorporating longitudinal studies that not only employ conventional neuropsychological assessments but also integrate newer, more specific neuropsychological tests for assessing specific perirhinal cortex function, such as the novel object recognition task developed by Frei et al. (2022), will be instrumental. It is also worth mentioning that our automated segmentation algorithm enables further examination of the PHC's role in early AD. This exploration could provide critical insights into AD pathology, as early PHC atrophy could explain certain cognitive symptoms (e.g., visuospatial: Epstein & Kanwisher, 1998).

Furthermore, we did not investigate cortical thickness values of left and right hemisphere separately. Brain atrophy in typical AD often presents asymmetrically, particularly emphasizing the vulnerability of the left hemisphere (Lubben et al., 2021). This emphasizes the importance of separate evaluation of the hemispheres (e.g., cortical thickness of the left and right mPRC) in future research and clinical assessments. Although the mPRC rises as a promising vital structural biomarker in the early phases of AD, adopting a multi-domain approach that potentially includes a range of biomarkers becomes increasingly more important as we delve into the mild cognitive impairment spectrum moving towards asymptomatic stages. Such investigations require large data sets, which are not feasible for manual segmentation, a shortfall we believe to have successfully addressed with our presented automated segmentation method. This strategy not only aims to improve individualized patient evaluations but also promises to refine diagnostic precision and foster early, customized interventions in the incipient stages of the disease.

## **5. Conclusion**

We aimed to replicate prior findings by Krumm et al. (2016), confirming early AD-associated cortical thinning within key parahippocampal gyrus regions via automated MRI-segmentation. The results

showed high consistency for cortical thickness between the manual and automated segmentation. Therefore, despite the potentially slightly higher sensitivity of manual segmentation in our sample, the automated method still emerges as a promising tool, especially due to its applicability to larger datasets. We underscore the importance of future longitudinal studies, which should not only include initially healthy individuals but also focus on measuring unilateral cortical thickness values and incorporate neuropsychological testing, particularly tasks specifically assessing the function of the perirhinal cortex. This strategy not only aims to enhance diagnostic precision but also to pave the way for early, targeted intervention strategies, ultimately contributing to the development of personalized treatment plans and advancing our collective understanding of AD pathology.



## References

- Alzubaidi, L., Zhang, J., Humaidi, A. J., Al-Dujaili, A., Duan, Y., Al-Shamma, O., ... & Farhan, L. (2021). Review of deep learning: Concepts, CNN architectures, challenges, applications, future directions. *Journal of Big Data*, 8(1), 53. <https://doi.org/10.1186/s40537-021-00444-8>
- Ashburner, J., & Friston, K. J. (2005). Unified segmentation. *NeuroImage*, 26(3), 839–851. <https://doi.org/10.1016/j.neuroimage.2005.02.018>
- Beck, A. T. (1961). An Inventory for Measuring Depression. *Archives of General Psychiatry*, 4(6), 561. <https://doi.org/10.1001/archpsyc.1961.01710120031004>
- Beck, A. T., Steer, R. A., & Brown, G. (2011). *Beck Depression Inventory–II* [dataset]. <https://doi.org/10.1037/t00742-000>
- Bell, C. C. (1994). DSM-IV: Diagnostic and Statistical Manual of Mental Disorders. *JAMA: The Journal of the American Medical Association*, 272(10), 828. <https://doi.org/10.1001/jama.1994.03520100096046>
- Bobinski, M., Wegiel, J., Tarnawski, M., Bobinski, M., Reisberg, B., de Leon, M. J., ... & Wisniewski, H. M. (1997). Relationships between Regional Neuronal Loss and Neurofibrillary Changes in the Hippocampal Formation and Duration and Severity of Alzheimer Disease. *Journal of Neuropathology & Experimental Neurology*, 56(4), 414–420. <https://doi.org/10.1097/00005072-199704000-00010>
- Braak, H., & Braak, E. (1991). Neuropathological staging of Alzheimer-related changes. *Acta Neuropathologica*, 82(4), 239–259. <https://doi.org/10.1007/BF00308809>
- Braak, H., & Del Tredici, K. (2006). Staging of cortical neurofibrillary inclusions of the Alzheimer's type. In M. Jucker, K. Beyreuther, C. Haass, R. M. Nitsch, & Y. Christen (Eds.), *Alzheimer: 100 Years and Beyond* (pp. 97–106). Springer. [https://doi.org/10.1007/978-3-540-37652-1\\_8](https://doi.org/10.1007/978-3-540-37652-1_8)
- Brodmann, K., & Garey, L. (2006). *Brodmann's Localisation in the cerebral cortex: The principles of comparative localisation in the cerebral cortex based on the cytoarchitectonics*. Springer. <https://doi.org/10.1007/b138298>

- Çiçek, Ö., Abdulkadir, A., Lienkamp, S. S., Brox, T., & Ronneberger, O. (2016). 3D U-Net: Learning Dense Volumetric Segmentation from Sparse Annotation. In S. Ourselin, L. Joskowicz, M. R. Sabuncu, G. Unal, & W. Wells (Eds.), *Medical Image Computing and Computer-Assisted Intervention – MICCAI 2016* (pp. 424–432). Springer International Publishing. [https://doi.org/10.1007/978-3-319-46723-8\\_49](https://doi.org/10.1007/978-3-319-46723-8_49)
- Dale, A. M., Fischl, B., & Sereno, M. I. (1999). Cortical Surface-Based Analysis: I. Segmentation and Surface Reconstruction. *NeuroImage*, *9*(2), 179–194. <https://doi.org/10.1006/nimg.1998.0395>
- Delis, D. C., Freeland, J., Kramer, J. H., & Kaplan, E. (1988). Integrating clinical assessment with cognitive neuroscience: Construct validation of the California Verbal Learning Test. *Journal of Consulting and Clinical Psychology*, *56*(1), 123–130. <https://doi.org/10.1037/0022-006X.56.1.123>
- Enkirch, S. J., Träschütz, A., Müller, A., Widmann, C. N., Gielen, G. H., Heneka, M. T., ... & Hattingen, E. (2018). The ERICA Score: An MR Imaging–based Visual Scoring System for the Assessment of Entorhinal Cortex Atrophy in Alzheimer Disease. *Radiology*, *288*(1), 226–333. <https://doi.org/10.1148/radiol.2018171888>
- Epstein, R., & Kanwisher, N. (1998). A cortical representation the local visual environment. *Nature*, *392*(6676), 598–601. Scopus. <https://doi.org/10.1038/33402>
- Fischl, B., Sereno, M. I., & Dale, A. M. (1999). Cortical Surface-Based Analysis: II: Inflation, Flattening, and a Surface-Based Coordinate System. *NeuroImage*, *9*(2), 195–207. <https://doi.org/10.1006/nimg.1998.0396>
- Folstein, M. F., Folstein, S. E., & McHugh, P. R. (1975). “Mini-mental state”: A practical method for grading the cognitive state of patients for the clinician. *Journal of Psychiatric Research*, *12*(3), 189–198. [https://doi.org/10.1016/0022-3956\(75\)90026-6](https://doi.org/10.1016/0022-3956(75)90026-6)
- Frei, M., Berres, M., Kivisaari, S. L., Henzen, N. A., Monsch, A. U., Reinhardt, J., ... & Krumm, S. (2022). Can you find it? Novel oddity detection task for the early detection of Alzheimer’s disease. *Neuropsychology*, No Pagination Specified-No Pagination Specified. <https://doi.org/10.1037/neu0000859>

- Giannakopoulos, P., Herrmann, F. R., Bussière, T., Bouras, C., Kövari, E., Perl, D. P., ... & Hof, P. R. (2003). Tangle and neuron numbers, but not amyloid load, predict cognitive status in Alzheimer's disease. *Neurology*, *60*(9), 1495–1500. <https://doi.org/10.1212/01.wnl.0000063311.58879.01>
- Gómez-Isla, T., Hollister, R., West, H., Mui, S., Growdon, J. H., Petersen, R. C., ... & Hyman, B. T. (1997). Neuronal loss correlates with but exceeds neurofibrillary tangles in Alzheimer's disease. *Annals of Neurology*, *41*(1), 17–24. <https://doi.org/10.1002/ana.410410106>
- Henzen, N. A., Reinhardt, J., Blatow, M., Kressig, R. W., & Krumm, S. (2023). Excellent Interrater Reliability for Manual Segmentation of the Medial Perirhinal Cortex. *Brain Sciences*, *13*(6), Article 6. <https://doi.org/10.3390/brainsci13060850>
- Isensee, F., Jaeger, P. F., Kohl, S. A. A., Petersen, J., & Maier-Hein, K. H. (2021). nnU-Net: A self-configuring method for deep learning-based biomedical image segmentation. *Nature Methods*, *18*(2), 203–211. <https://doi.org/10.1038/s41592-020-01008-z>
- Kaplan, E., Goodglass, H., & Weintraub, S. (1983). *Boston naming test*. Lea & Febiger.
- Koo, T. K., & Li, M. Y. (2016). A Guideline of Selecting and Reporting Intraclass Correlation Coefficients for Reliability Research. *Journal of Chiropractic Medicine*, *15*(2), 155–163. <https://doi.org/10.1016/j.jcm.2016.02.012>
- Krumm, S., Kivisaari, S. L., Probst, A., Monsch, A. U., Reinhardt, J., Ulmer, S., ... & Taylor, K. I. (2016). Cortical thinning of parahippocampal subregions in very early Alzheimer's disease. *Neurobiology of Aging*, *38*, 188–196. <https://doi.org/10.1016/j.neurobiolaging.2015.11.001>
- Kulason, S., Tward, D. J., Brown, T., Sicat, C. S., Liu, C.-F., Ratnanather, J. T., ... & Miller, M. I. (2019). Cortical thickness atrophy in the transentorhinal cortex in mild cognitive impairment. *NeuroImage: Clinical*, *21*, 101617. <https://doi.org/10.1016/j.nicl.2018.101617>
- Lubben, N., Ensink, E., Coetzee, G. A., & Labrie, V. (2021). The enigma and implications of brain hemispheric asymmetry in neurodegenerative diseases. *Brain Communications*, *3*(3), fcab211. <https://doi.org/10.1093/braincomms/fcab211>
- Molton, I. (2013). Geriatric Depression Scale. In M. D. Gellman & J. R. Turner (Eds.), *Encyclopedia of Behavioral Medicine* (pp. 857–858). Springer. [https://doi.org/10.1007/978-1-4419-1005-9\\_194](https://doi.org/10.1007/978-1-4419-1005-9_194)

- Morey, R. A., Petty, C. M., Xu, Y., Hayes, J. P., Wagner, H. R., Lewis, D. V., ... & McCarthy, G. (2009). A comparison of automated segmentation and manual tracing for quantifying hippocampal and amygdala volumes. *NeuroImage*, *45*(3), 855–866.  
<https://doi.org/10.1016/j.neuroimage.2008.12.033>
- Morris, J. C., Kimberly, A., Quaid, K., Holtzman, D. M., Kantarci, K., Kaye, J., Reiman, E. M., ... & Siemers, E. R. (2005). Role of biomarkers in studies of presymptomatic Alzheimer's disease. *Alzheimer's & Dementia*, *1*(2), 145–151. <https://doi.org/10.1016/j.jalz.2005.09.013>
- Reuter, M., Schmansky, N. J., Rosas, H. D., & Fischl, B. (2012). Within-subject template estimation for unbiased longitudinal image analysis. *Neuroimage*, *61*(4), 1402–1418.  
<https://doi.org/10.1016/j.neuroimage.2012.02.084>
- Ronneberger, O., Fischer, P., & Brox, T. (2015). U-Net: Convolutional Networks for Biomedical Image Segmentation. *arXiv:1505.04597 [Cs]*. <http://arxiv.org/abs/1505.04597>
- Rullmann, M., Brendel, M., Schroeter, M., Saur, D., Levin, J., Perneczky, R., ... & Tau, O. B. O. T. G. I. I. F. (2022). Multicenter 18F-PI-2620 PET for In Vivo Braak Staging of Tau Pathology in Alzheimer's Disease. *Biomolecules*, *12*. <https://doi.org/10.3390/biom12030458>
- Scheltens, P., & Pol, L. van de. (2012). Atrophy of medial temporal lobes on MRI in “probable” Alzheimer's disease and normal ageing: Diagnostic value and neuropsychological correlates. *Journal of Neurology, Neurosurgery & Psychiatry*, *83*(11), 1038–1040.  
<https://doi.org/10.1136/jnnp-2012-302562>
- Schwarz, A., Yu, P., Miller, B., Shcherbinin, S., Dickson, J., Navitsky, M. A., Joshi, A., Devous, M., & Mintun, M. (2016). Regional profiles of the candidate tau PET ligand 18F-AV-1451 recapitulate key features of Braak histopathological stages. *Brain : A Journal of Neurology*, *139* Pt 5, 1539–1550. <https://doi.org/10.1093/brain/aww023>
- Sone, D., Imabayashi, E., Maikusa, N., Okamura, N., Furumoto, S., Kudo, Y., ... & Matsuda, H. (2017). Regional tau deposition and subregion atrophy of medial temporal structures in early Alzheimer's disease: A combined positron emission tomography/magnetic resonance imaging

study. *Alzheimer's & Dementia : Diagnosis, Assessment & Disease Monitoring*, 9, 35–40.

<https://doi.org/10.1016/j.dadm.2017.07.001>

Sperling, R. A., Aisen, P. S., Beckett, L. A., Bennett, D. A., Craft, S., Fagan, A. M., ... & Phelps, C. H. (2011).

Toward defining the preclinical stages of Alzheimer's disease: Recommendations from the National Institute on Aging-Alzheimer's Association workgroups on diagnostic guidelines for Alzheimer's disease. *Alzheimer's & Dementia : The Journal of the Alzheimer's Association*, 7(3), 280–292. <https://doi.org/10.1016/j.jalz.2011.03.003>

Taylor, K. I., & Probst, A. (2008). Anatomic localization of the transentorhinal region of the perirhinal cortex. *Neurobiology of Aging*, 29(10), 1591–1596.

<https://doi.org/10.1016/j.neurobiolaging.2007.03.024>

Winblad, B., Palmer, K., Kivipelto, M., Jelic, V., Fratiglioni, L., Wahlund, L.-O., ... & Petersen, R. C. (2004).

Mild cognitive impairment--beyond controversies, towards a consensus: Report of the International Working Group on Mild Cognitive Impairment. *Journal of Internal Medicine*, 256(3), 240–246. <https://doi.org/10.1111/j.1365-2796.2004.01380.x>

### 3. GENERELLE DISKUSSION

Die Demenz, respektive die AK als ihre führende Ursache, stellt eine der grössten gesundheitlichen Herausforderungen des 21. Jahrhunderts dar. Dies resultiert aus einer immer älter werdenden Bevölkerung in Kombination mit der Tatsache, dass das Alter der grösste Risikofaktor für eine AK darstellt. Die Identifikation der frühesten kognitiven und strukturellen Veränderungen repräsentiert daher eines der bedeutendsten Ziele der Alzheimer-Forschung. Eine möglichst frühe Diagnose würde den Einsatz von Therapien zu einem Zeitpunkt geringster kognitiver und neuropathologischer Schäden erlauben. Die vorliegende Promotionsschrift konzentrierte sich deshalb auf den mPRC, welcher als erste kortikale Struktur von der neurofibrillären Taupathologie der typischen AK betroffen ist und somit ein vielversprechender früher und sensitiver kognitiver sowie struktureller Marker repräsentiert. In Studie I wurde ein neu entwickelter Test zur Messung der PRC-Funktion vorgestellt, der die Unterscheidung von Patientinnen und Patienten im frühen Stadium der AK von gesunden Kontrollpersonen erlaubte. In Studie II fanden wir zwischen zwei Ratern eine hervorragende Übereinstimmung manuell segmentierter kortikaler Dicken-Werte für parahippocampale Regionen (mPRC, IPRC und ERC). In Studie III haben wir die manuelle Segmentierung aus Studie II automatisiert und erzielten eine hohe Übereinstimmung zwischen den manuell und automatisiert generierten Werte für die kortikale Dicke parahippocampaler Regionen (mPRC, IPRC, ERC und PHC). Es folgt nun eine Diskussion der Ergebnisse der einzelnen Studien, bevor diese im Kontext der Bedeutung für die Verbesserung der Früherkennung der AK zusammengeführt werden.

#### 3.1. Der Odd-One-Out für die Früherkennung der Alzheimer-Krankheit

Wie eingehend thematisiert, konzentriert sich die Alzheimer-Diagnostik hauptsächlich auf der Beurteilung der episodischen Gedächtnisleistung, die in engem Zusammenhang mit Atrophie im ERC und HC steht (Hirni et al., 2013; Lipton & Eichenbaum, 2008). Zwar weist ein häufig genutzter semantischer Gedächtnistest (semantische Flüssigkeitsaufgabe) eine Korrelation mit der Integrität des PRC auf, aber gleichzeitig auch mit dem ERC und dem HC (Hirni et al., 2013). Das bedeutet, dass aktuell kein

routinemässig eingesetzter Test spezifisch die PRC-Funktion abbildet. Angesichts der frühen Beteiligung des PRC in der Neuropathologie der typischen AK und seiner zentralen Rolle in der visuellen Objektverarbeitung, präsentierten wir in Studie I eine innovative und vielversprechende visuelle Diskriminationsaufgabe. Bei diesem spezifischen PRC-Funktionstest gilt es, aus sechs komplexen und sehr ähnlichen Figuren jene zu identifizieren, die am stärksten von den anderen abweicht. Eine Aufgabe, für welche es notwendig ist, eine integrierte Wahrnehmungsrepräsentation aus einzelnen visuellen Merkmalen zu erstellen – eine Funktion, welche dem PRC zugeschrieben wird (Murray et al., 2007; Murray & Richmond, 2001). In einer Pilotstudie mit 50 Patientinnen und Patienten im Frühstadium einer AK und 50 gesunden Kontrollpersonen ermittelten wir die optimale Kombination aus Anzahl visueller Merkmale pro Figur sowie Anzahl und Art der abweichenden Variationen der Zielfigur. Aufbauend auf diesen Erkenntnissen führten wir eine Validierungsstudie mit 27 Patientinnen und Patienten im Frühstadium einer AK, 25 gesunden Kontrollpersonen und 26 Patientinnen und Patienten mit einer Depression durch. Grund für den Einbezug einer Depressionsgruppe war die Tatsache, dass eine klinisch relevanten depressiven Stimmungsproblematik oft ebenfalls mit Gedächtnisproblemen einhergeht. Dies kann die Abgrenzung zur AK in der Klinik erschweren, wobei ein spezifischer PRC-Funktionstest in diesem Falle die Differentialdiagnostik verbessern könnte (Rotomskis et al., 2015), da bei einer Depression keine Funktionsbeeinträchtigung des PRC zu erwarten ist. Unsere Ergebnisse zeigten, dass die visuelle Diskriminationsaufgabe eine gute Unterscheidung zwischen Patientinnen und Patienten im Frühstadium einer AK und gesunden Kontrollpersonen ermöglichte. Ein zusätzlicher differentialdiagnostischer Nutzen im Sinne einer Differenzierung der Alzheimergruppe zur Depressionsgruppe fand sich in unserer Stichprobe nicht. Eine massgebliche Limitation hierbei war der deutliche Altersunterschied zwischen den zwei Gruppen (Alzheimer vs. Depression: Mittelwertsunterschied von 16.2 Jahren), welcher den Grossteil der Varianz in der Testleistung erklärte. Entsprechend sollten zukünftigen Studien Gruppen verwenden, die hinsichtlich des Alters angeglichen sind, um eine präzisere Einschätzung der Testleistung zu ermöglichen. Des Weiteren erfordert die visuelle Diskriminationsaufgabe möglicherweise ein gewisses Mass an Aufmerksamkeit (z.B. die Aufrechterhaltung des visuellen Stimulus sowie eine Aufmerksamkeitsverschiebung zwischen den Figuren). Da Patientinnen und Patienten mit einer

Depression häufig Aufmerksamkeitsdefizite aufweisen (Rotomskis et al., 2015), könnte dies die Testleistung negativ beeinflusst haben. Zukünftige Studien könnten diesen Faktor durch den zusätzlichen Einsatz von Aufmerksamkeitstests, etwa zur Messung der visuellen Merkspanne und Arbeitsgedächtnis, berücksichtigen.

Die durchgeführte voxel-basierte Morphometrie (VBM)-Analyse zeigte einen Zusammenhang zwischen der Testleistung und vier signifikanten Clustern, insbesondere in den parahippocampalen Regionen einschliesslich des PRC und des ERC. Überraschenderweise hat die durchgeführte Analyse der interessierenden Regionen (ROI; «Regions of Interest») – die darauf abzielte, die Testleistung mit einer spezifischen Region (z.B. dem mPRC) in Verbindung zu bringen – keine Signifikanz erreicht. Solche Diskrepanzen zwischen VBM- und ROI-Analysen sind in der Literatur zur Neurobiologie nicht ungewöhnlich, da die interindividuelle Varianz in ROI-Analysen oft sehr gross ist (z.B. Giuliani et al., 2005; Seyed et al., 2020). Zukünftige Forschung könnte durch grössere Stichproben die interindividuelle Varianz besser adressieren. Weiter besteht die Möglichkeit, dass die funktionelle Überlappung benachbarter anatomischer Gebiete eine präzise Zuordnung der Testleistung zu spezifischen Regionen erschwerte. Jüngere Studien haben beispielsweise die Beteiligung des Parietallappens (im Sinne des dorsalen visuellen Verarbeitungspfades) an der Objekterkennung hervorgehoben, welcher in den frühen Phasen der AK die reduzierte PRC-Funktion kompensieren könnte (Freud et al., 2017). Trotz der Übereinstimmung unserer visuellen Reize mit wesentlichen klassischen Prinzipien der Gestalttheorie (z.B. Nähe und Verbundenheit) müssen wir in Betracht ziehen, dass unser eingesetzter PRC-Funktionstest vielleicht nicht primär die Fähigkeit erfasste, eine integrierte Wahrnehmungsrepräsentation aus einzelnen visuellen Merkmalen zu erstellen. Hierbei könnten funktionelle Bildgebungsverfahren, wie das funktionelle MRT (fMRT), wertvolle Einblicke in die bei der Aufgabenbearbeitung involvierten Gehirnregionen bieten. Als Proof-of-Concept, dass der mPRC tatsächlich nur in der Alzheimer-Gruppe atroph ist, haben wir die kortikale Dicke unserer ROI mit beiden anderen Gruppen verglichen. In Einklang mit dem postulierten hierarchischen Verlauf der neurofibrillären Taupathologie (Braak et al., 2006; Braak & Braak, 1991b), wies nur die Alzheimer-Gruppe eine signifikant verringerte kortikale Dicke im mPRC und ERC auf. Dieser Unterschied fand sich nicht für



den IPRC, was nicht nur das frühe Stadium unserer Alzheimer-Gruppe reflektierte, sondern erneut unterstreicht, wie wichtig es ist, den medialen und lateralen PRC in den Anfangsphasen der AK separat zu betrachten.

Ein herausragendes Merkmal des vorgestellten PRC-Funktionstests ist, dass er unabhängig von Sprache, Ausbildung und Gedächtnis funktioniert sowie durch seine einfache Umsetzung mittels Computer überzeugt. Insgesamt deutet vieles darauf hin, dass die vorgestellte visuelle Diskriminationsaufgabe ein vielversprechendes Instrument ist, Patientinnen und Patienten in einem frühen Alzheimer-Stadium von gesunden Personen zu differenzieren. Damit er jedoch optimal in der klinischen Diagnostik genutzt werden kann, gilt es, den Test in der Zukunft anhand dreier Hauptkriterien zu bewerten:

1. Seine Fähigkeit, basierend auf seiner Sensitivität, den Krankheitsverlauf der AK bereits in sehr frühen Stadien zu prognostizieren.
2. Sein Potenzial, frühzeitige kognitive Veränderungen der AK sensibler und spezifischer zu erkennen als herkömmlich verwendete Testverfahren, um so einen zusätzlichen diagnostischen Mehrwert zu bieten.
3. Seine Kapazität, die AK eindeutig von anderen Erkrankungen (z.B. vaskulären Hirnveränderungen, einer Parkinson-Krankheit oder einer Depression) abzugrenzen.

Um die oben erwähnten Kriterien eingehend zu überprüfen, erweisen sich Langzeitstudien mit initial gesunden älteren Studienteilnehmenden als besonders hilfreich. Im Laufe einer solchen Studie manifestieren sich bei einigen Probandinnen und Probanden kognitive Veränderungen, wobei ein Teil dieser Gruppe im Verlauf die Kriterien für ein MCI-Stadium aufgrund einer AK erfüllen. An diesem Punkt wird es möglich, retrospektiv zu bewerten, inwiefern unser neuer spezifischer PRC-Funktionstest in der Lage war, subtile kognitive Veränderungen im Rahmen der AK früher zu erkennen als gängige Standardtests (z.B. episodische Gedächtnisaufgaben). Die Stärke solcher Studien liegt darin, dass sie erlauben, die Effektstärken und prognostische Validität verschiedener Tests bei Individuen zu evaluieren, die im Verlauf eine symptomatische AK entwickeln. Durch eine umfassende neuropsychologische

Untersuchung könnten zudem mögliche Zusammenhänge zwischen Aufmerksamkeitsfunktionen – etwa gemessen durch visuelle Merkspanne und Arbeitsgedächtnis – und unserem PRC-Funktionstest mitberücksichtigt werden. Dieses Wissen könnte in zukünftigen Anwendungen genutzt werden, um für reduzierte Aufmerksamkeitsleistungen zu kontrollieren, was eine präzisere Einschätzung der PRC-Funktion ermöglichen würde. Zur weiteren Vertiefung der Erkenntnisse könnten ergänzende Studien Eye-Tracking-Technologien nutzen, um die Augenbewegungen verschiedener Patientengruppen sowie gesunder Kontrollpersonen während der Aufgabenbearbeitung zu analysieren. Dieser Ansatz würde es ermöglichen, feinere Unterschiede im visuellen Suchverhalten zu erfassen. Insbesondere könnte untersucht werden, ob Patientinnen und Patienten mit einer Beeinträchtigung des PRC schneller zwischen einzelnen Objekten hin und her wechseln, beispielsweise, weil sie auf den Vergleich einzelner Merkmale zwischen den Objekten zurückgreifen müssen. Weiter könnte durch den Einsatz des PRC-Funktionstests in einer Langzeitstudie, die gegenwärtig noch relativ lange Testdauer von rund 20 Minuten optimiert werden, indem nur die aussagekräftigsten Items identifiziert werden. Eine kompaktere Testdauer ist für eine zukünftige klinische Anwendungen besonders wünschenswert und wird am Ende der Promotionsarbeit im Ausblick nochmals ausführlicher thematisiert. Ein solcher kognitiver Marker entfaltet sein Potential vermutlich weniger im bereits fortgeschrittenem Alzheimer-Stadium, wenn der HC deutlich atroph ist und die Gedächtnisleistung entsprechend stark defizitär. Vielmehr sollte das Augenmerk auf Personen in einem präklinischen Stadium gerichtet werden. Beispielsweise Personen welche subjektiv eine Abnahme ihrer kognitiven Leistungsfähigkeit bemerken, in der alltäglichen Funktion aber nicht eingeschränkt sind und in den routinemässig eingesetzten neuropsychologischen Tests unauffällige Resultate erzielen (bekannt als «subjective cognitive decline»; SCD; Jessen et al., 2020).

Zusätzlich muss erwähnt werden, dass die vorliegende Dissertation den Fokus auf nur eine Funktion des PRC gerichtet hat. Der PRC zeichnet sich jedoch durch Verbindungen zu weiteren sensorischen Arealen aus (Suzuki & Amaral, 1994), wobei er neben visuellen auch auditive und sensomotorische Informationen verarbeitet, was ihm eine zentrale Bedeutung für das semantische Objektgedächtnis verleiht (Taylor et al., 2006, 2011). Diese Fähigkeit zur multimodalen

Informationsverarbeitung stellt eine ideale Basis dar, um zusätzliche, spezifische PRC-Funktionstests zu entwickeln. Besonders visuell-auditorische Integrationsaufgaben könnten hierbei äusserst interessant sein – ein Ansatzpunkt, der ebenfalls im Ausblick am Ende der Promotionsarbeit nochmals aufgegriffen wird.

### 3.2. Manuelle und automatisierte Segmentierung des medialen perirhinalen Kortex

Wie eingänglich erwähnt, werden ergänzend zur neuropsychologischen Untersuchung in der klinischen Routine der Memory Clinic standardmässig eine geriatrisch-neurologische Untersuchung sowie eine strukturelle Bildgebung durchgeführt. Besonders bei Patientinnen und Patienten mit subtilen kognitiven Defiziten kann die Bestimmung der genauen Ursache herausfordernd sein, was weiter erschwert wird durch die im Alter vermehrt auftretende Multimorbidität (Salive, 2013). In solchen Fällen gewinnt die Bedeutung von Biomarkern, insbesondere die strukturelle MRT-Bildgebung, erheblich an Gewicht und bietet in Kombination mit neuropsychologischen Bewertungen einen zusätzlichen diagnostischen Mehrwert (Klöppel et al., 2015). Vor allem ein Atrophie-Score des mPRC, beispielsweise gemessen an der kortikalen Dicke, könnte wegen seiner frühen und spezifischen Beteiligung im Kontext der AK, einen wertvollen Beitrag zur differentialdiagnostischen Unterscheidung leisten.

Studie II zeigte, dass zwei Rater mit dem angewendeten manuellen Segmentierungsprotokoll fast identische Werte für die kortikale Dicke des mPRC, IPRC und ERC erzielten. Zudem erwies sich das Protokoll selbst für einen unerfahrenen Rater als äusserst benutzerfreundlich. Für die Volumenschätzungen fanden sich für Regionen, deren Grenzen durch die Sulcus collateralis Variabilität beeinflusst werden (z.B. mPRC und IPRC) eine bedeutend tiefere Übereinstimmung zwischen den beiden Ratern (vgl. Intraklass-Korrelationskoeffizienten-Werte von .705 bis .874 für Volumina gegenüber .953 bis .986 für die kortikale Dicke). Dieses Ergebnis ist im Einklang mit bestehender Literatur, die den Einfluss der Sulcus collateralis Variabilität auf das Volumen benachbarter Regionen beschrieben (Insausti et al., 1998; Pruessner et al., 2002). Dickerson et al. (2009) konnten zeigen, dass das Volumen von MTL-

Subregionen (z.B. ERC und PRC), wenn auch nicht so ausgeprägt wie bei Patientinnen und Patienten mit einer AK, auch bei gesunden älteren Personen verringert war. Die kortikale Dicke hingegen war nur in der Alzheimer-Gruppe reduziert, nicht bei gesunden älteren Personen. Angesichts dieser Befunde stellt die kortikale Dicke möglicherweise ein sensibleres und zuverlässigeres Mass für Atrophie in Zusammenhang mit der AK dar, insbesondere für Regionen, deren Grenzen durch die Variabilität des Sulcus collateralis beeinflusst werden (z.B. mPRC und IPRC). Aufgrund der ausgezeichneten Übereinstimmung zwischen den beiden Ratern verzichteten wir auf eine erneute Segmentierung zur Ermittlung der Intra-Rater Reliabilität. Zukünftige Studien könnten sich dessen noch annehmen und gleichzeitig mehr als zwei Rater einschliessen.

Mit unserer Stichprobe haben wir nicht versucht, die Allgemeinbevölkerung abzubilden, sondern eher die Heterogenität des klinischen Alltags zu reflektieren, die aus Patientinnen und Patienten mit unterschiedlichen Störungsbildern und nur wenigen gesunden Personen besteht. Entsprechend könnte eine Replikationsstudie eine grössere Stichprobe anstreben, was zusätzlich auch erlauben würde, die kortikale Dicke der ROI zwischen den Gruppen zu vergleichen (im Sinne einer Proof-of-Concept Studie, dass der mPRC nur im Anfangsstadium der AK atroph ist und nicht bei anderen Störungsbildern). Die manuelle Segmentierung kommt mit dem Nachteil zeitintensiver Umsetzung, was beispielsweise für grössere Datensätze und für den klinischen Einsatz nicht tragbar ist. Während die automatisierte Segmentierung beispielsweise für den ERC bereits sehr gute Resultate erzielt (Desikan et al., 2006; Yushkevich et al., 2015), ist bisher keine zuverlässige Software für die kortikale Dicke des mPRC verfügbar.

Vor diesem Hintergrund widmete sich Studie III der Entwicklung eines Segmentierungstools zur automatisierten Berechnung der kortikalen Dicke parahippocampaler Regionen (mPRC, IPRC, ERC und PHC). Wir nutzten dafür U-Net, ein Deep-Learning-basiertes Softwarepaket, das ursprünglich für die Zellerkennung und -segmentierung entwickelt wurde (Ronneberger et al., 2015). Ein entscheidender Vorteil dieser Methode ist, dass die bestehende Modellarchitektur mit neuen Daten trainiert und auf spezifische Fragestellungen zugeschnitten werden kann. Für den Trainingsprozess haben wir MRT-Bilder mit manuell segmentierten Labels verwendet, welche die Position der ROI präzise markierten - basierend

auf dem in Studie II verwendeten Segmentierungsprotokoll. Durch das Training generierte das Modell Segmentierungsmasken, welche anschliessend in einem separaten Testdatensatz eingesetzt wurden, um die kortikale Dicke der ROI automatisiert zu bestimmen. Dieser Testdatensatz entsprach dem der Studie von Krumm et al. (2016), was uns erlaubte, das automatisierte Modell zu validieren und seine Fähigkeit zu prüfen, die erlernten Merkmale auf neue, unbekannte Daten anzuwenden. Die Ergebnisanalyse zeigte eine hohe Übereinstimmung zwischen den manuell und automatisiert generierten kortikalen Dicken aller ROI.

Durch die Analyse der automatisiert ermittelten kortikalen Dicken konnten wir zentrale Ergebnisse der Studie von Krumm et al. (2016) bestätigen. Dies umfasste insbesondere den Nachweis signifikanter Atrophie in der Alzheimer-Demenzgruppe im Vergleich zur gesunden Kontrollgruppe, im ERC, mPRC und IPRC. Im Gegensatz zu den Befunden von Krumm et al. (2016) zeigte sich jedoch eine signifikant reduzierte kortikale Dicke ausschliesslich im ERC, nicht im mPRC, wenn die aMCI-Gruppe mit der gesunden Kontrollgruppe verglichen wurde. Diese Diskrepanz könnte die Grenzen unseres aktuellen methodischen Ansatzes widerspiegeln. Da die automatisierte Segmentierung darauf trainiert wurde, die Ergebnisse der manuellen Segmentierung zu replizieren, ist ihre Genauigkeit zwangsläufig durch die Präzision der manuellen Segmentierungstechnik begrenzt. Es muss aber berücksichtigt werden, dass die manuelle Segmentierung, auch wenn sie in unserer Studie als Referenzstandard benutzt wurde, lediglich eine Schätzung der wahren kortikalen Dicke repräsentiert, da alle Methodologien naturgemäss Limitationen und potenzielle Verzerrungen aufweisen. Die Ergebnisse zeigten, dass die manuelle Segmentierung in unserer Stichprobe möglicherweise etwas genauer war, Unterschiede in der kortikalen Dicke zwischen der aMCI-Gruppe und der gesunden Kontrollgruppe abzubilden. Jedoch ist sie aufgrund ihres Zeitaufwandes für die klinische und wissenschaftliche Praxis nicht praktikabel. Beispielsweise benötigt man für den mPRC pro Person durchschnittlich 20 Minuten manuelle Arbeit, während unser Segmentierungstool diese Aufgabe in nur 5 Minuten automatisiert im Hintergrund berechnen kann. Folglich erweist sich die automatisierte Methode aufgrund ihrer hohen Übereinstimmung mit der manuellen Segmentierung, trotz eines möglichen Bias, als vielversprechende Alternative.

Nichtsdestotrotz bleiben die zukünftige Anwendung und Validierung unseres neuen automatisierten Tools von grosser Bedeutung.

Weiter muss erwähnt werden, dass wir in unserer Studie die kortikale Dicke der linken und rechten Hemisphäre der ROI nicht separat untersucht haben. Zukünftige Studien sollten eine getrennte Beurteilung (z.B. kortikale Dicke des linken und rechten mPRC) vornehmen. Dies ist besonders wichtig, da die Hirnatrophie bei der typischen AK oft asymmetrisch auftritt, insbesondere mit einer stärkeren Betonung der linken Hemisphäre (Lubben et al., 2021). Eine ideale und wünschenswerte Anwendung unseres automatisierten Segmentierungstools wäre im Rahmen einer Langzeitstudie mit ursprünglich gesunden Personen. Dieser Ansatz würde nicht nur erlauben, umfassende normative Daten zu sammeln, sondern auch eine retrospektive Analyse frühester kortikaler Veränderungen bei Teilnehmenden, die im Verlauf eine symptomatische AK entwickeln. Eine Herangehensweise, welche ebenfalls im Ausblick am Ende der Dissertationsarbeit erneut aufgegriffen wird. Mit der zusätzlichen Berechnung der kortikalen Dicke des PHC erlaubt unser automatisiertes Segmentierungstool zudem die Rolle dieser Region im frühen Verlauf der AK weiterführend zu untersuchen, ein Thema, das bisher noch nicht vollständig verstanden ist.

### 3.3. Der PRC/mPRC vor dem Hintergrund der Früherkennung der Alzheimer-Krankheit

Die vorliegende Promotionsarbeit hebt den mPRC bzw. den PRC als vielversprechende Marker für die frühesten strukturellen und kognitiven Veränderungen im Rahmen der AK hervor. Das weit verbreitete Biomarker-Modell der AK von Jack et al. (2010, 2013), postuliert eine sequenzielle Abfolge von pathologischen Veränderungen, beginnend mit der Akkumulation von A $\beta$ , gefolgt von Tau-Protein-Anomalien, neurodegenerativen Veränderungen und schliesslich kognitiven Defiziten (siehe Abbildung 5). Diese sequenzielle Ansicht wird jedoch kritisiert, da dieses Modell vorrangig auf Erkenntnissen der genetisch bedingten und seltenen familiären Form der AK basiert und möglicherweise nicht auf die häufigere sporadische Form der AK Anwendung findet (Frisoni et al., 2022). Stattdessen wird ein probabilistisches Modell diskutiert, in dem die Präsenz von A $\beta$ - und Tau-Pathologie das Risiko für die

Entwicklung einer symptomatischen AK erhöht, jedoch nicht deterministisch zur Krankheitsentwicklung führt (Frisoni et al., 2022). Dies steht im Einklang mit der eingänglich erwähnten Beobachtung, dass nicht alle Individuen mit nachweisbarer Alzheimer-typischer Neuropathologie kognitive Defizite entwickeln (z.B. Braak et al., 2011; Timmers et al., 2019). Entsprechend ist es notwendig, individuelle Krankheitsverläufe im Rahmen der Früherkennung und Therapie der AK zu berücksichtigen (Dubois et al., 2021; Stern, 2012).

Die Frage, ob im Verlauf der AK zuerst strukturelle oder neurokognitive Veränderungen auftreten, bleibt ein zentrales Forschungsthema. Langzeitstudien wie die von Hirni et al. (2016) legen nahe, dass kognitive Veränderungen möglicherweise viel früher als bisher erwartet auftreten. Beispielsweise bereits acht Jahre vor einer MCI-Diagnose, während deutliche strukturelle Unterschiede erst zum Zeitpunkt der Diagnose feststellbar waren (Hirni et al., 2016). Dies unterstreicht die Bedeutung neu entwickelter spezifischer kognitiver und struktureller Marker von kortikalen Regionen, welche im Rahmen der typischen AK durch die neurofibrilläre Taupathologie als erstes betroffen sind. Vor diesem Hintergrund könnten der in Studie I vorgestellte spezifische PRC-Funktionstest und das automatisierte Segmentierungstool für den mPRC aus Studie III entscheidend dazu beitragen, den zeitlichen Verlauf und das Zusammenspiel von kognitiven und strukturellen Veränderungen im Rahmen der AK weiter zu entschlüsseln. Aufgrund der Heterogenität und der Schwierigkeit kognitive Defizite in den frühesten Stadien der AK zuzuordnen, dürfen unsere Marker keineswegs als alleinstehende «Super-Marker» verstanden werden, sondern im Rahmen einer breiten multimodalen Diagnostik interpretiert werden. Wie eingehend aufgeführt ist die frühzeitige und präzise Identifikation von Personen, die eine symptomatische AK entwickeln, grundlegend für den erfolgreichen Einsatz therapeutischer Interventionen und unterstützt die Entwicklung massgeschneiderter Behandlungsstrategien. Dies wiederum erhöht die Chance, den Krankheitsverlauf effektiv zu beeinflussen und die Lebensqualität der Betroffenen nachhaltig zu verbessern. Der in Studie I vorgestellte PRC-Funktionstest und das automatisierte Segmentierungstool für den mPRC aus Studie III, liefern wertvolle Instrumente, um die

Alzheimer-Forschung voranzutreiben und tragen somit entscheidend zur Verbesserung der Früherkennung und Diagnostik der AK bei.

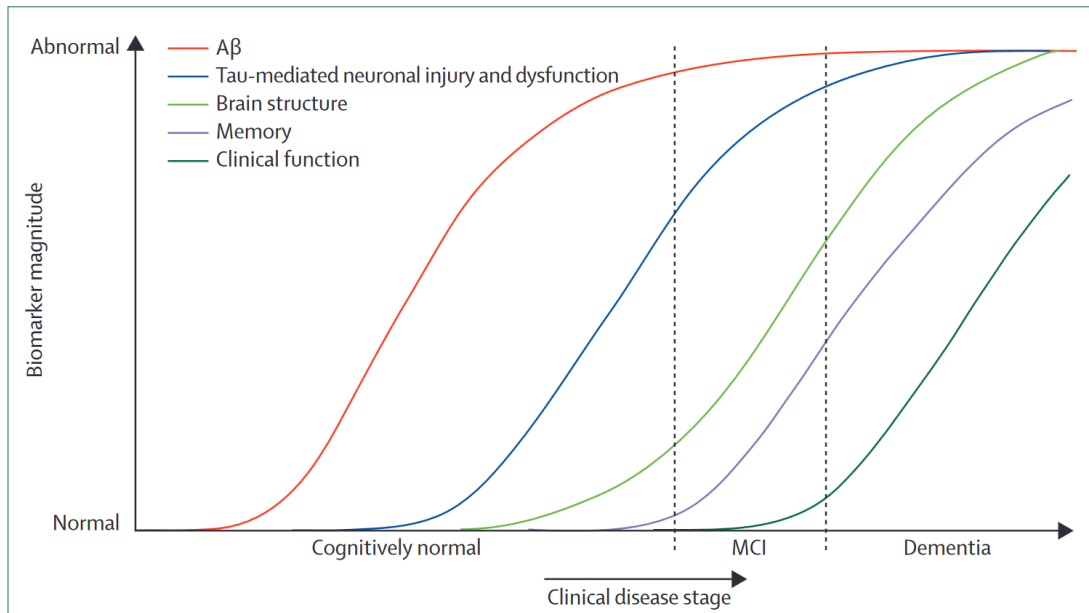


Abbildung 5. Kaskadenmodell der AK (Jack et al., 2013).

#### 4. AUSBLICK

Im Rahmen meiner Dissertation hatte ich die einzigartige Gelegenheit, an der Langzeitstudie „Hirnleistungen im Verlauf des Alterns“ unter der Leitung von Frau PD Dr. phil. Sabine Krumm mitzuwirken. Dieses Projekt, das rund 400 gesunde Personen über 65 Jahren umfasst, die im Abstand von zwei Jahren neuropsychologisch und mittels Bildgebung untersucht werden, bietet eine ideale Plattform, um die in den Studien I bis III gesammelten Erkenntnisse weiter zu vertiefen. Neben den herkömmlichen neuropsychologischen Tests, kommen auch die in Studie I vorgestellte visuelle Diskriminationsaufgabe sowie weitere neu entwickelte spezifische PRC-Funktionstests zum Einsatz (z.B. eine visuell-auditorische Integrationsaufgabe). Jeder Untersuchungszeitpunkt beinhaltet eine MRT-Bildgebung, was eine ideale Einsatzmöglichkeit für das in Studie III entwickelte automatisierte Segmentierungstool bietet. Zusätzlich



wurde in einem kleineren Sample die visuelle Diskriminationsaufgabe als fMRT-Paradigma durchgeführt, was ein tieferes Verständnis der involvierten Hirnregionen während der Aufgabenbearbeitung ermöglicht. Diese umfassende Herangehensweise erlaubt es, retrospektiv die ersten kognitiven und strukturellen Veränderungen von Studienteilnehmenden zu identifizieren, die im Verlauf eine symptomatische AK entwickeln. Darüber hinaus ermöglicht es die Evaluation von Effektstärken und prognostischer Validität sowie die Sammlung von Normdaten (z.B. der kortikalen Dicke des mPRC). Zusätzlich können weitere Einflussfaktoren untersucht werden, wie die differenziellen Effekte von Geschlecht, Bildungsniveau, Ernährung oder körperlicher Aktivität, die als mögliche Indikatoren für kognitive Reserve dienen könnten. Dieses Forschungsprojekt leistet in Kombination mit den Erkenntnissen der vorliegenden Promotionsarbeit einen bedeutenden Beitrag zur Verbesserung der Früherkennung und Diagnostik der AK. Es legt zudem wichtige Grundlagen für ein tieferes Verständnis des Krankheitsverlaufs sowie für die Entwicklung neuer Behandlungsstrategien und therapeutischer Ansätze.

Vor diesem Hintergrund sehe ich noch Potenzial, das Forschungsprojekt zu erweitern, indem die Nähe zur klinischen Praxis in der Memory Clinic genutzt wird. Ein ergänzendes Projekt könnte die Anwendbarkeit der visuellen Diskriminationsaufgabe aus Studie I in der klinischen Routine der Memory Clinic überprüfen. Dabei wäre es essenziell, in einem ersten Schritt den Test hinsichtlich der Bearbeitungszeit und der Durchführung zu optimieren. Eine auf maximal 10 Minuten ausgelegte, tablet-basierte Version scheint hierbei besonders wünschenswert. Idealerweise in Kombination mit zusätzlichen spezifischen PRC-Funktionstests, wie der visuell-auditorische Integrationsaufgabe aus der oben genannten Langzeitstudie. Die Anwendung in der klinischen Routine würde nicht nur erlauben die Praktikabilität neuer Instrumente in einem solchem Umfeld zu evaluieren, sondern auch zu deren Weiterentwicklung beitragen. Die Ergebnisse dieser klinischen Anwendung könnten dann mit Daten aus der Langzeitstudie verglichen werden, um die prognostische Validität und die Effektstärken der Tests weiter zu verfeinern. Diese frühen klinischen Berührungspunkte könnten helfen, den Übergang innovativer kognitiver PRC-Funktionstests in den klinischen Alltag zu beschleunigen und somit entscheidend zur Verbesserung der Früherkennung und Diagnostik der AK beitragen.

## REFERENZLISTE

- Aisen, P. S., Andrieu, S., Sampaio, C., Carrillo, M., Khachaturian, Z. S., Dubois, B., ... & Vellas, B. (2011). Report of the task force on designing clinical trials in early (predementia) AD. *Neurology*, *76*(3), 280–286. <https://doi.org/10.1212/WNL.0b013e318207b1b9>
- Albert, M. S., DeKosky, S. T., Dickson, D., Dubois, B., Feldman, H. H., Fox, N. C., ... & Phelps, C. H. (2011). The diagnosis of mild cognitive impairment due to Alzheimer's disease: Recommendations from the National Institute on Aging-Alzheimer's Association workgroups on diagnostic guidelines for Alzheimer's disease. *Alzheimer's & dementia: the journal of the Alzheimer's Association*, *7*(3), 270–279. <https://doi.org/10.1016/j.jalz.2011.03.008>
- Alzheimer, A. (1907). Über eine eigenartige Erkrankung der Hirnrinde. *Zeitschrift Für Psychiatrie*, (64), 146–148.
- Alzubaidi, L., Zhang, J., Humaidi, A. J., Al-Dujaili, A., Duan, Y., Al-Shamma, O., ... & Farhan, L. (2021). Review of deep learning: Concepts, CNN architectures, challenges, applications, future directions. *Journal of Big Data*, *8*(1), 53. <https://doi.org/10.1186/s40537-021-00444-8>
- American Psychiatric Association. (2013). *Diagnostic and statistical manual of mental disorder (5th ed.)*. Washington, DC: Author.
- Armstrong, M. J., Litvan, I., Lang, A. E., Bak, T. H., Bhatia, K. P., Borroni, B., ... & Weiner, W. J. (2013). Criteria for the diagnosis of corticobasal degeneration. *Neurology*, *80*(5), 496–503. <https://doi.org/10.1212/WNL.0b013e31827f0fd1>
- Ashburner, J., & Friston, K. J. (2005). Unified segmentation. *NeuroImage*, *26*(3), 839–851. <https://doi.org/10.1016/j.neuroimage.2005.02.018>
- Ballatore, C., Lee, V. M.-Y., & Trojanowski, J. Q. (2007). Tau-mediated neurodegeneration in Alzheimer's disease and related disorders. *Nature Reviews. Neuroscience*, *8*(9), 663–672. <https://doi.org/10.1038/nrn2194>
- Bastin, C., & Delhay, E. (2023). Targeting the function of the transentorhinal cortex to identify early cognitive markers of Alzheimer's disease. *Cognitive, Affective, & Behavioral Neuroscience*, *23*(4), 986–996. <https://doi.org/10.3758/s13415-023-01093-5>

- Bobinski, M., Wegiel, J., Tarnawski, M., Bobinski, M., Reisberg, B., de Leon, M. J., ... & Wisniewski, H. M. (1997). Relationships between Regional Neuronal Loss and Neurofibrillary Changes in the Hippocampal Formation and Duration and Severity of Alzheimer Disease. *Journal of Neuropathology & Experimental Neurology*, 56(4), 414–420. <https://doi.org/10.1097/00005072-199704000-00010>
- Braak, H., Alafuzoff, I., Arzberger, T., Kretschmar, H., & Del Tredici, K. (2006). Staging of Alzheimer disease-associated neurofibrillary pathology using paraffin sections and immunocytochemistry. *Acta Neuropathologica*, 112(4), 389–404. <https://doi.org/10.1007/s00401-006-0127-z>
- Braak, H., & Braak, E. (1985). On areas of transition between entorhinal allocortex and temporal isocortex in the human brain. Normal morphology and lamina-specific pathology in Alzheimer's disease. *Acta Neuropathologica*, 68(4), 325–332. <https://doi.org/10.1007/BF00690836>
- Braak, H., & Braak, E. (1991a). Demonstration of Amyloid Deposits and Neurofibrillary Changes in Whole Brain Sections. *Brain Pathology*, 1(3), 213–216. <https://doi.org/10.1111/j.1750-3639.1991.tb00661.x>
- Braak, H., & Braak, E. (1991b). Neuropathological staging of Alzheimer-related changes. *Acta Neuropathologica*, 82(4), 239–259. <https://doi.org/10.1007/BF00308809>
- Braak, H., Thal, D. R., Ghebremedhin, E., & Del Tredici, K. (2011). Stages of the Pathologic Process in Alzheimer Disease: Age Categories From 1 to 100 Years. *Journal of Neuropathology & Experimental Neurology*, 70(11), 960–969. <https://doi.org/10.1097/NEN.0b013e318232a379>
- Brookmeyer, R., & Abdalla, N. (2018). Estimation of lifetime risks of Alzheimer's disease dementia using biomarkers for preclinical disease. *Alzheimer's & Dementia*, 14(8), 981–988. <https://doi.org/10.1016/j.jalz.2018.03.005>
- Brown, M. W., & Aggleton, J. P. (2001). Recognition memory: What are the roles of the perirhinal cortex and hippocampus? *Nature Reviews Neuroscience*, 2(1), Article 1. <https://doi.org/10.1038/35049064>

- Bussey, T. J., Saksida, L. M., & Murray, E. A. (2005). The Perceptual-Mnemonic/Feature Conjunction Model of Perirhinal Cortex Function. *The Quarterly Journal of Experimental Psychology Section B*, 58(3–4b), 269–282. <https://doi.org/10.1080/02724990544000004>
- Cate, A. D., & Köhler, S. (2006). The missing whole in perceptual models of perirhinal cortex. *Trends in Cognitive Sciences*, 10(9), 396–397. <https://doi.org/10.1016/j.tics.2006.07.004>
- Chen, G., Xu, T., Yan, Y., Zhou, Y., Jiang, Y., Melcher, K., & Xu, H. E. (2017). Amyloid beta: Structure, biology and structure-based therapeutic development. *Acta Pharmacologica Sinica*, 38(9), Article 9. <https://doi.org/10.1038/aps.2017.28>
- Çiçek, Ö., Abdulkadir, A., Lienkamp, S. S., Brox, T., & Ronneberger, O. (2016). 3D U-Net: Learning Dense Volumetric Segmentation from Sparse Annotation. In S. Ourselin, L. Joskowicz, M. R. Sabuncu, G. Unal, & W. Wells (Hrsg.), *Medical Image Computing and Computer-Assisted Intervention – MICCAI 2016* (S. 424–432). Springer International Publishing. [https://doi.org/10.1007/978-3-319-46723-8\\_49](https://doi.org/10.1007/978-3-319-46723-8_49)
- Corkin, S. (1984). Lasting Consequences of Bilateral Medial Temporal Lobectomy: Clinical Course and Experimental Findings in H.M. *Seminars in Neurology*, 4(2), 249–259. <https://doi.org/10.1055/s-2008-1041556>
- Crutch, S. J., Schott, J. M., Rabinovici, G. D., Murray, M., Snowden, J. S., van der Flier, W. M., ... & Fox, N. C. (2017). Consensus classification of posterior cortical atrophy. *Alzheimer's & dementia: the journal of the Alzheimer's Association*, 13(8), 870–884. <https://doi.org/10.1016/j.jalz.2017.01.014>
- Davachi, L. (2006). Item, context and relational episodic encoding in humans. *Current Opinion in Neurobiology*, 16(6), 693–700. <https://doi.org/10.1016/j.conb.2006.10.012>
- Desikan, R. S., Ségonne, F., Fischl, B., Quinn, B. T., Dickerson, B. C., Blacker, D., ... & Killiany, R. J. (2006). An automated labeling system for subdividing the human cerebral cortex on MRI scans into gyral based regions of interest. *NeuroImage*, 31(3), 968–980. <https://doi.org/10.1016/j.neuroimage.2006.01.021>

- DeTure, M. A., & Dickson, D. W. (2019). The neuropathological diagnosis of Alzheimer's disease. *Molecular Neurodegeneration*, *14*(1), 32. <https://doi.org/10.1186/s13024-019-0333-5>
- Dickerson, B. C., Feczko, E., Augustinack, J. C., Pacheco, J., Morris, J. C., Fischl, B., & Buckner, R. L. (2009). Differential effects of aging and Alzheimer's disease on medial temporal lobe cortical thickness and surface area. *Neurobiology of Aging*, *30*(3), 432–440. <https://doi.org/10.1016/j.neurobiolaging.2007.07.022>
- Dubois, B., Hampel, H., Feldman, H. H., Scheltens, P., Aisen, P., Andrieu, S., ... & Jack, C. R. (2016). Preclinical Alzheimer's disease: Definition, natural history, and diagnostic criteria. *Alzheimer's & dementia: the journal of the Alzheimer's Association*, *12*(3), 292–323. <https://doi.org/10.1016/j.jalz.2016.02.002>
- Dubois, B., Padovani, A., Scheltens, P., Rossi, A., & Dell'Agnello, G. (o. J.). Timely Diagnosis for Alzheimer's Disease: A Literature Review on Benefits and Challenges. *Journal of Alzheimer's Disease*, *49*(3), 617–631. <https://doi.org/10.3233/JAD-150692>
- Dubois, B., Villain, N., Frisoni, G. B., Rabinovici, G. D., Sabbagh, M., Cappa, S., ... & Feldman, H. H. (2021). Clinical diagnosis of Alzheimer's disease: Recommendations of the International Working Group. *The Lancet Neurology*, *20*(6), 484–496. [https://doi.org/10.1016/S1474-4422\(21\)00066-1](https://doi.org/10.1016/S1474-4422(21)00066-1)
- Enkirch, S. J., Träschütz, A., Müller, A., Widmann, C. N., Gielen, G. H., Heneka, M. T., ... & Hattingen, E. (2018). The ERICA Score: An MR Imaging-based Visual Scoring System for the Assessment of Entorhinal Cortex Atrophy in Alzheimer Disease. *Radiology*, *288*(1), 226–333. <https://doi.org/10.1148/radiol.2018171888>
- Freud, E., Culham, J. C., Plaut, D. C., & Behrmann, M. (2017). The large-scale organization of shape processing in the ventral and dorsal pathways. *eLife*, *6*, e27576. <https://doi.org/10.7554/eLife.27576>
- Frisoni, G. B., Altomare, D., Thal, D. R., Ribaldi, F., van der Kant, R., Ossenkoppele, R., ... & Dubois, B. (2022). The probabilistic model of Alzheimer disease: The amyloid hypothesis revised. *Nature Reviews. Neuroscience*, *23*(1), 53–66. <https://doi.org/10.1038/s41583-021-00533-w>

- Gaugler, J. E., Ascher-Svanum, H., Roth, D. L., Fafowora, T., Siderowf, A., & Beach, T. G. (2013). Characteristics of patients misdiagnosed with Alzheimer's disease and their medication use: An analysis of the NACC-UDS database. *BMC Geriatrics*, *13*, 137. <https://doi.org/10.1186/1471-2318-13-137>
- Gauthier, S., Leuzy, A., Racine, E., & Rosa-Neto, P. (2013). Diagnosis and management of Alzheimer's disease: Past, present and future ethical issues. *Progress in Neurobiology*, *110*, 102–113. <https://doi.org/10.1016/j.pneurobio.2013.01.003>
- Giannakopoulos, P., Gold, G., Gunten, A. von, Hof, P. R., & Bouras, C. (2009). Pathological Substrates of Cognitive Decline in Alzheimer's Disease. *Dementia in Clinical Practice*, *24*, 20–29. <https://doi.org/10.1159/000197881>
- Giannakopoulos, P., Herrmann, F. R., Bussière, T., Bouras, C., Kövari, E., Perl, D. P., ... & Hof, P. R. (2003). Tangle and neuron numbers, but not amyloid load, predict cognitive status in Alzheimer's disease. *Neurology*, *60*(9), 1495–1500. <https://doi.org/10.1212/01.wnl.0000063311.58879.01>
- Giuliani, N. R., Calhoun, V. D., Pearlson, G. D., Francis, A., & Buchanan, R. W. (2005). Voxel-based morphometry versus region of interest: A comparison of two methods for analyzing gray matter differences in schizophrenia. *Schizophrenia Research*, *74*(2–3), 135–147. <https://doi.org/10.1016/j.schres.2004.08.019>
- Goedert, M., & Ghetti, B. (2007). Alois Alzheimer: His Life and Times. *Brain Pathology*, *17*(1), 57–62. <https://doi.org/10.1111/j.1750-3639.2007.00056.x>
- Gómez-Isla, T., Hollister, R., West, H., Mui, S., Growdon, J. H., Petersen, ... & Hyman, B. T. (1997). Neuronal loss correlates with but exceeds neurofibrillary tangles in Alzheimer's disease. *Annals of Neurology*, *41*(1), 17–24. <https://doi.org/10.1002/ana.410410106>
- Gorno-Tempini, M. L., Hillis, A. E., Weintraub, S., Kertesz, A., Mendez, M., Cappa, S. F., ... & Grossman, M. (2011). Classification of primary progressive aphasia and its variants. *Neurology*, *76*(11), 1006–1014. <https://doi.org/10.1212/WNL.0b013e31821103e6>
- Hirni, D. I., Kivisaari, S. L., Krumm, S., Monsch, A. U., Berres, M., Oeksuez, F., ... & Taylor, K. I. (2016). Neuropsychological Markers of Medial Perirhinal and Entorhinal Cortex Functioning are

- Impaired Twelve Years Preceding Diagnosis of Alzheimer's Dementia. *Journal of Alzheimer's Disease*, 52(2), 573–580. <https://doi.org/10.3233/JAD-150158>
- Hirni, D. I., Kivisaari, S. L., Monsch, A. U., & Taylor, K. I. (2013). Distinct neuroanatomical bases of episodic and semantic memory performance in Alzheimer's disease. *Neuropsychologia*, 51(5), 930–937. <https://doi.org/10.1016/j.neuropsychologia.2013.01.013>
- Insausti, R., Juottonen, K., Soininen, H., Insausti, A. M., Partanen, K., Vainio, P., ... & Pitkänen, A. (1998). MR volumetric analysis of the human entorhinal, perirhinal, and temporopolar cortices. *American Journal of Neuroradiology*, 19(4), 659–671.
- Jack, C. R., Albert, M. S., Knopman, D. S., McKhann, G. M., Sperling, R. A., Carrillo, M. C., ... & Phelps, C. H. (2011). Introduction to the recommendations from the National Institute on Aging-Alzheimer's Association workgroups on diagnostic guidelines for Alzheimer's disease. *Alzheimer's & Dementia: The Journal of the Alzheimer's Association*, 7(3), 257–262. <https://doi.org/10.1016/j.jalz.2011.03.004>
- Jack, C. R., Knopman, D. S., Jagust, W. J., Petersen, R. C., Weiner, M. W., Aisen, P. S., ... & Trojanowski, J. Q. (2013). Tracking pathophysiological processes in Alzheimer's disease: An updated hypothetical model of dynamic biomarkers. *The Lancet Neurology*, 12(2), 207–216. [https://doi.org/10.1016/S1474-4422\(12\)70291-0](https://doi.org/10.1016/S1474-4422(12)70291-0)
- Jack, C. R., Knopman, D. S., Jagust, W. J., Shaw, L. M., Aisen, P. S., Weiner, M. W., ... & Trojanowski, J. Q. (2010). Hypothetical model of dynamic biomarkers of the Alzheimer's pathological cascade. *The Lancet Neurology*, 9(1), 119–128. [https://doi.org/10.1016/S1474-4422\(09\)70299-6](https://doi.org/10.1016/S1474-4422(09)70299-6)
- Jack Jr., C. R., Bennett, D. A., Blennow, K., Carrillo, M. C., Dunn, B., Haeberlein, S. B., ... & Silverberg, N. (2018). NIA-AA Research Framework: Toward a biological definition of Alzheimer's disease. *Alzheimer's & Dementia*, 14(4), 535–562. <https://doi.org/10.1016/j.jalz.2018.02.018>
- Jessen, F., Amariglio, R. E., Buckley, R. F., van der Flier, W. M., Han, Y., Molinuevo, J. L., ... & Wagner, M. (2020). The characterisation of subjective cognitive decline. *The Lancet Neurology*, 19(3), 271–278. [https://doi.org/10.1016/S1474-4422\(19\)30368-0](https://doi.org/10.1016/S1474-4422(19)30368-0)

- Kivisaari, S. L., Probst, A., & Taylor, K. I. (2013). The Perirhinal, Entorhinal, and Parahippocampal Cortices and Hippocampus: An Overview of Functional Anatomy and Protocol for Their Segmentation in MR Images. In S. Ulmer & O. Jansen (Hrsg.), *fMRI: Basics and Clinical Applications* (S. 239–267). Springer. [https://doi.org/10.1007/978-3-642-34342-1\\_19](https://doi.org/10.1007/978-3-642-34342-1_19)
- Klöppel, S., Peter, J., Ludl, A., Pilatus, A., Maier, S., Mader, I., ... & for the A. D. N. Initiative (2015). Applying Automated MR-Based Diagnostic Methods to the Memory Clinic: A Prospective Study. *Journal of Alzheimer's Disease*, *47*(4), 939–954. <https://doi.org/10.3233/JAD-150334>
- Krumm, S., Kivisaari, S. L., Probst, A., Monsch, A. U., Reinhardt, J., Ulmer, S., ... & Taylor, K. I. (2016). Cortical thinning of parahippocampal subregions in very early Alzheimer's disease. *Neurobiology of Aging*, *38*, 188–196. <https://doi.org/10.1016/j.neurobiolaging.2015.11.001>
- Kumar, A., Sidhu, J., Goyal, A., & Tsao, J. W. (2023). Alzheimer Disease. In *StatPearls*. StatPearls Publishing. <http://www.ncbi.nlm.nih.gov/books/NBK499922/>
- Lerner, Y., Hendler, T., Ben-Bashat, D., Harel, M., & Malach, R. (2001). A hierarchical axis of object processing stages in the human visual cortex. *Cerebral Cortex (New York, N.Y.: 1991)*, *11*(4), 287–297. <https://doi.org/10.1093/cercor/11.4.287>
- Lipton, P. A., & Eichenbaum, H. (2008). Complementary roles of hippocampus and medial entorhinal cortex in episodic memory. *Neural Plasticity*, *2008*. <https://doi.org/10.1155/2008/258467>
- Littlewood, C., Seymour, J., & Owen, V. (2010). Does treating Alzheimer's disease early, delay institutionalisation? *International Journal of Geriatric Psychiatry*, *25*(12), 1307–1309. <https://doi.org/10.1002/gps.2446>
- Lopez, O. L., Becker, J. T., Wahed, A. S., Saxton, J., Sweet, R. A., Wolk, D. A., ... & DeKosky, S. T. (2009). Long-term effects of the concomitant use of memantine with cholinesterase inhibition in Alzheimer disease. *Journal of neurology, neurosurgery, and psychiatry*, *80*(6), 600–607. <https://doi.org/10.1136/jnnp.2008.158964>
- Maass, A., Landau, S., Baker, S. L., Horng, A., Lockhart, S. N., La Joie, R., ... & Jagust, W. J. (2017). Comparison of multiple tau-PET measures as biomarkers in aging and Alzheimer's disease. *NeuroImage*, *157*, 448–463. <https://doi.org/10.1016/j.neuroimage.2017.05.058>



- Mattsson, N., Brax, D., & Zetterberg, H. (2010). To Know or Not to Know: Ethical Issues Related to Early Diagnosis of Alzheimer's Disease. *International Journal of Alzheimer's Disease*, 2010, 841941. <https://doi.org/10.4061/2010/841941>
- McKhann, G. M., Knopman, D. S., Chertkow, H., Hyman, B. T., Jack, C. R., Kawas, C. H., ... & Phelps, C. H. (2011). The diagnosis of dementia due to Alzheimer's disease: Recommendations from the National Institute on Aging-Alzheimer's Association workgroups on diagnostic guidelines for Alzheimer's disease. *Alzheimer's & dementia : the journal of the Alzheimer's Association*, 7(3), 263–269. <https://doi.org/10.1016/j.jalz.2011.03.005>
- Monsch, Büla, Hermelink, Kressig, Martensson, Mosimann, Müri, Vögeli, & von Gunten. (2012). Konsensus 2012 zur Diagnostik und Therapie von Demenzkranken in der Schweiz. *Praxis*, 101(19), 1239–1249. <https://doi.org/10.1024/1661-8157/a001085>
- Moss, H. E., Rodd, J. M., Stamatakis, E. A., Bright, P., & Tyler, L. K. (2005). Anteromedial Temporal Cortex Supports Fine-grained Differentiation among Objects. *Cerebral Cortex*, 15(5), 616–627. <https://doi.org/10.1093/cercor/bhh163>
- Murray, E. A., Bussey, T. J., & Saksida, L. M. (2007). Visual perception and memory: A new view of medial temporal lobe function in primates and rodents. *Annual Review of Neuroscience*, 30, 99–122. <https://doi.org/10.1146/annurev.neuro.29.051605.113046>
- Murray, E. A., & Richmond, B. J. (2001). Role of perirhinal cortex in object perception, memory, and associations. *Current Opinion in Neurobiology*, 11(2), 188–193. [https://doi.org/10.1016/S0959-4388\(00\)00195-1](https://doi.org/10.1016/S0959-4388(00)00195-1)
- Murray, M. E., Graff-Radford, N. R., Ross, O. A., Petersen, R. C., Duara, R., & Dickson, D. W. (2011). Neuropathologically defined subtypes of Alzheimer's disease with distinct clinical characteristics: A retrospective study. *Lancet neurology*, 10(9), 785–796. [https://doi.org/10.1016/S1474-4422\(11\)70156-9](https://doi.org/10.1016/S1474-4422(11)70156-9)
- O'Neil, E. B., Cate, A. D., & Köhler, S. (2009). Perirhinal Cortex Contributes to Accuracy in Recognition Memory and Perceptual Discriminations. *The Journal of Neuroscience*, 29(26), 8329–8334. <https://doi.org/10.1523/JNEUROSCI.0374-09.2009>

- Ossenkoppelle, R., Pijnenburg, Y. A. L., Perry, D. C., Cohn-Sheehy, B. I., Scheltens, N. M. E., Vogel, J. W., ... & Rabinovici, G. D. (2015). The behavioural/dysexecutive variant of Alzheimer's disease: Clinical, neuroimaging and pathological features. *Brain*, *138*(9), 2732–2749.  
<https://doi.org/10.1093/brain/awv191>
- Palmer, S., & Rock, I. (1994). Rethinking perceptual organization: The role of uniform connectedness. *Psychonomic Bulletin & Review*, *1*(1), 29–55. <https://doi.org/10.3758/BF03200760>
- Piaceri, I., Nacmias, B., & Sorbi, S. (2013). Genetics of familial and sporadic Alzheimer's disease. *Frontiers in Bioscience-Elite*, *5*(1), Article 1. <https://doi.org/10.2741/E605>
- Polsinelli, A. J., & Apostolova, L. G. (2022). Atypical Alzheimer Disease Variants. *Continuum (Minneapolis, Minn.)*, *28*(3), 676–701. <https://doi.org/10.1212/CON.0000000000001082>
- Price, J. L., & Morris, J. C. (1999). Tangles and plaques in nondemented aging and “preclinical” Alzheimer's disease. *Annals of Neurology*, *45*(3), 358–368. [https://doi.org/10.1002/1531-8249\(199903\)45:3<358::AID-ANA12>3.0.CO;2-X](https://doi.org/10.1002/1531-8249(199903)45:3<358::AID-ANA12>3.0.CO;2-X)
- Pruessner, J. C., Köhler, S., Crane, J., Pruessner, M., Lord, C., Byrne, A., ... & Evans, A. C. (2002). Volumetry of temporopolar, perirhinal, entorhinal and parahippocampal cortex from high-resolution MR images: Considering the variability of the collateral sulcus. *Cerebral Cortex*, *12*(12), 1342–1353. Scopus. <https://doi.org/10.1093/cercor/12.12.1342>
- Raslau, F. D., Mark, I. T., Klein, A. P., Ulmer, J. L., Mathews, V., & Mark, L. P. (2015). Memory Part 2: The Role of the Medial Temporal Lobe. *American Journal of Neuroradiology*, *36*(5), 846–849.  
<https://doi.org/10.3174/ajnr.A4169>
- Rasmussen, J., & Langerman, H. (2019). Alzheimer's Disease – Why We Need Early Diagnosis. *Degenerative Neurological and Neuromuscular Disease*, *9*, 123–130.  
<https://doi.org/10.2147/DNND.S228939>
- Reuter, M., Schmansky, N. J., Rosas, H. D., & Fischl, B. (2012). Within-subject template estimation for unbiased longitudinal image analysis. *Neuroimage*, *61*(4), 1402–1418.  
<https://doi.org/10.1016/j.neuroimage.2012.02.084>

- Ronneberger, O., Fischer, P., & Brox, T. (2015). U-Net: Convolutional Networks for Biomedical Image Segmentation. *arXiv:1505.04597 [cs]*. <http://arxiv.org/abs/1505.04597>
- Rotomskis, A., Margevičiūtė, R., Germanavičius, A., Kaubrys, G., Budrys, V., & Bagdonas, A. (2015). Differential diagnosis of depression and Alzheimer's disease with the Addenbrooke's Cognitive Examination-Revised (ACE-R). *BMC Neurology*, *15*, 57. <https://doi.org/10.1186/s12883-015-0315-3>
- Rullmann, M., Brendel, M., Schroeter, M., Saur, D., Levin, J., Perneczky, R., ... & Tau, O. B. O. T. G. I. I. F. (2022). Multicenter 18F-PI-2620 PET for In Vivo Braak Staging of Tau Pathology in Alzheimer's Disease. *Biomolecules*, *12*. <https://doi.org/10.3390/biom12030458>
- Salive, M. E. (2013). Multimorbidity in older adults. *Epidemiologic Reviews*, *35*, 75–83. <https://doi.org/10.1093/epirev/mxs009>
- Scheltens, P., & Pol, L. van de. (2012). Atrophy of medial temporal lobes on MRI in “probable” Alzheimer's disease and normal ageing: Diagnostic value and neuropsychological correlates. *Journal of Neurology, Neurosurgery & Psychiatry*, *83*(11), 1038–1040. <https://doi.org/10.1136/jnnp-2012-302562>
- Scheltens, P., Strooper, B. D., Kivipelto, M., Holstege, H., Chételat, G., Teunissen, C. E., ... & van der Flier, W. M. (2021). Alzheimer's disease. *Lancet (London, England)*, *397*(10284), 1577–1590. [https://doi.org/10.1016/S0140-6736\(20\)32205-4](https://doi.org/10.1016/S0140-6736(20)32205-4)
- Schweizerische Alzheimervereinigung. (2023, January 20). Zahlen und Fakten zur Demenz. Retrieved from <http://www.alz.ch/index.php/zahlen-zur-demenz.html>
- Seyedi, S., Jafari, R., Talaei, A., Naseri, S., Momennezhad, M., Moghaddam, M. D., & Akbari-Lalimi, H. (2020). Comparing VBM and ROI analyses for detection of gray matter abnormalities in patients with bipolar disorder using MRI. *Middle East Current Psychiatry*, *27*(1), 69. <https://doi.org/10.1186/s43045-020-00076-3>
- Sone, D., Imabayashi, E., Maikusa, N., Okamura, N., Furumoto, S., Kudo, Y., ... & Matsuda, H. (2017). Regional tau deposition and subregion atrophy of medial temporal structures in early Alzheimer's disease: A combined positron emission tomography/magnetic resonance imaging

- study. *Alzheimer's & Dementia : Diagnosis, Assessment & Disease Monitoring*, 9, 35–40.  
<https://doi.org/10.1016/j.dadm.2017.07.001>
- Sperling, R. A., Aisen, P. S., Beckett, L. A., Bennett, D. A., Craft, S., Fagan, A. M., ... & Phelps, C. H. (2011). Toward defining the preclinical stages of Alzheimer's disease: Recommendations from the National Institute on Aging-Alzheimer's Association workgroups on diagnostic guidelines for Alzheimer's disease. *Alzheimer's & dementia : the journal of the Alzheimer's Association*, 7(3), 280–292. <https://doi.org/10.1016/j.jalz.2011.03.003>
- Spillantini, M. G., & Goedert, M. (2013). Tau pathology and neurodegeneration. *The Lancet Neurology*, 12(6), 609–622. [https://doi.org/10.1016/S1474-4422\(13\)70090-5](https://doi.org/10.1016/S1474-4422(13)70090-5)
- Squire, L. R., Stark, C. E. L., & Clark, R. E. (2004). The medial temporal lobe. *Annual Review of Neuroscience*, 27, 279–306. <https://doi.org/10.1146/annurev.neuro.27.070203.144130>
- Stern, Y. (2012). Cognitive reserve in ageing and Alzheimer's disease. *Lancet neurology*, 11(11), 1006–1012. [https://doi.org/10.1016/S1474-4422\(12\)70191-6](https://doi.org/10.1016/S1474-4422(12)70191-6)
- Suzuki, W. A., & Amaral, D. G. (2003). Where are the perirhinal and parahippocampal cortices? A historical overview of the nomenclature and boundaries applied to the primate medial temporal lobe. *Neuroscience*, 120(4), 893–906. [https://doi.org/10.1016/S0306-4522\(03\)00281-1](https://doi.org/10.1016/S0306-4522(03)00281-1)
- Suzuki, W. L., & Amaral, D. G. (1994). Perirhinal and parahippocampal cortices of the macaque monkey: Cortical afferents. *Journal of Comparative Neurology*, 350(4), 497–533.  
<https://doi.org/10.1002/cne.903500402>
- Taylor, K. I., Devereux, B. J., & Tyler, L. K. (2011). Conceptual structure: Towards an integrated neurocognitive account. *Language and Cognitive Processes*, 26(9), 1368–1401.  
<https://doi.org/10.1080/01690965.2011.568227>
- Taylor, K. I., Moss, H. E., Stamatakis, E. A., & Tyler, L. K. (2006). Binding crossmodal object features in perirhinal cortex. *Proceedings of the National Academy of Sciences*, 103(21), 8239–8244.  
<https://doi.org/10.1073/pnas.0509704103>

- Taylor, K. I., & Probst, A. (2008). Anatomic localization of the transentorhinal region of the perirhinal cortex. *Neurobiology of Aging*, *29*(10), 1591–1596.  
<https://doi.org/10.1016/j.neurobiolaging.2007.03.024>
- Thal, D. R., Rüb, U., Orantes, M., & Braak, H. (2002). Phases of A beta-deposition in the human brain and its relevance for the development of AD. *Neurology*, *58*(12), 1791–1800.  
<https://doi.org/10.1212/wnl.58.12.1791>
- Timmers, T., Ossenkoppele, R., Wolters, E. E., Verfaillie, S. C. J., Visser, D., Golla, S. S. V., ... & van Berckel, B. N. M. (2019). Associations between quantitative [18F]flortaucipir tau PET and atrophy across the Alzheimer's disease spectrum. *Alzheimer's Research & Therapy*, *11*(1), 60.  
<https://doi.org/10.1186/s13195-019-0510-3>
- Townley, R. A., Graff-Radford, J., Mantyh, W. G., Botha, H., Polsinelli, A. J., Przybelski, S. A., ... & Jones, D. T. (2020). Progressive dysexecutive syndrome due to Alzheimer's disease: A description of 55 cases and comparison to other phenotypes. *Brain Communications*, *2*(1), fcaa068.  
<https://doi.org/10.1093/braincomms/fcaa068>
- Tulving, E. (1972). Episodic and semantic memory. In *Organization of memory* (S. xiii, 423–xiii, 423). Academic Press.
- Tyler, L. K., Stamatakis, E. A., Bright, P., Acres, K., Abdallah, S., Rodd, J. M., & Moss, H. E. (2004). Processing objects at different levels of specificity. *Journal of Cognitive Neuroscience*, *16*(3), 351–362. <https://doi.org/10.1162/089892904322926692>
- van Dyck C. H., Swanson C. J., Aisen P., Bateman R. J., Chen C., Gee M., ... & Iwatsubo T. (2023). Lecanemab in Early Alzheimer's Disease. *New England Journal of Medicine*, *388*(1), 9–21.  
<https://doi.org/10.1056/NEJMoa2212948>
- Villa, C., Lavitrano, M., Salvatore, E., & Combi, R. (2020). Molecular and Imaging Biomarkers in Alzheimer's Disease: A Focus on Recent Insights. *Journal of Personalized Medicine*, *10*(3), Article 3. <https://doi.org/10.3390/jpm10030061>
- World Health Organization. (2023). Ageing and health. Retrieved August 10, 2023, from <https://www.who.int/news-room/fact-sheets/detail/ageing-and-health>

- Winblad, B., Palmer, K., Kivipelto, M., Jelic, V., Fratiglioni, L., Wahlund, L.-O., ... & Petersen, R. C. (2004). Mild cognitive impairment--beyond controversies, towards a consensus: Report of the International Working Group on Mild Cognitive Impairment. *Journal of Internal Medicine*, 256(3), 240–246. <https://doi.org/10.1111/j.1365-2796.2004.01380.x>
- Wisse, L. E. M., Chételat, G., Daugherty, A. M., de Flores, R., la Joie, R., Mueller, S. G., ... & Carr, V. A. (2021). Hippocampal subfield volumetry from structural isotropic 1 mm<sup>3</sup> MRI scans: A note of caution. *Human Brain Mapping*, 42(2), 539–550. <https://doi.org/10.1002/hbm.25234>
- Wu, T., Lin, C., & Weng, R. (2003). Probability Estimates for Multi-Class Classification by Pairwise Coupling. *Advances in Neural Information Processing Systems*, 16. [https://proceedings.neurips.cc/paper\\_files/paper/2003/hash/03e7ef47cee6fa4ae7567394b99912b7-Abstract.html](https://proceedings.neurips.cc/paper_files/paper/2003/hash/03e7ef47cee6fa4ae7567394b99912b7-Abstract.html)
- Yushkevich, P. A., Pluta, J. B., Wang, H., Xie, L., Ding, S.-L., Gertje, E. C., ... & Wolk, D. A. (2015). Automated volumetry and regional thickness analysis of hippocampal subfields and medial temporal cortical structures in mild cognitive impairment. *Human Brain Mapping*, 36(1), 258–287. <https://doi.org/10.1002/hbm.22627>

## CURRICULUM VITAE

### Persönliche Angaben

Name: Nicolas Alexander Henzen  
Geburtsdatum und -ort: 03.07.1992 in Visp (VS)

### Ausbildung

Seit 02/2020 **Doktorat in Psychologie**  
Memory Clinic, Universitäre Altersmedizin FELIX PLATTER, Basel  
SupervisorInnen: PD Dr. phil. Sabine Krumm, Prof. Dr. phil. Klaus Opwis,  
Prof. em. Dr. phil. Andreas U. Monsch  
Thema der Dissertation: *Early Detection of Alzheimer's Disease*

Seit 10/2022 **Master of Advanced Studies (MAS) in Neuropsychology**  
Universität Zürich

09/2020 – 10/2022 **Diploma of Advanced Studies (DAS) in Neuropsychology**  
Universität Zürich

09/2017 – 01/2020 **Master of Science in Psychologie**  
Universität Zürich  
Thema der Masterarbeit: *Microstate Analysis in Children and Young  
Adolescents with Attention-Deficit/Hyperactivity Disorder During  
Resting-State EEG*  
Betreuer: Prof. Dr. phil. Nicolas Langer

09/2014 – 08/2017 **Bachelor of Science in Psychologie mit Nebenfächern Recht und  
Management & Economics**  
Universität Zürich

Berufserfahrung:

Seit 02/2023 **Assistenzpsychologe**  
Memory Clinic, Universitäre Altersmedizin FELIX PLATTER, Basel

Seit 03/2024 **Dozent in Vertretung für Neurophysiologie, -anatomie und  
Biopsychologie**  
Kalaidos Fachhochschule Zürich

09/2018 – 12/2019 **Forschungsmitarbeiter**  
Lehrstuhl Methoden der Plastizitätsforschung, Universität Zürich  
Projekt: Untersuchung der Stabilität von kognitiven Fähigkeiten

07/2018 – 09/2018 **Praktikum in klinischer Neuropsychologie**  
Neurozentrum – Luzerner Kantonsspital, Luzern  
Betreuer: PD Dr. phil. Tobias Pflugshaupt

## Während des Doktorats

Mitarbeit im Forschungsprojekt «Hirnfunktionen im Verlauf des Alterns – Langzeitstudie»

Forschungsleitung: PD Dr. phil. Sabine Krumm

Memory Clinic, Universitäre Altersmedizin FELIX Platter, Basel

- Neuropsychologische Datenerhebung und -prüfung
- Datenbezogene Supervision von PraktikantInnen und Masterstudierenden

Mitarbeit im Forschungsprojekt «Früh- und Differentialdiagnose der Alzheimer Krankheit»

Thema: *Blutmarker in der Verbesserung der Diagnostik von Hirnleistungsstörungen*

Forschungsleitung: Prof. em. Dr. phil. Andreas U. Monsch, Prof. Dr. med. Marc Sollberger

Memory Clinic, Universitäre Altersmedizin FELIX PLATTER, Basel in Kollaboration mit Predemtec AG, Gossau, St. Gallen

- Rekrutierung und neuropsychologische Datenerhebung bei einer gesunden Kontrollgruppe

## Publikationen

- Frei, M., Berres, M., Kivisaari, S. L., Henzen, N. A., Monsch, A. U., Reinhardt, J., Blatow, M., Kressig, R. W., & Krumm, S. (2023). Can you find it? Novel oddity detection task for the early detection of Alzheimer's disease. *Neuropsychology*, 37(7), 717–740.
- Henzen, N. A., Reinhardt, J., Blatow, M., Kressig, R. W., & Krumm, S. (2023). Excellent Interrater Reliability for Manual Segmentation of the Medial Perirhinal Cortex. *Brain Sciences*, 13(6), Article 6.
- Menne, F., Henzen, N. A., Sollberger, M., Monsch, A. U., & Schipke, C. G. (2023). Influence of preanalytical and analytical factors on the quantification of six regulatory serum proteins. *Bioanalysis*, 15(19), 1157–1167.

## Wissenschaftliche Vorträge:

04/2023: *Der mediale perirhinale Kortex vor dem Hintergrund der Früherkennung der Alzheimer-Krankheit*, Memory Clinic Seminars; Universitäre Altersmedizin FELIX PLATTER, Basel

02/2022: *Topografie & funktionelle Neuroanatomie zweier ausgewählter Strukturen (Teil II: Perirhinaler Cortex)*, Memory Clinic Seminars; Universitäre Altersmedizin FELIX PLATTER, Basel

05/2021: *Intraclass Correlation of Manual and Automated Segmentation of Medial and Lateral Perirhinal Kortex*, Memory Clinic Seminars; Universitäre Altersmedizin FELIX PLATTER, Basel

## Wissenschaftliche Posterpräsentationen (online):

- Henzen, N. A., Abdulkadir, A., Reinhardt, J., Blatow, M., Kressig, R. W., & Krumm, S. (2023). Out-of-the box automated computation of cortical thickness of the medial perirhinal cortex does not replace segmentation by hand. *Alzheimer's & Dementia*, 19(S17), e078850.
- Henzen, N. A., Reinhardt, J., Blatow, M., Kressig, R. W., & Krumm, S. (2021). Very high interrater reliability for manual segmentation of the medial perirhinal cortex. *Alzheimer's & Dementia*, 17(S4), e052922.